HUN-REN Biological Research Centre
Institute of Biochemistry
Synthetic and Systems Biology Unit

University of Szeged
Faculty of Natural Sciences and Informatics
Doctoral School of Biology

Ph.D. Thesis

Integrating rational design principles to develop resistance-limiting antibiotics for Gram-negative pathogens

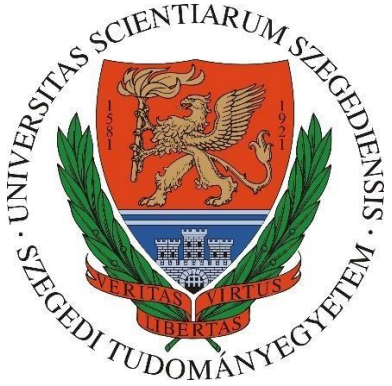

Author: Elvin Maharramov

Supervisor: Prof. Dr. Csaba Pál

Szeged, 2026

“Science knows no country, because knowledge belongs to humanity, and is the torch which illuminates the world.”

Louis Pasteur, 1872

Table of Contents

List of abbreviations

1. **Introduction** 1
   1.1. Global burden of antimicrobial resistance 1
   1.2. Mechanisms of antibiotic resistance 2
      1.2.1 Enzymatic inactivation 4
      1.2.2 Target modification 6
      1.2.3 Efflux system 7
      1.2.4 Reduced permeability 7
   1.3 Strategies for designing antibiotics resilient to resistance 8
      1.3.1 Permeabilizers: overcoming the outer-membrane barrier 9
      1.3.2 Targeting LPS biogenesis and transport: promising yet unrealized opportunities 10
      1.3.3 Non-canonical strategies that target the membrane envelope 12
   1.4 Integrating available strategies to rationally design future antibiotics 13
2. **Aims** 15
3. **Methods and materials** 16
   3.1. Strains, antibiotics, and media 16
   3.2. Membrane permeabilization assay 16
   3.3. Frequency-of-Resistance assay 17
   3.4. High-throughput laboratory evolution 17
   3.5. High-Throughput MIC measurements 18
   3.6. *In vitro* growth measurements 18
   3.7. Whole-genome sequencing and variant analysis 18
   3.8. Comparative mutational analysis 19
   3.9. AcrAB efflux system screening 19
   3.10. Genome-wide overexpression library screening 20
   3.11. ORF identification from overexpression library 21
   3.12. Functional metagenomic screens 21
   3.13. Annotation of antibiotic resistance genes (ARGs) 22
   3.14. Phylogenetic and geographic analysis of ARGs 22
   3.15. Quantifying bacterial survival under antibiotic exposure 23
   3.16. Statistics and reproducibility 24
4. **Results** 25

4.1. Antibiotic classification 25
4.2. Short-term resistance development measured by frequency of resistance 27
4.3. Adaptive laboratory evolution to measure resistance emergence under prolonged antibiotic exposure 29
4.4. Fitness cost of resistance evolution 31
4.5. Resistance mechanisms to dual-target permeabilizers 32
4.6. Cross-resistance of polymyxin adapted lines 35
4.7. Resistance to dual-target permeabilizers by gene amplification is limited 36
4.8. Mobile resistance genes to dual-target permeabilizers are rare in the environment 37
4.9. Killing kinetics of dual-target permeabilizers 40
5. **Discussion** 44
6. **Summary** 48
7. **Personal contributions** 50
8. **Acknowledgement** 51
9. **References** 52
10. **List of publications** 67

List of abbreviations

AB	*Acinetobacter baumannii*
ABC	ATP-binding cassette
ABC-F	ATP-binding cassette F family
ACP	Acyl carrier protein
ALE	Adaptive laboratory evolution
AMR	Antimicrobial resistance
APR	Apramycin sulfate
ARG	Antibiotic resistance gene
ASKA	A Complete Set of *E. coli* K-12 ORF Archive (ASKA) library
ATCC	American Type Culture Collection
AUC	Area under the (growth) curve
BAM	β-barrel assembly machinery
BLAST	Basic Local Alignment Search Tool
BLI	β-lactamase inhibitor
BWA	Burrows–Wheeler Aligner
CAMP	Cationic antimicrobial peptide
CARD	Comprehensive Antibiotic Resistance Database
CLSI	Clinical and Laboratory Standards Institute
COG	Clusters of Orthologous Groups
COL	Colistin
DOX	Doxycycline
DT	Dual-target
EC	*Escherichia coli*
ERA	Eravacycline
EUCAST	European Committee on Antimicrobial Susceptibility Testing
FASII	Fatty-acid synthesis II
FoR	Frequency of resistance
GEN	Gentamicin
GEP	Gepotidacin
GFP	Green fluorescent protein
HEPES	4-(2-hydroxyethyl)-1-piperazineethanesulfonic acid

IM	Inner membrane
IPTG	Isopropyl β-D-1-thiogalactopyranoside
KEGG	Kyoto Encyclopedia of Genes and Genomes
KP	*Klebsiella pneumoniae*
KPC	*Klebsiella pneumoniae* carbapenemase
LB	Lysogeny broth
LPS	Lipopolysaccharide
MDR	Multidrug resistant
MER	Meropenem
MHB	Mueller–Hinton broth
MIC	Minimum inhibitory concentration
MOX	Moxifloxacin
MS	Minimal salts media
NDM	New Delhi metallo-β-lactamase
NPN	N-phenyl-1-naphthylamine
OM	Outer membrane
OMA	Omadacycline
ORF	Open reading frame
OXA	Oxacillinase (class D β-lactamase)
PA	*Pseudomonas aeruginosa*
PBS	Phosphate-buffered saline
PBP	Penicillin-binding protein
PD	Pharmacodynamic
PK	Pharmacokinetic
PMB	Polymyxin B
POL	POL7306
RND	Resistance-nodulation-division (efflux family)
SCH	SCH79797
SEN	Sensitive (antibiotic-sensitive)
SNP	Single-nucleotide polymorphism
SPR	SPR206
ST	Single-target
SUO	Sulopenem
TRD	Tridecaptin M152-P3

UTI	Urinary tract infection
WHO	World Health Organization
WT	Wild type
YFP	Yellow fluorescent protein
ZOL	Zoliflodacin

1. Introduction

1.1. Global burden of antimicrobial resistance

Antibiotic resistance represents a significant challenge to global health, jeopardizing years of medical advancements. It undermines routine medical care, increases morbidity and mortality, and imposes substantial costs on health systems (Naghavi et al., 2024).

A high percentage of resistant infections found in clinical settings can be linked to a certain group of pathogens. The World Health Organization (WHO) has consistently reported the need for urgent strategies to prevent and control antimicrobial resistance in these priority pathogens over the past few years. In these reports, priority pathogens were categorized into three groups (Critical, High, Medium) according to their immediate public threat level. According to the most recent report in 2024 (World Health Organization, 2024), Gram-negative bacterial pathogens retained their “critical” classification from the earlier report in 2017 (World Health Organization, 2017). This group includes carbapenem-resistant *Acinetobacter baumannii*, as well as carbapenem and cephalosporin-resistant *Enterobacterales*, including *Escherichia coli*, *Klebsiella pneumoniae*, *Citrobacter*, *Serratia*, *Morganella*, and *Enterobacter* species. It is particularly alarming, as these pathogens are able to resist carbapenem treatment regimes, which was long considered the "last resort" for serious gram-negative infections (Sheu et al., 2019). In 2019 alone, drug-resistant bacterial infections were directly responsible for an estimated 1.27 million deaths and associated with ~4.95 million deaths globally (Fig. 1; Murray et al., 2022), despite the introduction of several new antibiotics and antibiotic adjuvants(Miller & Arias, 2024). This corresponds to roughly 1 in 11 infection-related deaths (≈ 9%) being directly attributable to antimicrobial resistance (AMR) in 2019 (Ikuta et al., 2022). Notably, four of the top six pathogens with high mortality rate are Gram-negative organisms (*E. coli, K. pneumoniae, A. baumannii, Pseudomonas aeruginosa*), reflecting the outsized impact of Gram-negative resistance on global health (Fig. 1). This epidemiological burden underscores the urgent need for new strategies to combat AMR on a global scale. Without changing how antibiotics are developed and deployed, small advances are rapidly undone by bacterial adaptation.

Having outlined the clinical burden and the pathogens of greatest concern, the next step is to examine the mechanistic landscape of resistance. Understanding common pathways that repeatedly emerge across species and drug classes is essential for building a general framework to guide rational antibiotic design.

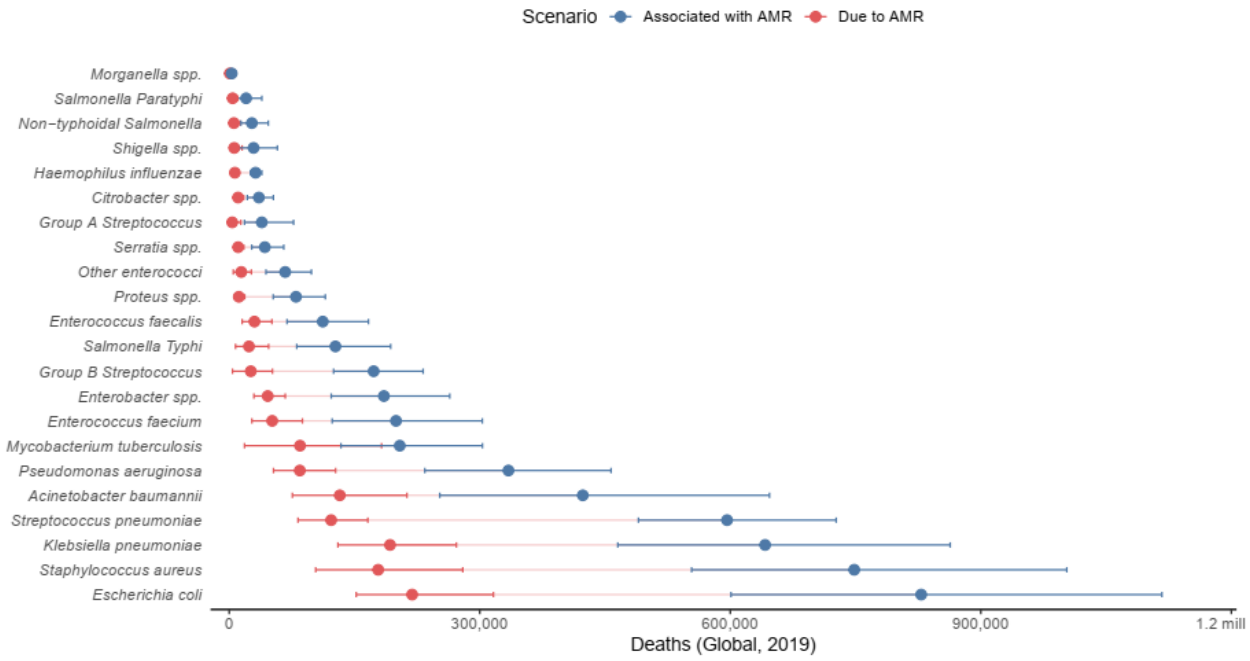

Figure 1. Global deaths associated with and attributable to antimicrobial resistance (AMR) by pathogens in 2019. Horizontal dot–error plots show estimated global deaths for major bacterial pathogens. **Blue points** denote deaths **associated with AMR** (infections caused by bacteria resistant to ≥1 routinely used antimicrobial). **Red points** denote deaths **due to AMR** (excess mortality attributable to resistance compared with a scenario in which infections are drug-susceptible). Horizontal bars represent 95% confidence interval. Pathogens are ordered by burden. The x-axis indicates global deaths in 2019 (up to ~1.2 million). Modified from Murray et al. (2022).

1.2. Mechanisms of antibiotic resistance

Understanding how bacteria become resistant is challenging: resistance predates modern medicine, and bacteria use diverse mechanisms to withstand antimicrobial pressure (Dcosta et al., 2011). Clarifying these molecular routes helps us (i) identify general resistance patterns, (ii) optimize use of existing drugs, (iii) design new antibiotics less prone to resistance, and (iv) develop new countermeasures (MacNair et al., 2024; Theuretzbacher, 2025b). Broadly, resistance arises in two ways: intrinsic resistance, driven by structural or functional traits that block drug action, and acquired resistance, gained through mutations or horizontal gene transfer (Darby et al., 2023).

For example, the outer membrane of Gram-negative bacteria acts as a permeability barrier, limiting entry of many antibiotics. This helps explain why some classes (*e.g.,* macrolides) show poor activity against Gram-negatives (Table 1; Myers & Clark, 2021; Vaara, 1993). Intrinsic resistance can also stem from the absence or replacement of a target, as with triclosan, where species that lack FabI or carry triclosan-insensitive ENR isoenzymes (*e.g.,* FabV in *Pseudomonas*) are inherently nonsusceptible (Zhu et al., 2010).

Table 1. Bacterial species and the antibiotics intrinsic resistance. Table is adapted from Reygaert (2018).

Bacteria	Antibiotics with intrinsic resistance
***Bacteroides* (anaerobes)**	aminoglycosides, many β-lactams, quinolones
All gram positives	aztreonam
All gram negatives	glycopeptides, lipopeptides
Enterococci	aminoglycosides, cephalosporins, lincosamides
Escherichia coli	macrolides
***Klebsiella* spp.**	ampicillin
***Acinetobacter* spp.**	ampicillin, glycopeptides
Pseudomonas aeruginosa	sulfonamides, ampicillin, 1st and 2nd generation cephalosporins, chloramphenicol, tetracycline
Serratia marcescens	macrolides
Listeria monocytogenes	cephalosporins

Bacteria can also develop resistance through genetic mutations, which results in the emergence of novel traits that facilitate survival. These mechanisms can be roughly divided into four main strategies, each of which stands for a unique method of counteracting the effects of antibiotics (Fig. 2; Darby et al., 2023).

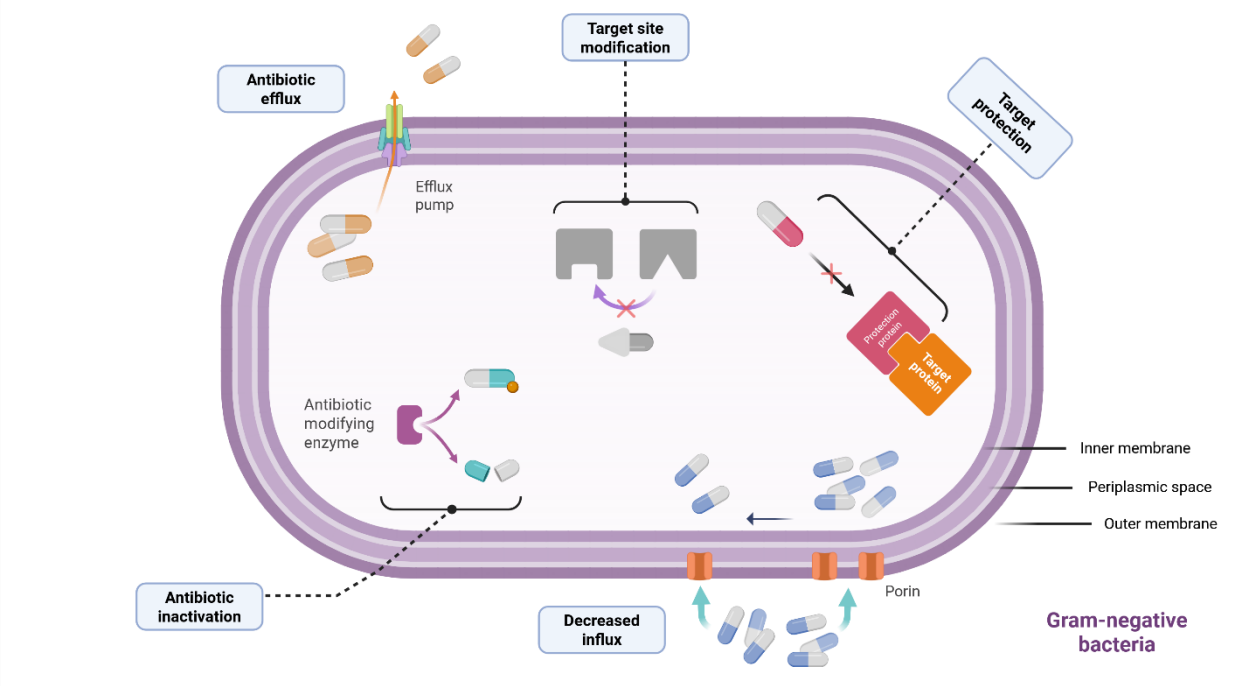

Figure 2. Core mechanisms of antibiotic resistance in Gram-negative bacteria. Schematic of a Gram-negative cell envelope (outer membrane, periplasm, inner membrane) highlights the principal ways bacteria reduce antibiotic efficacy. 1) **Decreased influx:** reduced porin number or altered porin selectivity lowers drug entry into the periplasm (common for β-lactams and fluoroquinolones). 2) **Active efflux:** multidrug efflux pumps expel chemically diverse antibiotics from the cell, decreasing intracellular concentrations. 3) **Antibiotic inactivation:** periplasmic or cytosolic enzymes chemically modify or hydrolyze drugs (for example, β-lactamases; aminoglycoside-modifying enzymes). 4) **Target-site modification:** mutations or enzymatic alterations of drug

targets prevent binding (for example, changes in DNA gyrase/topoisomerase IV, ribosomal RNA/proteins, or lipid A for polymyxins). 5) **Target protection:** proteins that shield or remove antibiotics from their targets (for example, Qnr proteins protecting DNA gyrase; ABC-F factors protecting the ribosome). Together, these mechanisms, often present in combination, either limit drug accumulation or diminish target engagement, resulting in clinical resistance. Illustration adapted from Darby et al. (2023) and created with Biorender.com.

1.2.1 Enzymatic inactivation

One of the most widespread bacterial resistance strategies is the synthesis of enzymes that chemically modify or inactivate antimicrobial drugs before they reach their targets. Antibiotics can be modified in two main ways: either by transferring a chemical group or by degrading the antibiotic and rendering it inactive (Fig. 3; Darby et al., 2023). β-lactamases, which hydrolyze the β-lactam ring and are essential for the action of carbapenems, cephalosporins, and penicillins, serve as an example of the latter strategy (Fig. 3a; Tooke et al., 2019). The emergence of β-lactamases is one of the most studied examples of bacterial adaptation to antibiotic pressure. With over 7,000 different β-lactamase variations discovered so far, the variety of these enzymes is simply enormous (Naas et al., 2017). Based on their amino acid sequences and catalytic processes, these enzymes are divided into four main functional classes (A, B, C, and D) (Tooke et al., 2019).

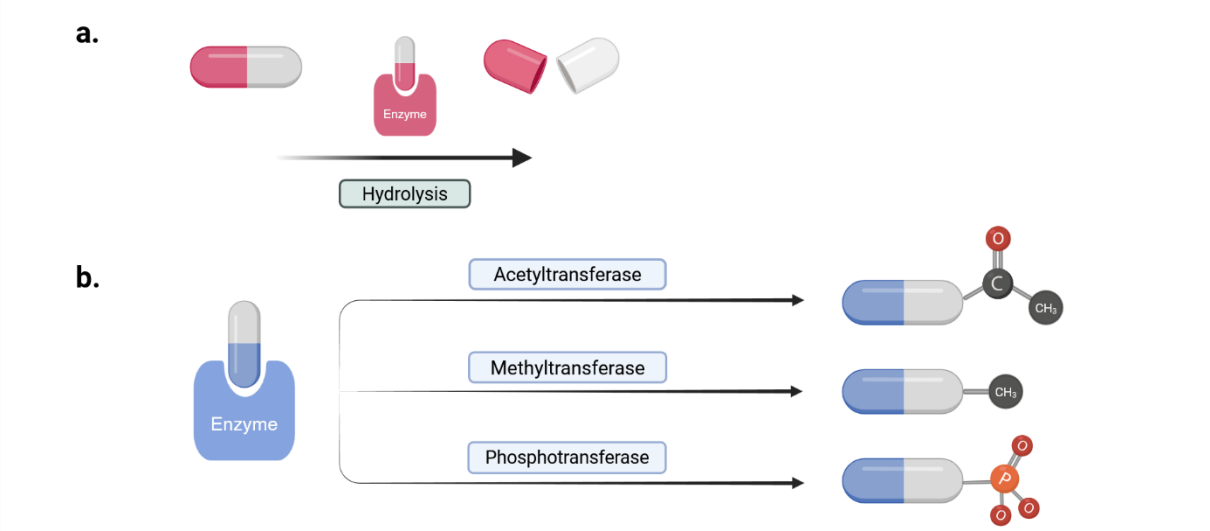

Figure 3. Enzymatic inactivation of antibiotics. (a) **Hydrolysis:** drug-inactivating enzymes cleave susceptible bonds, yielding inactive fragments (*e.g.*, β-lactamases opening the β-lactam ring). (b) **Covalent modification:** transferases attach small groups to the drug scaffold, such as acetyl (acetyltransferases), methyl (methyltransferases), or phosphate (phosphotransferases), thereby diminishing target binding and/or stability (classically seen with aminoglycosides, chloramphenicol, and some macrolides). Figure adapted from Darby et al. (2023) and created with Biorender.com

These enzymes are particularly problematic because they can render carbapenems, one of the last-resort antibiotics, to be ineffective. It is therefore expected that the WHO's 2024 antibiotic-resistance report classified carbapenem-resistant *A. baumannii* and *Enterobacterales* as critical-priority pathogens (World Health Organization, 2024). Carbapenem resistance typically arises from carbapenemase production or the synthesis of extended-spectrum β-lactamases together with porin loss (Codjoe &

Donkor, 2017). Carbapenemases, including KPC (class A), NDM (class B), and OXA (class D), can hydrolyze penicillins, cephalosporins, and carbapenems, drastically decreasing the number of available treatment options for a specific infection (Halat & Moubareck, 2020).

Although several new antibiotics have been developed to overcome existing resistance mechanisms, most are simply derivatives of older drugs. Cefiderocol, a novel siderophore-cephalosporin approved by the FDA in 2019, was designed to treat carbapenem-resistant Gram-negative pathogens, especially metallo-β-lactamase-producing *P. aeruginosa* and *A. baumannii* (Bianco et al., 2024; Theuretzbacher et al., 2025). However, a recent study reported that carbapenemases NDM-15, NDM-22, and NDM-27 can already confer resistance to cefiderocol (Daruka et al., 2025). Furthermore, systematic review and meta-analysis found high rates of cefiderocol non-susceptibility among NDM β-lactamase–producing *Enterobacterales* and *A. baumannii*, undermining its novelty (Karakonstantis et al., 2024). Similarly, sulopenem, thiopenem β-lactam antibiotic approved by FDA in 2024, has already encountered resistance mediated by environmental DNA fragments encoding NDM β-lactamases (Daruka et al., 2025).

Tetracycline-inactivating enzymes, which catalyze the oxidation of tetracyclines, provide yet another notable example of the inactivation of antibiotics. The most well-known is the Tet(X) family, which has been identified in numerous bacterial classes and has the ability to spread horizontally on transposable elements to impart high-level resistance to tetracyclines (T. He et al., 2019; Markley & Wencewicz, 2018). The environmental prevalence of these enzymes is positively correlated with tetracycline use (Gasparrini et al., 2020). Consequently, newer antibiotics like eravacycline and omadacycline, which were approved by the FDA in 2018, are already facing resistance mediated by environmental *tetX* enzymes (Daruka et al., 2025).

In addition to β-lactamases and tetracycline-inactivating enzymes, bacteria produce a wide range of antibiotic-modifying enzymes that transfer chemical groups to drugs, thereby inactivating them. For example, aminoglycoside-modifying enzymes (AMEs) can acetylate, phosphorylate, or adenylate aminoglycoside antibiotics, preventing their binding to the bacterial ribosome (Fig. 3b; Darby et al., 2023). In addition to chromosomes, many AMEs are encoded by mobile genetic elements, which facilitate their horizontal spread across environments (Partridge et al., 2018; M. S. Ramirez & Tolmasky, 2010). Apramycin, a novel aminoglycoside currently in clinical development, largely evades most common AMEs but can still be inactivated by the ApmA acetyltransferase (Bordeleau et al., 2021). However, recent findings demonstrate that bacteria harboring DNA fragments from environmental samples encoding acetyltransferases exhibit reduced susceptibility to apramycin, suggesting that derivatives of older antibiotics may already be vulnerable to the same resistance mechanisms that rendered previous generations ineffective (Daruka et al., 2025).

1.2.2 Target modification

When bacteria are unable to break down antibiotics, they often change the cellular targets that these drugs bind (Fig. 4). This strategy keeps vital biological processes intact while rendering antibiotics useless. Various target modification methods are sometimes highly unique to particular kinds of antibiotics. The fluoroquinolones antibiotics, for instance, bind close to the active site of crucial topoisomerase enzymes to inhibit them (Hooper & Jacoby, 2016). Point mutations in the quinolone resistance-determining regions (QRDRs) of the *gyrA*, *gyrB*, *parC*, and *parE* genes reduce fluoroquinolone binding affinity while maintaining enzyme activity (Varughese et al., 2018). Furthermore, the acquisition of the *qnr* gene, a family of genes carried on plasmids often seen in Gram-negative bacteria that protect topoisomerases from inhibition by quinolones, combined with *gyrA* point mutations can result in high-level resistance (Darby et al., 2023).

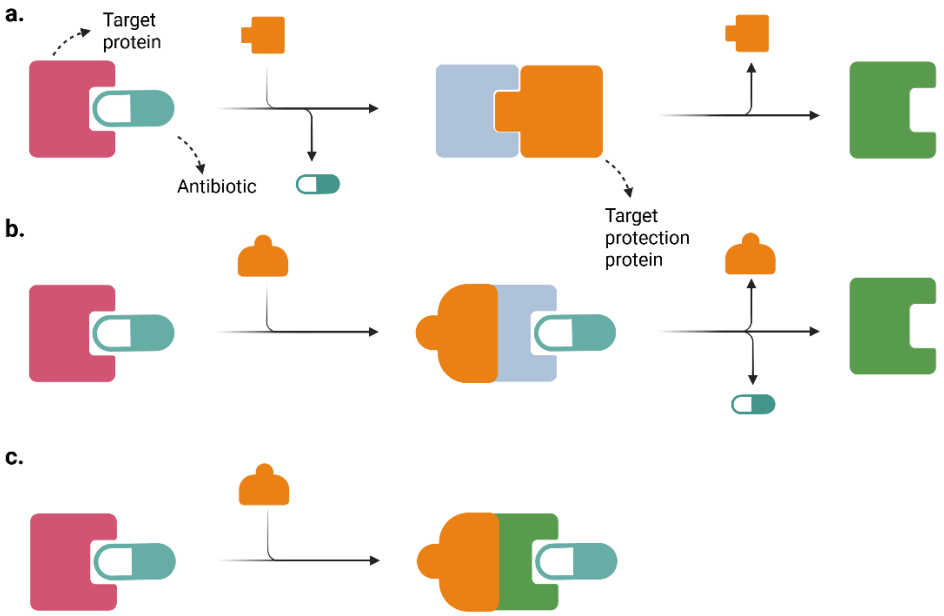

Figure 4. Target protection as a resistance mechanism. Schematic illustrates how target protection proteins (orange) can rescue an antibiotic-inhibited target (pink/blue) without mutating it. **(a)** The protector transiently occupies the drug-binding pocket, displacing the antibiotic and leaving an active target that resumes function (green). **(b)** The protector binds at a distinct site and remodels the target ejecting the bound drug; both proteins then dissociate, and activity is restored. **(c)** The protector remains associated with the target, capping the binding surface or stabilizing a drug-poor conformation, thereby preventing (re)binding while allowing catalysis. Examples include ribosomal protection proteins (TetM/TetO, ABC-F factors) and quinolone protection proteins (Qnr/PRP). Figure adapted from Darby et al. (2023) and created with Biorender.com

1.2.3 Efflux system

Bacterial defense strategies also include the active export of drugs via efflux pumps. Although all bacteria have numerous efflux pumps, these pumps are especially crucial in mediating antimicrobial resistance in Gram-negative bacteria. Efflux pumps work in tandem with the impermeable double membrane, adding to the inherent resistance of bacteria to many drugs (Krishnamoorthy et al., 2017). It has also been shown that the downregulation of efflux pumps in bacteria reduces the frequency at which resistance evolves within a population (Ricci et al., 2006). Efflux transporters are classified into six groups, with the resistance-nodulation-division (RND) family providing the most clinically relevant levels of resistance in Gram-negative bacteria (Alav et al., 2021). Overexpression of RND pumps in clinical isolates can lead to multidrug resistance (MDR) due to their ability to export several drugs with different structures and chemical properties (Blair et al., 2014).

The AcrAB-TolC system, a member of the RND family, allows *E. coli* and other *Enterobacteriaceae* to efflux wide range of antimicrobials, including β-lactams, fluoroquinolones, tetracyclines, and macrolides. Similarly, the MexAB-OprM system contributes to the intrinsic resistance of *P. aeruginosa* against multiple antibiotic classes (Huang et al., 2022).

Efflux pump expression is often regulated by local repressor proteins, and mutations affecting these repressors can lead to pump overexpression and increased resistance. For instance, in *Salmonella typhimurium*, *acrAB-tolC* expression is controlled by RamA, which itself is regulated by RamR (Abouzeed et al., 2008).

Importantly, the regulatory network extends beyond efflux alone. Global regulators such as MarA, SoxS, and Rob, which also influence *acrAB-tolC* expression, are involved in maintaining membrane integrity, DNA repair, biofilm formation, quorum sensing, and virulence. These pleiotropic roles highlight that efflux pump regulation is embedded within a broader genetic network that supports bacterial survival under diverse stress conditions (Chubiz, 2023).

1.2.4 Reduced permeability

The bacterial cell envelope is the initial line of defense against antimicrobial agents. Changes in the cell envelope's permeability can have a major impact on antibiotic efficacy, particularly for drugs that must pass through the cell membrane to reach their targets. This is especially important in Gram-negative bacteria, which have a double-membrane structure that makes the cellular envelope relatively impermeable, resulting in intrinsic resistance to many antibiotics used against Gram-positive pathogens. This poses a significant challenge to the development of novel antimicrobials that can penetrate the cell envelope (Saxena et al., 2023).

Gram-negative bacteria commonly use porin alterations as a resistance strategy. These porins allow hydrophilic compounds, such as many antibiotics, to pass through the outer membrane. The creation of porins with altered selectivity, as well as their deletion, can drastically lower antibiotic absorption (Davin-Regli et al., 2024). For instance, changes to *Enterobacteriaceae*'s OmpC and OmpF porins can result in β-lactam resistance (Masi et al., 2022), whereas *P. aeruginosa*'s loss of the OprD porin is linked to carbapenem resistance (H. Li et al., 2012).

In addition to drug entry through porins, the structure of the outer membrane itself also contributes to reduced antibiotic activity. For instance, modifications of lipopolysaccharides (LPS) in the outer membrane can confer resistance, particularly against cationic antimicrobial peptides (CAMP) such as polymyxins. The addition of 4-amino-4-deoxy-L-arabinose (Ara4N) or phosphoethanolamine (pEtN) to lipid A decreases the overall negative charge of the outer membrane, thereby reducing polymyxin binding and leading to resistance (Daruka et al., 2025; Spohn et al., 2019). These modifications are commonly regulated by two-component systems such as PmrAB and PhoPQ (Olaitan et al., 2014; Poirel et al., 2017). Additionally, in *K. pneumoniae*, inactivation of the small transmembrane protein MgrB, a negative regulator of PhoPQ, is a frequent mechanism underlying acquired colistin resistance (Cannatelli et al., 2014).

These recurring resistance mechanisms, such as enzymatic inactivation, target alteration, active efflux, and reduced permeability, represent continuous limitations on antibiotic design. From this perspective, the current drug discovery pipeline is not merely a catalog of candidate molecules but rather a testing ground for strategies aimed at overcoming or circumventing these barriers.

1.3 Strategies for designing antibiotics resilient to resistance

After the “Golden Age” of antibiotic discovery, the number of novel chemotypes and targets declined sharply. Today’s pipeline is dominated by refinements of existing classes or combinations with β-lactamase inhibitors, which provide short-term clinical value but often struggle to ensure long-term efficacy (Theuretzbacher, 2025b; Theuretzbacher et al., 2025). This underscores the need to identify the key factors that shape resistance risk and integrate them into the antibiotic development process.

The permeability barrier of Gram-negative pathogens makes them particularly difficult to treat. Compared with Gram-positive infections, far fewer long-lasting effective options exist, and as a result, current development efforts are heavily focused toward Gram-negative bacteria.

The clinical pipeline itself serves as a practical measure of discovery activity. To date, the most consistent advances have come from novel β-lactamase inhibitors, which protect β-lactam antibiotics (*e.g.*, penicillins and cephalosporins) from enzymatic hydrolysis. Together with beta-lactam antibiotics, this pipeline dominates the discovery of novel antibiotics in clinical trials (Fig. 5; Theuretzbacher, 2025a).

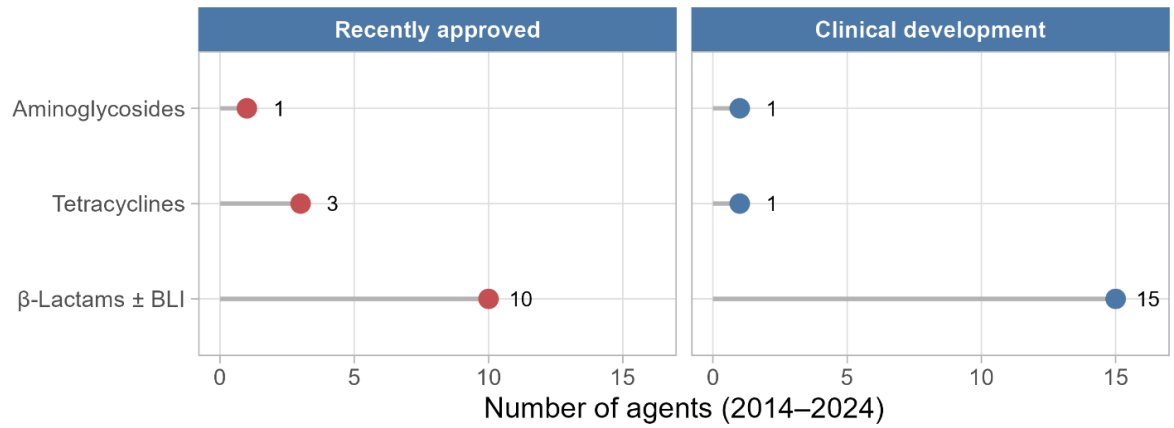

Figure 5. Recent approvals and clinical pipeline for selected antibiotic classes (2014–2024). Dot plots show the number of systemic agents **recently approved** (left) and **in clinical development** (right) for three major classes. Numbers next to each dot indicate counts of distinct agents in each category. The figure highlights the dominance of β-lactam/BLI combinations in both recent approvals and the current pipeline. Adapted from Theuretzbacher et al. (2025)

However, as highlighted in Chapter 1.2.1, β-lactamases are highly diverse and continue to evolve (Bush & Jacoby, 2010). Metallo-β-lactamases and inhibitor-resistant variants can undermine the efficacy of even the most advanced β-lactamase inhibitors (Karaiskos et al., 2025). Moreover, not all β-lactam resistance is enzymatic; mutations that diminish binding affinity to penicillin-binding proteins (PBPs) or the acquisition of alternative PBPs via plasmids can also compromise these novel therapies (Sethuvel et al., 2023).

The greatest challenge remains the development of first-in-class agents, whether by identifying new targets or by exploiting novel mechanisms of action against established ones. Unsurprisingly, progress in this area has been minimal (Butler et al., 2023). Despite substantial investment from both industry and academia, only a handful of compounds with genuinely novel activity against Gram-negative pathogens have reached the pipeline.

1.3.1 Permeabilizers: overcoming the outer-membrane barrier

One of the major challenges in the discovery of new antibiotics active against Gram-negative bacteria lies in their unique double-membrane structure. The outer membrane (OM) serves as a selective permeability barrier composed of an asymmetric bilayer, where lipopolysaccharides (LPS) form the outer leaflet and phospholipids occupy the inner one. This barrier greatly restricts the diffusion of hydrophobic and large hydrophilic molecules, thereby shielding essential cellular targets from antibiotic access (Delcour, 2008; May & Grabowicz, 2018). In addition to passive exclusion, efflux pumps embedded in the OM further reduce intracellular drug accumulation, collectively conferring a formidable intrinsic resistance to many otherwise potent compounds (Ntallis et al., 2025).

Permeabilizers are agents that compromise this barrier, either transiently or permanently, to facilitate the entry of antibiotics or other molecules. Classical examples include cationic peptides such as polymyxins, which bind to the negatively charged phosphate groups of LPS, displacing divalent cations (Mg^{2+}, Ca^{2+}) and destabilizing the OM. This electrostatic disruption increases membrane permeability, leading to leakage of periplasmic contents and cell death (Falagas & Kasiakou, 2006). Importantly, at sublethal concentrations, such molecules can also potentiate otherwise impermeant antibiotics, such effect that underlies the concept of "permeabilizer-based combination therapy" (Yan et al., 2019).

Beyond these traditional examples, the term *permeabilizer* has expanded to include synthetic and semi-synthetic compounds that either directly perturb the OM or exploit OM components (such as LPS or BamA) to gain entry (D. M. Ramirez et al., 2022; Si et al., 2023). These molecules need not be limited to membrane disruption; rather, their ability to transiently increase permeability is integral to their mechanism of action (Dhanda et al., 2025). This distinction is crucial, because several newly discovered antibiotics combine membrane permeabilization with a second, independent intracellular target, yielding what we refer to as *dual-target permeabilizers* (*e.g.,* POL7306, tridecaptin M152-P3, SCH79797) (Jangra et al., 2019; Luther et al., 2019; J. K. Martin et al., 2020). Such compounds merge rapid bactericidal action with a reduced probability of resistance, since effective survival would require simultaneous adaptation to both envelope damage and intracellular inhibition.

Understanding permeabilizers is therefore fundamental to the rationale discussed in the following sections. In Chapter 1.3.2, I explore strategies that target the assembly and maintenance of the Gram-negative envelope, particularly the biosynthesis and transport of LPS, a central determinant of permeability. The mechanisms described there define the structural and biochemical basis of how the outer membrane maintains its integrity and thus explain why disrupting or bypassing it through permeabilizers can be so effective. In turn, this sets the stage for the dual-target design concepts introduced later, where membrane permeabilization acts not merely as an access mechanism but as a direct, complementary mode of killing that minimizes resistance evolution.

1.3.2 Targeting LPS biogenesis and transport: promising yet unrealized opportunities

Building upon this concept, several efforts have focused on directly targeting the molecular pathways that construct and maintain the outer membrane barrier itself. Within the current antibiotic pipeline, one of the most intensively explored directions targets LPS biosynthesis and transport. LPS consists of three structural elements: the lipid A membrane anchor, the core oligosaccharide, and the O-antigen, with lipid A forming the outer leaflet of the outer membrane. Its production is governed by an extensive biosynthetic and regulatory network that integrates enzymes from fatty-acid metabolism, phospholipid synthesis, and diverse LPS-modification pathways (Fig. 6; Romano & Hung, 2023).

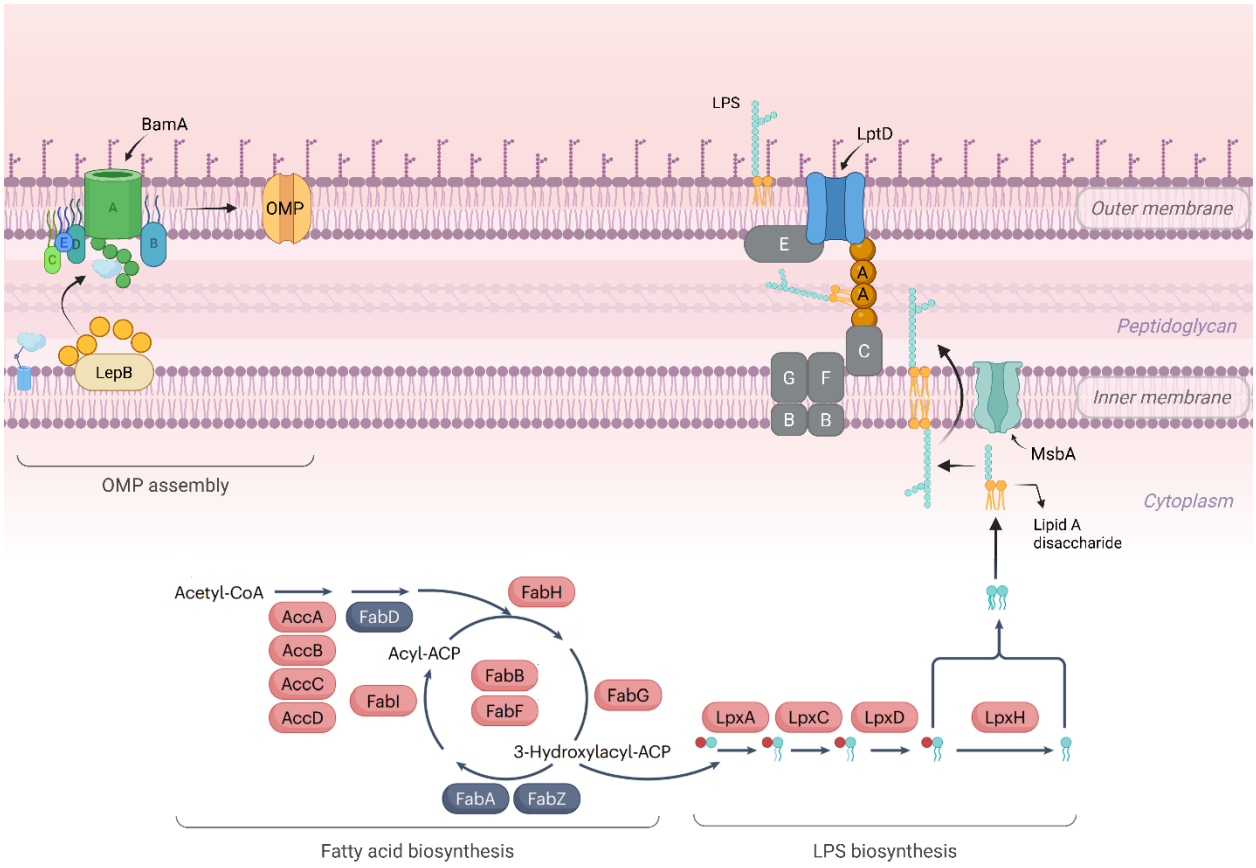

Figure 6. Gram-negative envelope biogenesis: lipid A/LPS production and OMP assembly. Schematic of the Gram-negative cell envelope showing key pathways that build and traffic outer-membrane components. **Bottom left, fatty-acid biosynthesis (FASII):** acetyl-CoA is carboxylated by **AccA–D**, transferred to ACP by **FabD**, and elongated via **FabH/G/Z/A/B/F/I** to produce 3-hydroxy-acyl-ACPs. These acyl donors feed **lipid A/LPS biosynthesis** (**LpxA → LpxC → LpxD → LpxH**) to generate a lipid A disaccharide. **MsbA** flips nascent lipid A–core to the periplasmic leaflet of the inner membrane. The **Lpt** machine, consisting of the IM ABC transporter **LptB$_2$FGC**, periplasmic **LptA** oligomers, and the OM translocon **LptD/E**, mediates LPS extraction, translocation across the periplasm, and insertion into the outer leaflet of the OM. In parallel, β-barrel **outer-membrane proteins (OMPs)** are exported to the periplasm, processed by signal peptidase **LepB**, and assembled into the OM by the **Bam complex (BamA–E)**. Adapted from Theuretzbacher et al. (2023) and created with Biorender.com

The enzymes of the lipid A pathway, encoded by the *lpx* family, are highly conserved across species and localized to the cytoplasm or the inner face of the inner membrane. Among these, LpxA, LpxC, and LpxD have emerged as prominent drug targets (Theuretzbacher et al., 2023). However, clinical translation has proven to be difficult. Although potent LpxC inhibitors have been developed, their advancement has been constrained by cardiovascular toxicity, while dual-targeting approaches that exploit the structural similarity of LpxA and LpxD have been hampered by the complexity of their enzymatic reactions (F. Cohen et al., 2019; Han et al., 2020; Kroeck et al., 2019; Surivet et al., 2020).

Following lipid A–core assembly, LPS is flipped into the periplasm and transported to the cell surface by the Lpt (lipopolysaccharide transport) machinery, a seven-protein complex in which the loss of any component causes defective or modified LPS accumulation (Okuda et al., 2016). Of these proteins, LptD has been studied most extensively due to its surface exposure (Botte et al., 2022). LptD is a β-

barrel outer-membrane protein whose assembly depends on BamA, the central subunit of the β-barrel assembly machinery (BAM) (Lee et al., 2019). The last stages of LPS assembly at the cell surface are mediated by LptD.

One of the earliest notable leads against an outer-membrane protein LptD was murepavadin, a peptidomimetic with specificity for *P. aeruginosa* (Srinivas et al., 2010). Although it showed promising activity, Phase 3 trials were halted due to nephrotoxicity (Prasad et al., 2022). Subsequent work produced chimeric molecules that engage both LPS and BamA at the outer membrane (*e.g.,* POL7306), broadening anti-Gram-negative activity (Fig. 6; Luther et al., 2019).

BamA itself is an essential protein that catalyzes the folding and insertion of β-barrel proteins like porins and LptD. It is one of the two crucial outer-membrane proteins, along with LptD. Because BamA is a β-barrel rather than a classical enzyme with a discrete active site, it has often been considered "undruggable" for small molecules (Lewis et al., 2024). Consistent with this view, purely synthetic BamA inhibitors have been hard to produce. A partial solution has been the development of OMPTAs (outer-membrane-protein-targeting antibiotics), chimeric polymyxin–cyclic polycations that harness polymyxin's strong affinity for LPS to achieve potent antibacterial activity, despite forming only weak direct contacts with BamA (Luther et al., 2019).

While LPS-pathway enzymes and assembly factors remain attractive, safety liabilities and delivery constraints have slowed clinical translation. This has motivated alternative envelope-focused strategies that do not exclusively depend on LPS binding.

1.3.3 Non-canonical strategies that target the membrane envelope

Other notable early stage leads with *in vivo* activity against Gram-negative bacteria include tridecaptins. They represent a particularly interesting re-emerging class of non-ribosomal antimicrobial peptides (NRAPs) with potent efficacy against critical priority Gram-negative pathogens (Bann et al., 2021). Tridecaptin M, recently isolated from *Paenibacillus* sp., selectively binds the Gram-negative variant of lipid II at the outer leaflet of the inner membrane, thereby disrupting the proton-motive force. In addition, tridecaptins interact with LPS, though via a molecular mechanism distinct from polymyxins (Cochrane et al., 2016; Jangra et al., 2019). Because NRAPs are assembled by non-ribosomal peptide synthetases (NRPSs), they can incorporate both proteinogenic and non-proteinogenic residues and undergo enzyme-mediated tailoring (Calcott et al., 2020; Felnagle et al., 2008). This biosynthetic flexibility provides a rich platform for chemical optimization of potency, stability, and pharmacological properties.

Another promising example is SCH79797, a repurposed small molecule with broad-spectrum activity mediated by dual mechanisms: disruption of the Gram-negative outer membrane through engagement of the mechanosensitive channel MscL, and inhibition of folate biosynthesis (J. K. Martin et al., 2020;

Wray et al., 2022). Notably, while combination therapies pairing dihydrofolate reductase (DHFR) inhibitors (*e.g.*, trimethoprim) with membrane disruptors often display antagonism, combining both mechanisms within a single scaffold have been associated with a low frequency of resistance and high potency (J. K. Martin et al., 2020). Because SCH79797 depolarizes membranes via MscL rather than through LPS binding, it highlights a complementary strategy for envelope disruption.

Together, these non-traditional approaches illustrate how envelope function can be compromised using small molecules or tailored peptides. By moving beyond strictly LPS-centric strategies, such agents broaden the scope of outer-membrane targeting and point toward rational designs that integrate multiple activities within a single scaffold to minimize resistance emergence.

1.4 Integrating available strategies to rationally design future antibiotics

In response to the urgent need for effective treatment options, two key strategies have gained prominence: (i) antibiotics that target immutable aspects of bacterial physiology, and (ii) multi-targeting antibiotics, in which a single molecule inhibits multiple bacterial targets (Breukink & de Kruijff, 2006; Lewis, 2020; Shukla et al., 2023; Silver, 2007).

The first strategy focuses on cellular structures that are not directly protein-encoded and thus less susceptible to mutation-driven resistance. For example, compounds that disrupt cell-envelope integrity exploit bacterial vulnerabilities that cannot be easily altered by point mutations (Lewis, 2020; Q. Li et al., 2021). Lipid II, a peptidoglycan precursor, demonstrates such a target and has been proposed as a promising candidate for drugs with inherently low resistance potential (Breukink & de Kruijff, 2006; Ling et al., 2015). In these cases, while resistance may still arise, it often comes at the cost of diminished virulence or reduced bacterial fitness.

The second strategy relies on designing molecules that act against multiple targets simultaneously. In principle, resistance emergence would require multiple concurrent mutations. In practice, this approach has limitations. Single mutations that offer significant advantages against one target or class are frequently seen in natural bacterial populations. Prolonged usage of antibiotics might enhance these precursors, thereby promoting resistance to dual-target drugs that are still under development (Szili et al., 2019). Moreover, resistance can evolve through indirect mechanisms such as reduced permeability, enzymatic inactivation, or altered efflux specificity, which may bypass the intended multi-target effect (Darby et al., 2023).

Given these considerations, I hypothesize that the most durable approaches will combine multiple mechanisms of action with a particular emphasis on membrane disruption. By contrast, drugs that act on a single membrane-associated function or two intracellular protein targets may remain vulnerable to envelope-level adaptations or pre-existing resistance mutations.

To test this hypothesis, we employ a series of complementary assays in Gram-negative, critical-priority pathogens. We selected 16 antibiotics covering diverse classes, including compounds that have been recently approved or remain in preclinical development, to better reflect the current drug discovery pipeline. For systematic comparison, I classified these drugs into four groups, with our primary focus on dual-target permeabilizers, agents that disrupt the bacterial outer membrane while simultaneously targeting another cellular pathway. This group includes POL7306, tridecaptin M152-P3, and SCH79797. Resistance development against these antibiotics is evaluated in parallel with three control groups: (i) single-target permeabilizers, such as polymyxin; (ii) dual-target non-permeabilizers, demonstrated by gepotidacin; and (iii) single-target non-permeabilizers, representing antimicrobials with well-defined single mechanisms of action (*e.g.,* aminoglycosides, tetracyclines). By integrating laboratory evolution with functional metagenomics and gene overexpression screens across these antibiotic–bacteria combinations, I systematically quantify resistance potential, map the genetic pathways driving adaptation, and evaluate scaffolds that are least prone to resistance. This framework not only provides a comparative assessment of current drug candidates but also offers empirical evidence to guide the rational design of next-generation antibiotics that maximize efficacy while limiting the risk of resistance evolution.

2. Aims

The overarching aim of this study is to define the principles underlying the development of antibiotics that are less prone to bacterial resistance, with a particular focus on agents that simultaneously disrupt membrane integrity and inhibit a distinct cellular pathway. I hypothesize that such "dual-target permeabilizers" impose evolutionary constraints that limit the emergence of resistance compared to drugs that act on a single membrane-associated pathway or two intracellular protein targets.

To address this:

- We first examine how resistance evolves in clinically relevant Gram-negative pathogens (*E. coli, K. pneumoniae, A. baumannii, P. aeruginosa*) when exposed to 16 different antibiotics, testing whether antibiotics that simultaneously disrupt membrane integrity and inhibit a distinct cellular pathway reduce the likelihood of resistance development.
- The genetic and mechanistic bases of resistance are then investigated, including the contribution of *de novo* mutations in target sites or efflux pumps, the role of gene amplification, and the potential acquisition of resistance through mobile genetic elements.
- To evaluate the environmental prevalence and transfer risk of resistance factors, functional metagenomic screens are applied from human, soil, and clinical microbiome sources.
- Finally, the bactericidal activity of membrane-permeabilizing antibiotics is assessed by quantifying population dynamics during exposure to lethal concentrations, thereby clarifying whether rapid killing contributes to their reduced resistance frequency.

Together, these aims are designed to systematically evaluate whether antibiotics that target both membrane integrity and additional cellular pathways (*i.e.,* dual-target permeabilizers) can overcome the evolutionary pressures that typically drive resistance. By integrating laboratory evolution, genetic analysis, functional metagenomics, and time-kill experiments, the study seeks to establish a framework to guide the future design of antibiotics with limited resistance.

3. Methods and materials

3.1. Strains, antibiotics, and media

This study employed a diverse collection of bacterial strains to investigate resistance phenomena. For the frequency-of-resistance (FoR) and adaptive laboratory evolution (ALE) experiments, two strains were chosen for each species: *Escherichia coli* ATCC 25922, *Klebsiella pneumoniae* ATCC 10031, *Acinetobacter baumannii* ATCC 17978, and *Pseudomonas aeruginosa* ATCC BAA-3107 represented the antibiotic-sensitive (SEN) cohort, whereas *E. coli* NCTC 13846, *K. pneumoniae* ATCC 700603, *A. baumannii* ATCC BAA-1605, and *P. aeruginosa* LESB58 constituted the multi-drug resistant (MDR) cohort. Functional metagenomic screens were later performed in *E. coli* ATCC 25922 and *K. pneumoniae* ATCC 10031 to capture environmental resistance determinants. To characterize dose–kill kinetics, an *E. coli* ATCC 25922 strain co-expressing yellow fluorescent protein (YFP, encoded on pZS2R, chloramphenicol-resistant) and red fluorescent protein (mCherry, also on pZS2R, chloramphenicol-resistant) was employed.

Sixteen antibiotics spanning four distinct modes of action were tested, including eleven novel compounds currently in various clinical trial phases and five established antibiotics with extensive clinical histories (names, abbreviations, and detailed properties are presented in Table 2). Antibiotics were either custom-synthesized in-house or procured from commercial suppliers. Upon preparation, each stock solution was filter-sterilized and stored at –20 °C until use. Cation-adjusted Mueller–Hinton Broth 2 (MHB; Millipore) served as the primary growth medium unless specified otherwise. In the case of SCH79797 (SCH), which inhibits folate biosynthesis, medium composition was switched to Minimal Salt (MS) in order to maximize antibacterial activity; this MS medium comprised 1 g/L $(NH_4)_2SO_4$, 3 g/L KH_2PO_4, 7 g/L K_2HPO_4, and was supplemented with 1.2 mM sodium citrate dihydrate ($Na_3C_6H_5O_7 \cdot 2H_2O$), 0.4 mM $MgSO_4$, 0.54 µg/mL $FeCl_3$, 1 µg/mL thiamine HCl, 0.2% Casamino Acids, and 0.2% glucose.

3.2. Membrane permeabilization assay

The outer membrane–permeabilizing effects of selected antibiotics on *E. coli* ATCC 25922 were quantified using the hydrophobic fluorescent probe 1-N-phenylnaphthylamine (NPN; Merck) in accordance with established protocols (Helander & Mattila-Sandholm, 2000). Initially, *E. coli* ATCC 25922 was inoculated into MHB and incubated overnight at 37 °C to saturation. Two hundred microliters of this overnight culture were then diluted into 20 mL fresh MHB and grown with shaking until mid-logarithmic phase (OD_{600} = 0.4–0.6). Cells were harvested by centrifugation (1,100 × g, 10 minutes), washed twice, and resuspended in a buffer containing 5 mM HEPES (pH 7.0) and 5 mM glucose to an OD_{600} of 0.4–0.6. One hundred microliters of this bacterial suspension, adjusted to four times the minimum inhibitory concentration (MIC) of each antibiotic, were mixed in a black 96-well

plate (Revvity PhenoPlate-96) with 50 µL freshly prepared NPN solution and 50 µL of HEPES buffer. After equilibrating at room temperature for 15 minutes, fluorescence was measured immediately using a Biotek Synergy H1 microplate reader (excitation 350 nm, emission 410 nm). Untreated *E. coli* served as a negative control, whereas polymyxin B (10 µg/mL)–treated cells provided a positive control. Relative fluorescence units were calculated by normalizing each antibiotic-treated well to the untreated control.

3.3. Frequency-of-Resistance assay

To assess how frequently spontaneous resistant mutants emerge within a bacterial population, FoR assays were performed following established guidelines (Bell & MacLean, 2018; Ling et al., 2015; Luria & Delbrück, 1943; Nyerges et al., 2020). Each overnight culture (grown in MHB at 37 °C, 250 RPM) was centrifuged, washed twice in fresh MHB, and adjusted to approximately 10^{10} stationary-phase cells per sample. These suspensions were then plated onto MHB agar plates containing antibiotic concentrations of 2×, 4×, 8×, and 20× the empirically determined MIC. Plates were incubated at 37 °C for 48 hours, with each concentration tested in triplicate. Simultaneously, total viable counts were determined by serially diluting and plating aliquots of the washed cells on antibiotic-free MHB agar. After 18 hours of incubation at 37 °C, colony-forming units (CFUs) were counted to calculate the initial cell density. Resistance frequency was defined as the ratio of colonies growing on antibiotic-containing plates to the total viable CFU count. From plates yielding colonies at the highest antibiotic concentration, ten individual colonies were picked for subsequent MIC determination and whole-genome sequencing.

3.4. High-throughput laboratory evolution

Adaptive laboratory evolution (ALE) experiments were designed to select for maximal resistance, following a high-throughput protocol (Bódi et al., 2017; Spohn et al., 2019). For each antibiotic–ancestral strain combination, ten parallel populations were initiated in 96-well plates at an antibiotic concentration that produced approximately 50% growth inhibition, as determined by preliminary dose–response assays. Cultures were incubated in MHB at 37 °C with continuous shaking (300 RPM) for 72 hours. At the end of each incubation, optical density at 600 nm (OD_{600}) was measured; wells showing $OD_{600} > 0.2$ at the highest antibiotic concentration were deemed to have sufficient growth to proceed. Twenty microliters from each qualifying well were transferred into four fresh wells arranged in a chessboard layout, each containing MHB supplemented with incrementally higher antibiotic concentrations (0.5×, 1×, 1.5×, and 2.5× the previous concentration). This layout also facilitated cross-contamination checks. Transfer and selection steps were repeated for twenty consecutive passages, ultimately yielding 728 evolved lines across all antibiotic–strain combinations.

3.5. High-Throughput MIC measurements

Minimum inhibitory concentrations (MICs) of all ancestral and evolved strains were determined via an automated broth microdilution approach in accordance with Clinical and Laboratory Standards Institute (CLSI) guidelines. Utilizing 384-well microtiter plates (Greiner), a robotic liquid handling system dispensed 11–16 twofold serial dilutions of each antibiotic into wells containing 60 µL of MHB. Each well was inoculated with a bacterial suspension at 5×10^5 cells/mL. Plates were incubated at 37 °C with continuous shaking (900 RPM, 3 mm throw) for 18 hours, with two biological replicates per strain. Post-incubation, OD_{600} was measured by a Biotek Synergy microplate reader. The MIC was recorded as the lowest antibiotic concentration yielding $OD_{600} < 0.05$ (after subtraction of blank OD readings). Relative MIC for each evolved strain was calculated by dividing its MIC by that of the ancestral strain.

3.6. *In vitro* growth measurements

To evaluate the fitness effects of resistance mutations, growth curves were generated for bacterial variants with available whole-genome sequences. Early stationary-phase cultures were prepared by growing each strain in MHB at 37 °C with shaking (Dunai et al., 2019). Inoculum size of 5×10^4 cells from these cultures were inoculated into 60 µL MHB in 384-well microtiter plates (Greiner), with at least nine replicates per variant (three biological replicates, each with three technical replicates). Plates were incubated at 37 °C under continuous shaking in a BioTek Synergy HL1 microplate reader. Optical density at 600 nm (OD_{600}) was recorded every 5 minutes for 24 hours. From the kinetic growth data, the area under the growth curve (AUC) was calculated over the 24-hour period. AUC serves as an integrated proxy for fitness, incorporating both the exponential growth rate and the final biomass achieved by each strain.

3.7. Whole-genome sequencing and variant analysis

To elucidate genetic changes underlying antibiotic resistance, 2–5 evolved lines from the FoR and ALE experiments were selected for whole-genome sequencing. Resistant populations were grown overnight in antibiotic-free medium, and genomic DNA was isolated using the GenElute Bacterial Genomic DNA Kit (Sigma). DNA was eluted twice in 60 µL RNase-free water, after which 60 µL of the eluate was concentrated using the Zymo DNA Clean & Concentrator Kit. DNA concentration was measured with a Qubit Fluorometer and normalized to 1 ng/µL. Sequencing libraries were constructed with the Nextera XT DNA library preparation kit (Illumina) following the manufacturer's instructions and were sequenced on an Illumina NextSeq 500 platform, generating 2 × 150 bp paired-end reads.

Sequencing reads were mapped to their respective reference genomes using the Burrows–Wheeler Aligner (BWA) (H. Li & Durbin, 2009). PCR duplicates were identified and removed using Picard MarkDuplicates and reads with more than six mismatches were discarded. Single nucleotide polymorphisms (SNPs) and small insertions or deletions (INDELs) were called with Freebayes

(Garrison & Marth, 2012) and filtered via vcffilter (Garrison et al., 2022), retaining only variants with a quality score exceeding 100. All candidate variants were manually inspected using the Integrative Genomics Viewer (IGV) to identify potential artifacts (Robinson et al., 2011). Variants present in the ancestral genome were excluded from further analysis. Mutations found in more than nine independent lines were considered likely ancestral and thus removed; those detected in six to nine lines were also manually reviewed. Variants located within repetitive regions of 40 bp or longer were discarded. Additionally, lines exhibiting mutations in DNA mismatch repair genes (*mutL*, *mutS*, *mutY*) or harboring more than nineteen total mutations (indicative of hypermutator phenotypes) were excluded from downstream analyses.

For eight different strains (*E. coli* ATCC 25922, *K. pneumoniae* ATCC 10031, *A. baumannii* ATCC 17978, *P. aeruginosa* ATCC BAA-3107, *K. pneumoniae* ATCC 700603, *A. baumannii* ATCC BAA-1605, *P. aeruginosa* LESB 58, and *E. coli* NCTC 13846) genomic sequences and annotations were retrieved from the ATCC database or NCBI (accession numbers FM209186.1 and NZ_UFZG00000000.1). All genes, including hypothetical open reading frames, were functionally annotated using PANNZER2 (Törönen et al., 2018; Törönen & Holm, 2022). Orthologous gene groups across these strains were identified with OrthoFinder (version 2.5.4), facilitating cross-strain comparisons of mutation targets (Emms & Kelly, 2015, 2019).

3.8. Comparative mutational analysis

To explore the genomic adaptations associated with different antibiotics, a comparative mutational analysis pipeline was implemented in R (version 4.3.2) (R Core Team, 2022). The clusterProfiler package was used to perform KEGG pathway enrichment analyses on lists of mutated genes, mapping them onto *E. coli* K-12 MG1655 pathways for consistency (Wu et al., 2021). To extend functional insights, these gene lists were merged with Clusters of Orthologous Groups (COG) annotations using the COG database (Tatusov et al., 1997). This combined approach enabled comprehensive profiling of resistance-associated pathways across all evolved lines.

3.9. AcrAB efflux system screening

To investigate the role of AcrAB efflux in antibiotic susceptibility, we compared efflux-deficient and overexpression strains of *E. coli* K-12 BW25113. The Δ*acrB* mutant was generated via P1 transduction according to established protocols, whereas the overexpression strain was constructed by transforming BW25113 with a multicopy plasmid (pUC*acrAB*) encoding the *acrAB* operon; a control strain carried the empty vector pUC118 (Baba et al., 2006; Nishino & Yamaguchi, 2001). The pUC*acrAB* plasmid was kindly provided by Kunihiko Nishino and Akihito Yamaguchi (Osaka University). Because *acrAB* expression is driven by its native promoters on pUC*acrAB*, no external induction was necessary. Antibiotic susceptibility testing was performed using a modified broth dilution method in 96-well microtiter plates containing fresh MHB (or MS medium for SCH) (Wiegand et al., 2008). Ten-step serial

dilutions of each antibiotic were prepared from stock solutions (two wells per concentration per strain). For plasmid-bearing strains, ampicillin (100 µg/mL) was included to maintain the plasmid. Cultures were diluted to 5 × 10^5 CFU/mL prior to inoculation. One column in each plate contained only medium to determine background OD. Plates were incubated at 37 °C with continuous shaking (900 RPM, 3 mm throw) for 18 hours. OD_{600} was measured using a Biotek Synergy 2 microplate reader. MIC was defined as the lowest antibiotic concentration yielding an $OD_{600} < 0.05$ after background subtraction. Relative MIC values were calculated by expressing each strain's MIC on a $\log_2$ scale:

$$\text{relative MIC}_{\text{pUC}acrAB} = log_2 \frac{\text{MIC}_{\text{pUC}acrAB}}{\text{MIC}_{\text{pUC118}}}$$

$$\text{relative MIC}_{\Delta acrB} = log_2 \frac{\text{MIC}_{\Delta acrB}}{\text{MIC}_{\text{wt}}}$$

3.10. Genome-wide overexpression library screening

A genome-wide overexpression screen was conducted using the *E. coli* K-12 ASKA library (pCA24N-$ORF_{GFP[-]}$) to identify genes whose overexpression confers antibiotic resistance (Kitagawa et al., 2005). Frozen aliquots of the pooled ASKA library (GFP minus) in *E. coli* K-12 BW25113 were inoculated into 5 mL MHB supplemented with chloramphenicol (20 µg/mL) and grown at 37 °C until an OD_{600} of approximately 0.8 was reached. For pre-induction, cultures were treated with 50 µM IPTG at 30 °C for 1 hour under constant agitation (200 RPM). The induced cells were then diluted to 5 × 10^5 CFU in 50 µL and evenly spread on MHB agar plates containing 100 µM IPTG, 10 µg/mL chloramphenicol, and an antibiotic concentration gradient (OmniTray format) (Bryson & Szybalski, 1952). Plates were incubated at 37 °C for 24 hours in duplicate. For each antibiotic, a control plate containing an equal number of cells transformed with an empty vector (pCA24N-noORF) was used to establish the inhibition zone in the absence of overexpressed ORFs. Colonies that grew beyond the inhibition zone were visually identified and collected to form a pooled "resistant colony" sample for each antibiotic.

Plasmid DNA was then extracted from each pooled sample using the GeneJET Plasmid Miniprep Kit (Thermo Scientific). To eliminate genomic DNA contamination, 1 µg of plasmid DNA was incubated with Exonuclease I (20 U/µL; 2.5 U total) and Lambda Exonuclease (10 U/µL; 10 U total) in ≤50 µL reaction volume at 37 °C for 30 minutes, followed by heat inactivation at 80 °C for 15 minutes. Digested plasmid DNA was purified using the Zymo DNA Clean & Concentrator Kit. Sequencing libraries were prepared from the purified plasmids with the Nextera XT DNA library preparation kit and assessed for quality on an Agilent BioAnalyzer 2100 (High Sensitivity DNA Chip). Libraries were then sequenced on an Illumina NextSeq 500 system using the NextSeq 500/550 Mid Output Kit v2.5 (300 cycles).

3.11. ORF identification from overexpression library

To pinpoint which ORFs were responsible for antibiotic resistance, raw sequencing reads were processed as follows. First, two 150 bp sequences flanking the plasmid integration site (denoted “E” (end) and “S” (start)) were identified within the fastq files using the Smith–Waterman alignment algorithm (Smith & Waterman, 1981). Reads containing sequence matches to these flanking regions, allowing a Hamming distance of up to 10, were retained. Reads with at least 15 bp alignment to both a plasmid junction (E or S) and the ORF were kept; those failing this criterion were replaced with “dummy” sequences to preserve file integrity. Retained reads were then mapped to the *E. coli* K-12 MG1655 reference genome using BWA with a custom Burrows–Wheeler Transform implementation (H. Li & Durbin, 2009). ORFs were identified as contiguous regions bounded by E and S sequences with ≥15 bp continuous coverage. Each putative ORF was validated by checking for the presence of stop codons and ensuring a minimum length of 15 bp. ORF annotations were assigned by comparing to the genome’s GTF file, prioritizing protein-coding sequences. ORFs exhibiting greater length than the annotated coding sequence were also noted, and identity scores (percentage of identical bases) to the reference CDS were reported.

3.12. Functional metagenomic screens

Functional metagenomic screens were carried out to discover resistance-conferring DNA fragments from environmental and clinical sources. Previously constructed metagenomic libraries captured resistomes from (i) river sediment and soil samples at seven antibiotic-polluted industrial sites in India; (ii) fecal samples from ten healthy European volunteers (five male, five female; ages 26–42; no antibiotic exposure for at least one year); and (iii) a pool of 68 multidrug-resistant clinical isolates (Apjok et al., 2023). Environmental DNA was isolated using the DNeasy PowerSoil Kit (Qiagen), while genomic DNA from clinical isolates was obtained with the GenElute Bacterial Genomic DNA Kit (Sigma). DNA was enzymatically sheared, and fragments ranging from 1.5 to 5 kb were selected to capture full-length resistance genes, although some larger elements may have been excluded. Fragments were cloned into a medium-copy-number plasmid featuring 10-nt barcodes (up- and down-tags) flanking each insert. Resulting library sizes varied from 2 to 6 million clones, with an average insert size of approximately 2 kb.

To screen these libraries, *K. pneumoniae* ATCC 10031 was transformed via DEEPMINE bacteriophage transduction, which employs hybrid T7 phage particles optimized for functional metagenomics in clinical strains (Apjok et al., 2023). For *E. coli* ATCC 25922, electroporation was used. The DEEPMINE protocol was modified by generating hybrid phages lacking gp11, gp12, and gp17 genes, and by utilizing a new phage tail donor plasmid carrying ΦSG-JL2 tail genes and the T7 packaging signal (Daruka et al., 2025; Yosef et al., 2017). Functional selections were conducted on MHB agar plates containing antibiotic gradients; plates were incubated at 37 °C for 24 hours (Kintses et al., 2019;

Szybalski, 1954). Control plates carrying empty metagenomic vectors (no inserts) were used to define baseline inhibition zones. Resistant colonies, identified in regions beyond the inhibition zone, were harvested for plasmid extraction. Plasmid DNA was isolated using the GeneJET Miniprep Kit (Thermo Scientific) and subjected to Exonuclease I and Lambda Exonuclease treatment (as described above) to remove genomic contamination. Purified plasmids were then sequenced by two complementary approaches: Illumina sequencing flanking barcodes and full-length Nanopore sequencing of the inserts and barcodes.

3.13. Annotation of antibiotic resistance genes (ARGs)

To identify and classify ARGs within metagenomic inserts, Nanopore consensus sequences were first matched to corresponding selection experiments using Illumina-derived 8 nt barcodes. Illumina reads were demultiplexed based on these barcodes, and each set was linked to its Nanopore consensus sequence via the unique 10 nt insert barcodes. To minimize redundancy and false positives, contigs were filtered by retaining only barcodes with the highest Nanopore read counts and contigs supported by at least eight Nanopore reads and five Illumina reads. Open reading frames within these contigs were predicted using Prodigal v2.6.3 (Hyatt et al., 2010). Predicted ORFs were annotated via BLASTx (NCBI BLAST v2.12.0) against the CARD and ResFinder databases, applying an E-value cutoff of 10^{-5} (Alcock et al., 2020; Altschul et al., 1990; Bortolaia et al., 2020). ORFs were clustered at 95% identity and coverage using CD-HIT v4.8.1, retaining one representative per cluster (Fu et al., 2012). Inserts were then classified based on the presence of ARGs and whether those ARGs corresponded to the selecting antibiotic. To ensure that host-derived sequences were excluded, ORFs were compared by BLASTp against host proteomes (from UniProt), and any ORF exhibiting more than 80% sequence similarity to a host protein was removed. Finally, the likely origin of each insert was determined by searching Nanopore contigs against the NCBI Prokaryotic RefSeq Genomes database using BLASTn (NCBI BLAST v2.12.0), followed by taxonomic assignment through R and the taxizedb package (Chamberlain S, 2024; Grenié et al., 2023; O'Leary et al., 2016; R Core Team, 2022).

3.14. Phylogenetic and geographic analysis of ARGs

Building upon previous large-scale surveys of *E. coli* resistance, 26,881 *E. coli* genomes were retrieved from the NCBI RefSeq database in February 2022. After filtering for complete metadata, 16,272 genomes were retained (Pursey et al., 2023). *In silico* Clermont phylogrouping was performed using the EzClermont command-line tool, and host plus geographic metadata were extracted from biosample records via Biopython's Bio.Entrez utilities (Clermont et al., 2013; Waters et al., 2020). Hosts were categorized into three groups, *i.e.,* "Human," "Agricultural/Domestic Animals," and "Wild Animals", by applying regular expressions to the host field. Geographic locations were aggregated into 20 subregions based on Natural Earth data. For each genome, a BLASTp search was conducted against the predicted ARG ORFs identified via functional metagenomic screens, with hits requiring ≥90% amino

acid identity and ≥90% query coverage and being present in no more than 10% of the genomes. This analysis enabled mapping of ARG prevalence across host types, phylogroups, and geographic regions.

3.15. Quantifying bacterial survival under antibiotic exposure

Killing kinetics for each antibiotic were measured by exposing bacterial cultures to antibiotics in 96-well deep-well plates and quantifying viability after four hours via microplating CFU counts and/or fluorescent viability staining (Lázár et al., 2022). First, single colonies of each strain (including YFP- and mCherry-tagged *E. coli*, *K. pneumoniae*, and *A. baumannii*) were grown overnight in MHB at 37 °C with shaking (160 RPM), with chloramphenicol (10 µg/mL) added for plasmid maintenance in fluorescent *E. coli*. Overnight cultures were diluted 1:5000 in fresh MHB and grown to an OD_{600} of 0.25. Cells were then concentrated by centrifugation and aliquoted into 50 µL glycerol stocks (~2.2×10^9 cells), which were stored at –80 °C. To prepare assay plates, 235 µL MHB (or MS for SCH) was dispensed into each well of a 96-well plate, and antibiotics were added using a Tecan D300e digital dispenser to create a 12-step dilution series ranging from 0.5× to 30× MIC. For single-dose clearance assays, antibiotics were prepared at 10× MIC in at least three technical replicates per strain–antibiotic pair. No-cell and no-antibiotic wells were included as negative and positive controls, respectively.

For dose–response assays involving fluorescent *E. coli*, frozen YFP- and mCherry-expressing stocks were thawed, mixed in a 1:1 ratio, and diluted 1:1000 in 30 mL MHB; cultures were incubated at 37 °C, 160 RPM for 45 minutes to recover. Fifteen microliters of this suspension (~10^7 CFU) were then inoculated into each antibiotic-containing well (total volume 250 µL). For single-dose clearance assays of *E. coli*, *K. pneumoniae*, and *A. baumannii*, frozen stocks of each strain were thawed, diluted 1:1000 in 30 mL MHB, and grown to OD_{600} = 0.25 at 37 °C, 160 RPM; 15 µL (~10^7 CFU) were transferred into each 10× MIC well. Plates were incubated for 4 hours at 37 °C with shaking (160 RPM).

Following antibiotic exposure, dose–response samples were serially diluted fivefold in phosphate-buffered saline (PBS), cells were washed three times (centrifugation at 4,500 RPM, 15 minutes, 4 °C; resuspension in PBS) to remove residual antibiotic, and 8 µL microdrops of each dilution (undiluted to 5^{-8}) were plated onto OmniTray plates containing 45 mL of 70% MHB agar. Plates were incubated for 18 hours at 37 °C. Post-incubation, plates were imaged for YFP fluorescence (excitation 500 ± 10 nm, emission 606 ± 94 nm), mCherry fluorescence (excitation 556 ± 24 nm, emission 690 ± 100 nm), and brightfield using a custom macroscope equipped with a Basler a2A840-45ucPRO camera. Colonies were manually counted to determine CFU/mL based on dilution factors. For single-dose clearance assays, viable cell counts were obtained by staining with the QUANTOM™ Viable Cell Staining Kit and using the QUANTOM Tx™ Microbial Cell Counter (Logos Biosystems) according to the manufacturer's instructions.

3.16. Statistics and reproducibility

All experiments were conducted with a minimum of two independent replicates to ensure data reliability. No sample size was predetermined using statistical methods. Experiments were neither random nor performed under blind conditions. Data processing and statistical analyses were undertaken in R (version 4.3.2). The tidyverse packages (*e.g.*, dplyr, ggplot2, readr) were used for data manipulation and visualization, while statistical tests were conducted using base R's stats package and rstatix. KEGG pathway annotations of gene lists were generated via the clusterProfiler package. Dose–response curves were plotted in MATLAB. Unless otherwise stated, all statistical tests were two-tailed, with a significance threshold set at $p < 0.05$.

4. Results

4.1. Antibiotic classification

First, we classified 16 antibiotics used in this study based on (i) their number of targets in bacterial physiology and (ii) whether they permeabilize the bacterial membrane (Table 2). We assigned antibiotics as single or dual target based on the literature. Next, we tested membrane permeabilization using the *N*-phenyl-1-naphthylamine (NPN) uptake assay. Drugs that disrupted the membrane caused a rapid increase in fluorescence compared with other antibiotics (Fig. 7). Accordingly, we further classified antibiotics as permeabilizers or non-permeabilizers. Together, this yielded four categories defined by target number and membrane activity (Fig. 8).

Table 2. This table lists all antibiotics tested, organized by their mode of action. We distinguish four groups: single-target non-permeabilizers, dual-target non-permeabilizers, single-target permeabilizers, and dual-target permeabilizers. Compounds marked with an asterisk (tridecaptin M152-P3, POL7306, and SCH79797) are in pre-clinical development and belong to the dual-target permeabilizer category.

Antibiotic	Abbreviation	Antibiotic Class	Mode of action group	Date of approval/clinical phase
Omadacycline	OMA	Tetracyclines	Single target non-permeabilizers	2018
Eravacycline	ERA			2018
Doxycycline	DOX			1967
Apramycin	APR	Aminoglycosides		Phase 1
Gentamicin	GEN			1964
Sulopenem	SUO	Carbapenems		Phase 3
Meropenem	MER			1996
Delafloxacin	DEL	Topoisomerase inhibitors	Dual target non-permeabilizers	2017
Gepotidacin	GEP			Phase 3
Zoliflodacin	ZOL			Phase 3
Moxifloxacin	MOX			1999
Tridecaptin M152-P3	TRD*	Targeting membrane integrity and an additional cellular pathway	Dual target permeabilizers	pre-clinical
POL7306	POL*			pre-clinical
SCH79797	SCH*			pre-clinical
SPR206	SPR	Polymyxins	Single target permeabilizers	Phase 2
Polymyxin B	PMB			1964

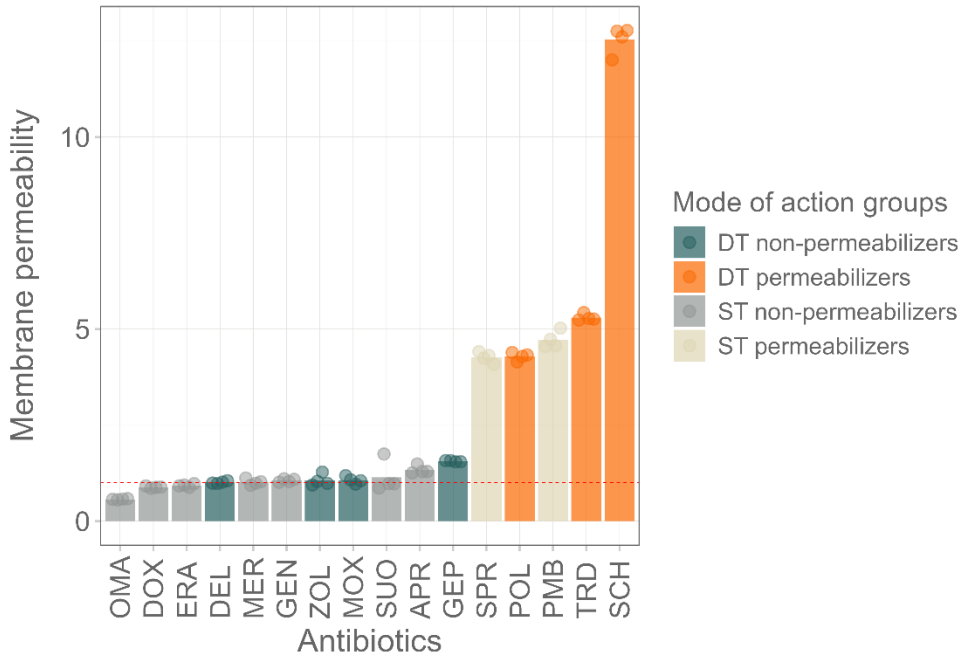

Figure 7. Antibiotic induced membrane permeabilization. Barplots show four replicates per antibiotic with NPN fluorescence (normalized to control) after 4× MIC exposure in *E. coli* ATCC 25922. The fluorescence intensity of NPN increased due to the permeabilization of the bacterial outer membrane by SCH79797 (SCH), tridecaptin M152-P3 (TRD), POL7306 (POL), SPR206 (SPR) and polymyxin B (PMB). The dashed line marks mean control fluorescence.

In the first category, we grouped three preclinical antibiotics: tridecaptin M152-P3, POL7306, and SCH-79797, all of which permeabilize the outer membrane and are proposed to act through dual mechanisms. We refer to these as dual-target (DT) permeabilizers, which serve as our primary study group based on the hypothesis that the most effective antibiotic development strategies will combine multiple mechanisms of action with a particular emphasis on membrane disruption. The remaining three categories function as control groups. The second category consists of peptide-based antibiotics such as polymyxin B and SPR206, which act primarily through membrane lysis, and are designated single-target (ST) permeabilizers. Conventional antibiotics with a single intracellular target that do not disrupt the membrane were classified as ST non-permeabilizers. Finally, antibiotics with dual-target mechanisms that lack membrane-permeabilizing activity and largely represented by topoisomerase inhibitors were classified as DT non-permeabilizers. This classification provides a systematic framework to compare how different target specificity and amount together with membrane disruption influence the likelihood of resistance evolution across four Gram-negative species (Maharramov et al., 2025).

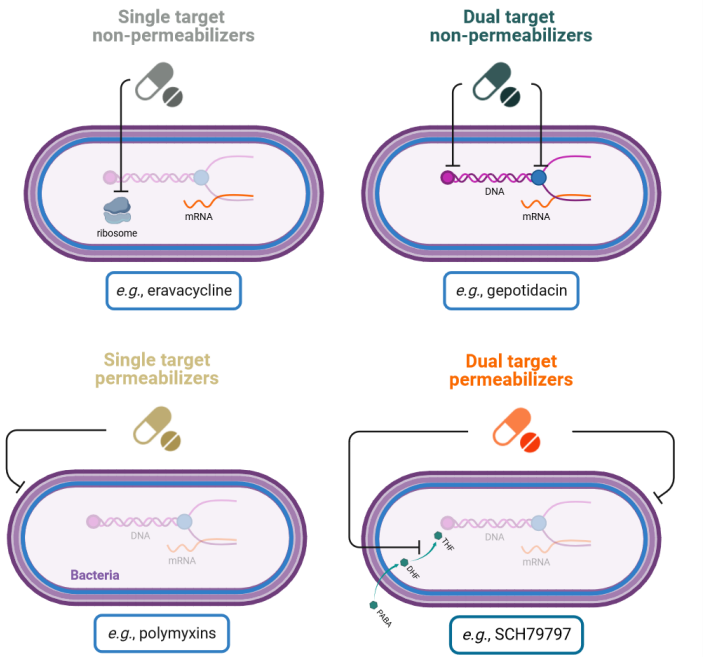

Figure 8. Overview of the four primary mode-of-action categories. This schematic illustrates representative mechanisms for each antibiotic group. Reproduced from Maharramov et al., 2025.

4.2. Short-term resistance development measured by frequency of resistance

To assess how readily bacteria develop resistance to various antibiotics, we evaluated one multidrug-resistant strain and one antibiotic-sensitive strain each of *Escherichia coli*, *Klebsiella pneumoniae*, *Acinetobacter baumannii*, and *Pseudomonas aeruginosa*. Building on previously established protocols for measuring spontaneous resistance frequencies (FoR assays) at multiple antibiotic concentrations, we first excluded any antibiotic–strain combination that exhibited reduced baseline susceptibility (MIC > 4 µg/mL) (Bell & MacLean, 2018; Daruka et al., 2025; Ling et al., 2015; Luria & Delbrück, 1943; Nyerges et al., 2020). For the remaining combinations, approximately 10^{10} cells of each strain were plated on agar containing a concentration of the antibiotic to which the strain was initially susceptible and incubated for two days. To quantify resistance, we compared the minimum inhibitory concentration (MIC) of any emerging mutants to that of the corresponding wild-type strain, expressing this as a relative MIC. Across all four species, resistance emerged rapidly when strains were exposed to ST permeabilizers, DT non-permeabilizers, or ST non-permeabilizers.

In sharp contrast, DT permeabilizers exhibited a markedly low likelihood of resistance development. Specifically, populations challenged with POL7306, tridecaptin M152-P3, or SCH79797 showed, on average, less than a fourfold increase in resistance levels (Fig. 9).

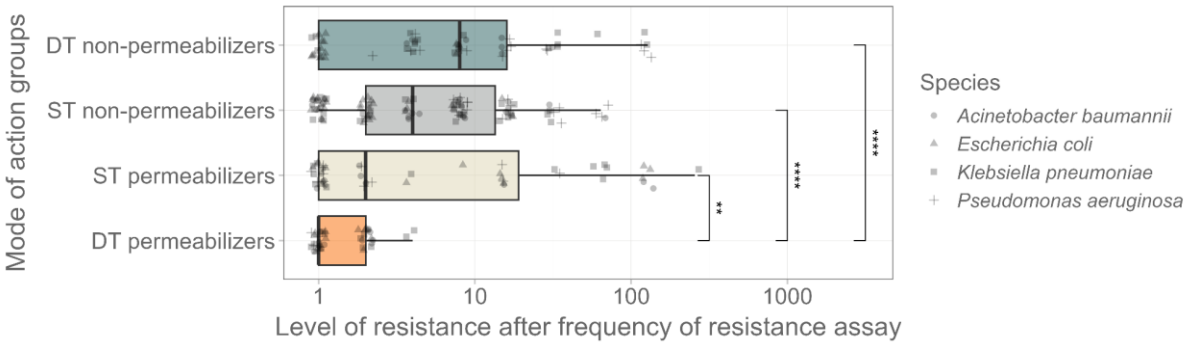

Figure 9. Resistance levels after the frequency-of-resistance assay. Each point corresponds to one lineage derived from the FoR assay, with different shapes denoting distinct bacterial species. Resistance is expressed as the relative MIC. A Kruskal–Wallis test ($\chi^2 = 28.312$, df = 3, $p < 0.0001$) indicates significant differences among the four antibiotic categories. Pairwise comparisons (Dunn's post hoc with Benjamini–Hochberg correction) revealed that DT permeabilizers exhibit significantly lower resistance increases compared to the other groups (**, $p < 0.01$; ****, $p < 0.0001$). Non-significant comparisons are omitted for clarity. Adapted from Maharramov et al., 2025.

By comparison, resistance to polymyxin B increased by more than 128-fold in the *A. baumannii* multidrug-resistant strain and in the *E. coli* and *K. pneumoniae* sensitive strains exposed to SPR206 (Fig. 10). It is noteworthy that no resistant mutants arose for polymyxin B in the *A. baumannii* and *K. pneumoniae* sensitive strains, nor in the multidrug-resistant *E. coli* strain. However, because FoR assays cannot detect exceedingly rare mutations or combinations thereof, they may underestimate the bacterial potential for resistance (Bell & MacLean, 2018). Consequently, it was essential to determine how prolonged antibiotic exposure influences resistance evolution.

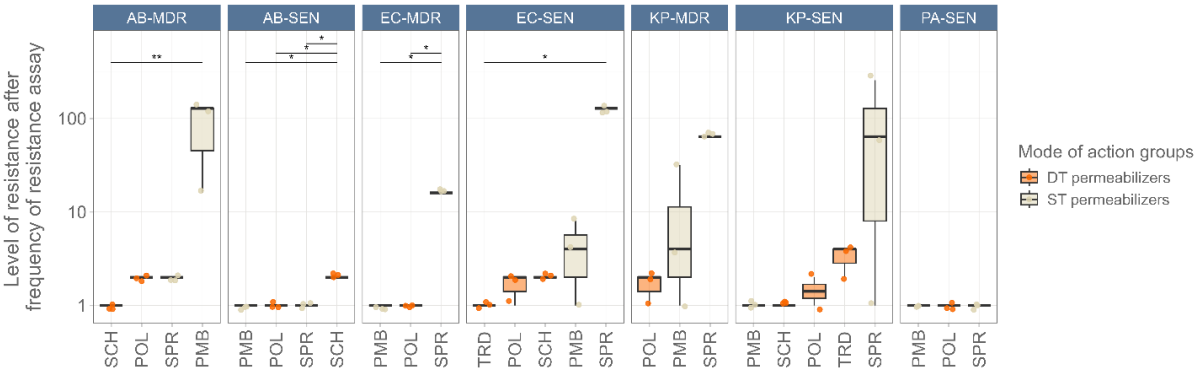

Figure 10. Resistance levels after FoR assay, by strain. Comparison of DT and ST permeabilizer resistance level is shown for each strain. Level of resistance indicates fold-change in relative MIC from FoR assays. Each point represents a single evolved line. Dunn's post hoc test (Benjamini–Hochberg correction) indicates significant differences: **, $p < 0.01$; *, $p < 0.05$. Abbreviations: *A. baumannii* (AB), *E. coli* (EC), *K. pneumoniae* (KP), and *P. aeruginosa* (PA), while MDR and SEN are multidrug resistant and sensitive strains, respectively.

4.3. Adaptive laboratory evolution to measure resistance emergence under prolonged antibiotic exposure

Next, we subjected the same collection of strains to adaptive laboratory evolution (ALE), aiming to maximize resistance over a longer, but fixed, timeframe (Daruka et al., 2025). As expected, ALE produced substantially higher resistance levels than those observed in FoR assays.

Remarkably, however, the resistance achieved against DT permeabilizers remained significantly lower than that seen for all other antibiotic classes (Fig. 11). For instance, after 60 days of continuous evolution, the maximal increase in resistance was only fourfold for *A. baumannii* and the *E. coli* sensitive strain exposed to SCH79797, whereas lineages evolved against polymyxin B exhibited more than a 1,024-fold increase in resistance.

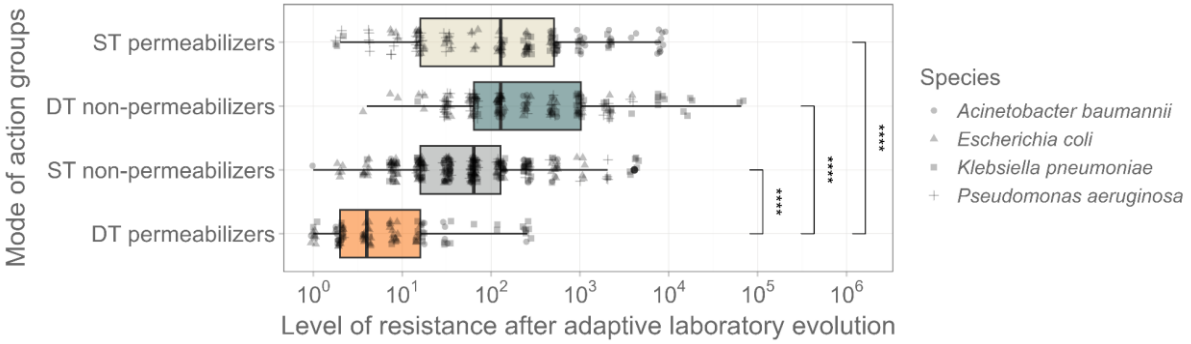

Figure 11. Level of resistance after adaptive laboratory evolution. Resistance levels were assessed by using relative MIC values calculated by dividing the MIC of the evolved line by that of the corresponding ancestor. Each data point represents a distinct adaptive laboratory evolved line, with species differentiation denoted by shape. Significant variation in resistance levels was observed across different modes of action groups (Kruskal-Wallis test, chi-squared = 205.014, df = 3, $p < 0.0001$). All pairwise comparisons between groups showed significant differences (Dunn's post-hoc test with Benjamini-Hochberg correction, **** indicates $p < 0.0001$). To reduce redundancy, *p*-values from comparisons involving other than the DT permeabilizers were excluded. Adapted from Maharramov et al., 2025.

When we analyzed antibiotic–strain pairs individually, DT permeabilizers displayed significantly lower median resistance levels than ST permeabilizers in 69% of comparisons (Fig. 12), and there were no cases in which an ST permeabilizer yielded lower relative MICs than any DT permeabilizer.

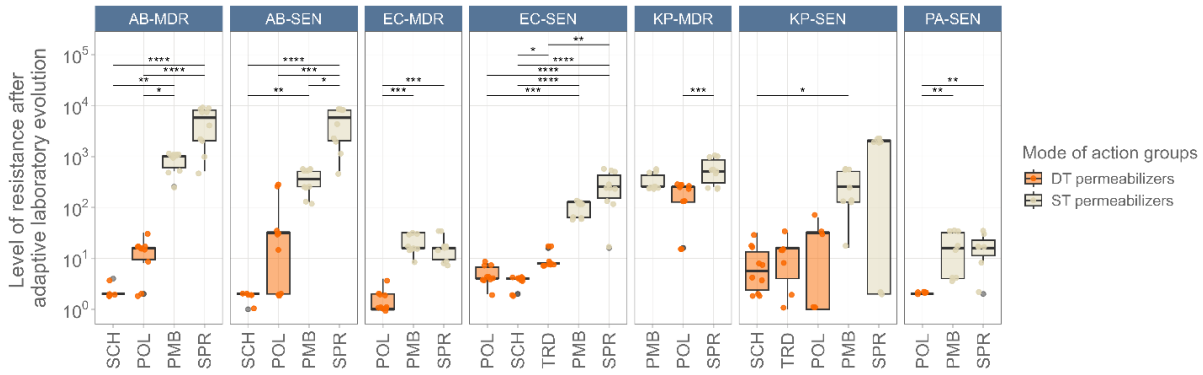

Figure 12. Resistance levels after ALE for DT and ST permeabilizers, by strain. This panel presents the level of resistance as relative MIC after ≈60 days of ALE for each strain (AB, EC, KP, PA; MDR and SEN). Each point is one evolved line. Dunn's post hoc tests (Benjamini–Hochberg correction) indicate significance levels: ****, $p < 0.0001$; ***, $p < 0.001$; **, $p < 0.01$; *, $p < 0.05$.

Notably, the capacity to evolve resistance to POL7306 and to SCH79797 varied substantially among species (Fig. 13). For example, *A. baumannii* evolved elevated resistance only to POL7306, whereas *K. pneumoniae* increased resistance to both POL7306 and SCH79797.

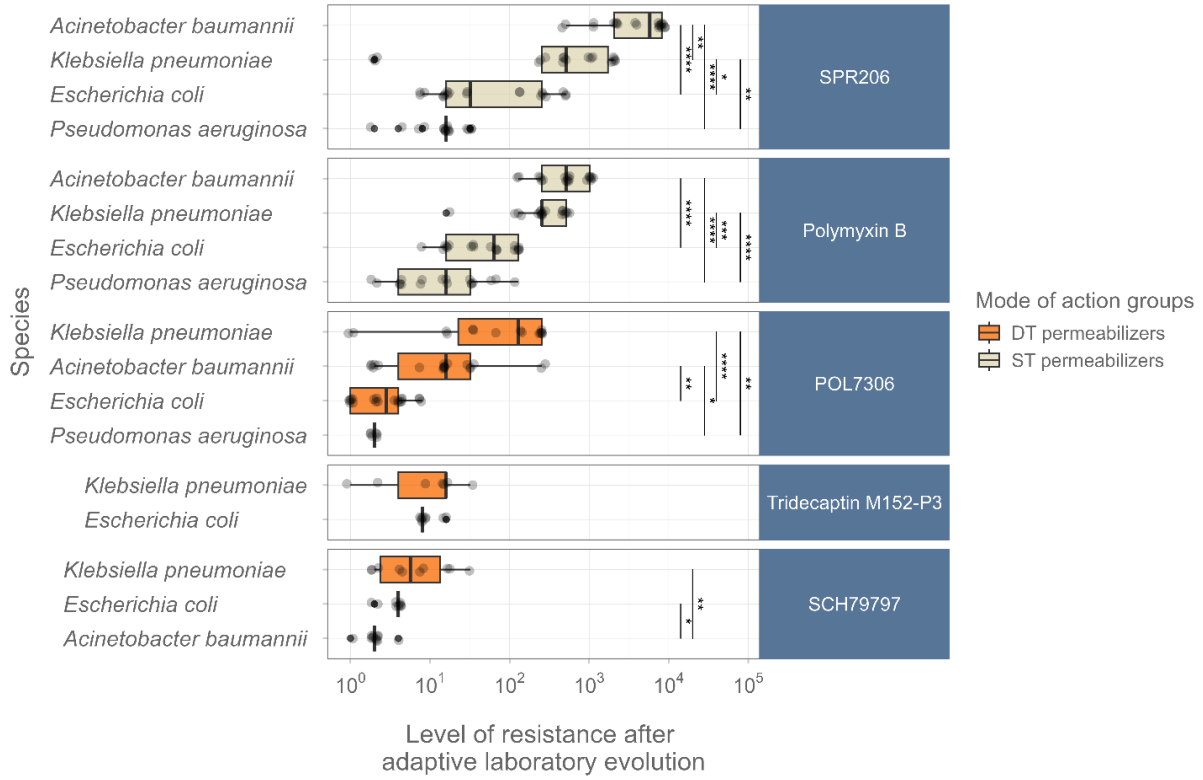

Figure 13. Species-specific resistance patterns after adaptive evolution. Here, each point represents one evolved lineage; shapes denote species. Relative MIC is plotted for each strain–antibiotic combination that had initial susceptibility (MIC ≤ 4 µg/mL). Species-level variation was significant for POL7306 (Kruskal–Wallis $\chi^2 = 25.6$, df = 3, $p < 0.0001$) and for SCH79797 ($\chi^2 = 11.86$, df = 2, $p < 0.01$). Specifically, *A. baumannii* and *K. pneumoniae* exhibited higher resistance to POL7306, whereas *K. pneumoniae* showed increased resistance to SCH79797. Pairwise comparisons via Dunn's post hoc tests (Benjamini–Hochberg correction) indicate significance levels: ****, $p < 0.0001$; ***, $p < 0.001$; **, $p < 0.01$; *, $p < 0.05$.

Because *P. aeruginosa* exhibited reduced initial susceptibility (MIC > 4 µg/mL) to other DT permeabilizers, only POL7306 was evaluated in that species. Overall, resistance levels attained via ALE remained significantly lower for DT permeabilizers than for ST permeabilizers (Dunn's post hoc test with Benjamini–Hochberg correction, $p < 0.01$).

4.4. Fitness cost of resistance evolution

In natural settings, the emergence of antibiotic resistance is often constrained by the associated fitness cost (Melnyk et al., 2015). To examine this constraint, we measured *in vitro* growth of 385 antibiotic-adapted lines (all of which exhibited elevated resistance after ALE) and their corresponding ancestors in antibiotic-free medium. If resistance evolution were limited by deleterious effects on growth, one would expect a negative correlation between fitness and resistance level (Melnyk et al., 2015). Indeed, for two DT permeabilizers, such as SCH79797 and tridecaptin M152-P3, we observed significant negative correlations between resistance and fitness (Pearson's $R = -0.79$ and -0.55, respectively; $p < 0.05$; Fig. 14). Interestingly, two ST non-permeabilizers, apramycin sulfate and eravacycline, also displayed similarly strong negative correlations (Pearson's $R = -0.74$ and -0.55, respectively; $p < 0.05$; Fig. 14).

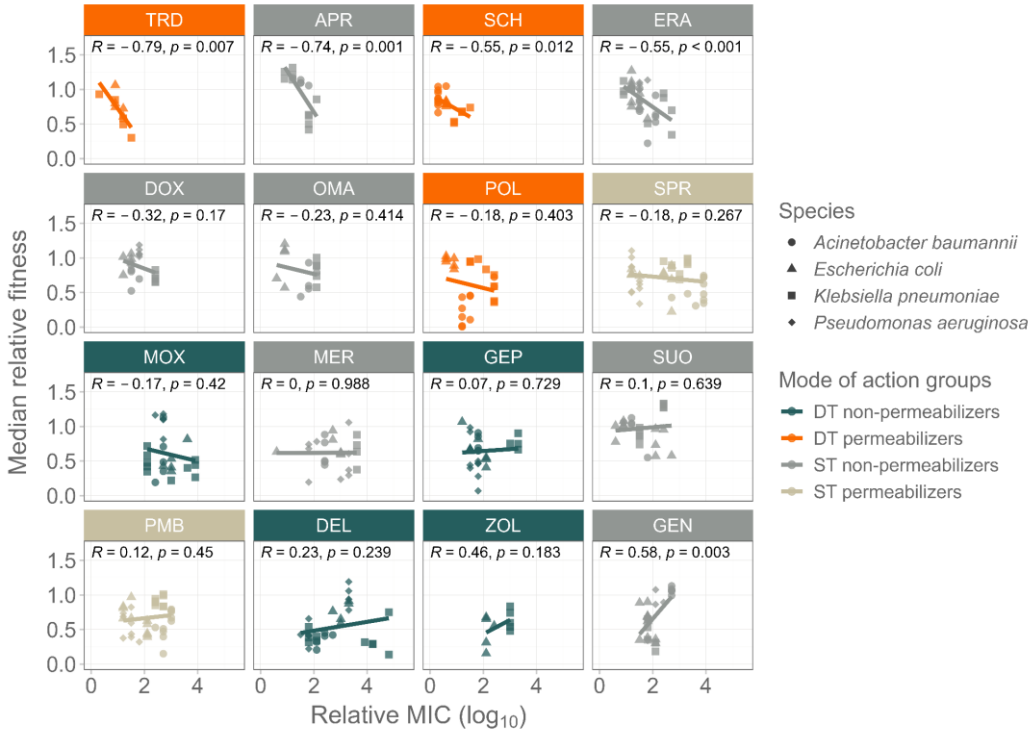

Figure 14. Correlation between evolved resistance and fitness. Each point represents one of the 385 ALE-adapted lines; colors indicate the mode-of-action group to which the line was adapted. The x-axis shows $\log_{10}$ relative MIC, and the y-axis displays median relative fitness. Relative fitness calculated as area under the growth curve of the evolved line divided by that of the ancestor, measured in antibiotic-free medium. For correlation analysis Pearson method (R) was used. Reproduced from Maharramov et al., 2025.

4.5. Resistance mechanisms to dual-target permeabilizers

We next examined the non-synonymous mutations accumulated during laboratory evolution, focusing on lines adapted to DT permeabilizers versus those adapted to other antibiotic classes. Notably, the set of mutated genes in DT permeabilizer–adapted lines was largely distinct from those in lines adapted to ST permeabilizers (Fig. 15). In fact, 80% of mutated genes were antibiotic-specific, and no single mutation was shared across all five antibiotics examined (Fig. 16). POL7306, in particular, showed a higher proportion (8.12%) of overlap with ST permeabilizer–associated mutations than did tridecaptin M152-P3 (2.5%) or SCH79797 (0.6%), consistent with POL7306's structural and functional similarity to polymyxin B (Luther et al., 2019).

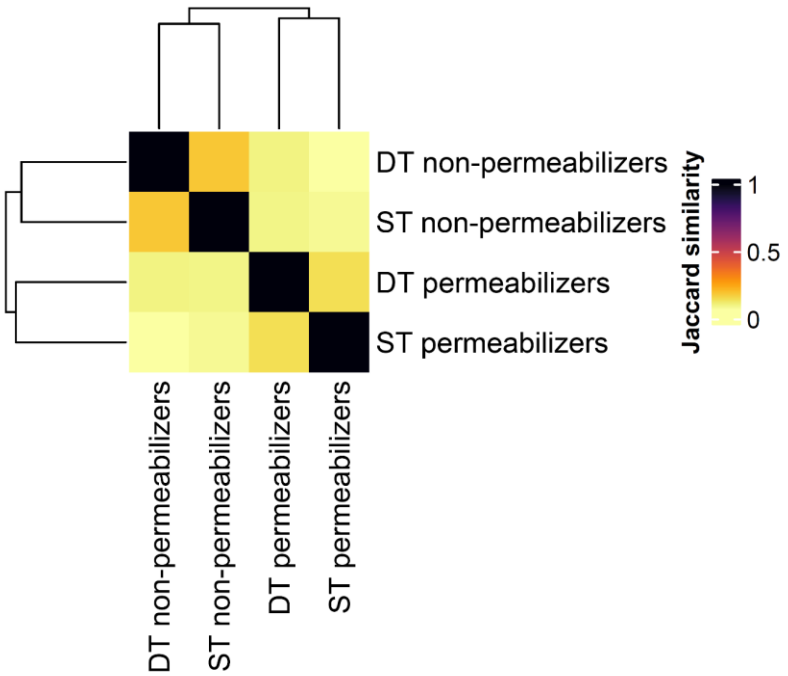

Figure 15. Similarity of mutational profiles across mode-of-action groups. This heatmap illustrates pairwise Jaccard similarity scores for genes mutated during ALE in response to antibiotics from different mode-of-action groups. Scores range from 0 (yellow, no overlap) to 1 (black, complete overlap). Antibiotics are clustered (complete linkage) based on Euclidean distances between mean Jaccard scores, highlighting which groups share more common mutational targets.

Several genes involved in cell envelope biogenesis and regulation were repeatedly mutated in lines adapted to SPR206, polymyxin B, POL7306, and tridecaptin M152-P3 (Fig. 17). For example, the two-component sensor system BasS–BasR and the outer membrane phospholipase PldA were mutated in response to polymyxin B, SPR206, and POL7306. Mutations in PhoPQ family members (*phoQ* and *qseC*) and in *lpxA*, which are critical for lipopolysaccharide (LPS) and lipid A biosynthesis, were found exclusively in lines adapted to ST permeabilizers (Khunsri et al., 2023; Theuretzbacher et al., 2023). In tridecaptin M152-P3–adapted lines, we also observed mutations in genes related to LPS

biosynthesis/regulation (*e.g., lptD*) and phospholipid trafficking (*e.g., mlaA*) (Balibar & Grabowicz, 2015; Grabowicz et al., 2013; Gu et al., 2015; Kaur & Mingeot -Leclercq, 2024; Lo Sciuto et al., 2018).

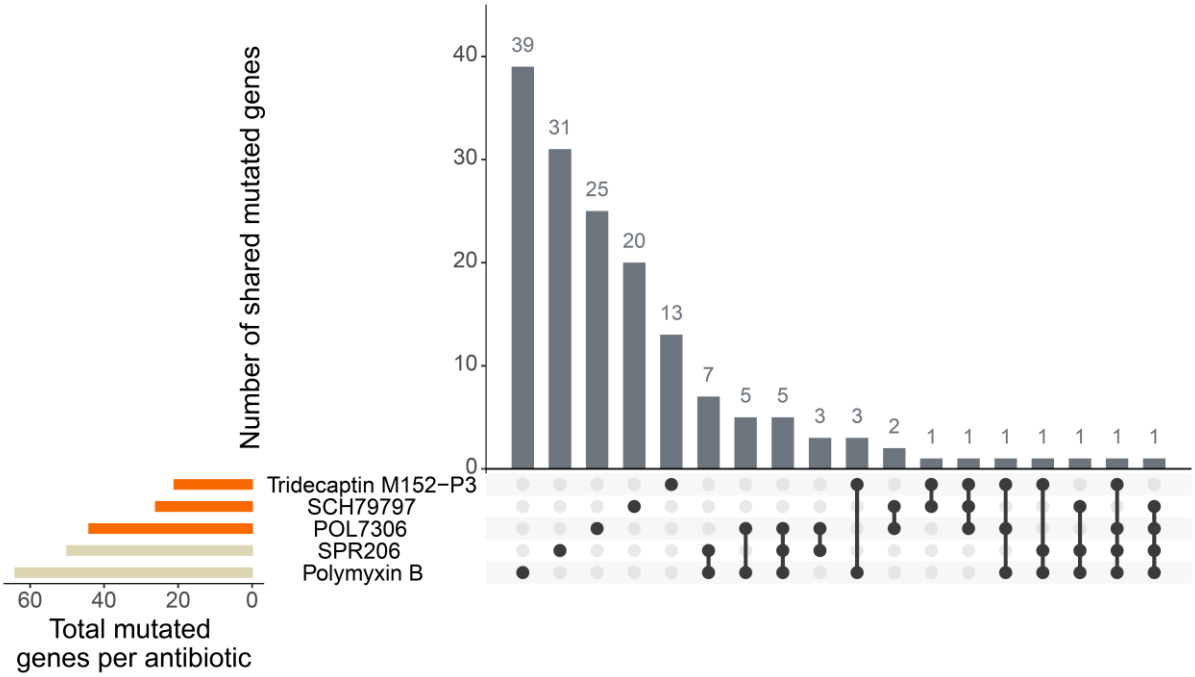

Figure 16. Overlap of frequently mutated genes among permeabilizer antibiotics. This plot depicts the number of protein-coding genes that acquired non-synonymous mutations in lines evolved to five membrane-targeting antibiotics: two ST permeabilizers (polymyxin B, SPR206) and three DT permeabilizers (SCH79797, tridecaptin M152-P3, POL7306). Horizontal bars at left indicate the total number of mutated genes per antibiotic. Vertical bars show the number of genes shared by the connected antibiotics (dots). Single dots correspond to genes mutated exclusively in one antibiotic's evolved lines. Overall, 80% of mutated genes (128 genes) are unique to a single antibiotic, and no gene was mutated across all five antibiotics. Adapted from Maharramov et al., 2025.

By contrast, lines adapted to SCH79797 carried mutations in *acrR*, the repressor of the AcrAB-TolC multidrug efflux pump (Fig. 17; Baquero & Alenazy, 2022; Blanco et al., 2016). Given that SCH79797 is a small molecule with an intracellular target, it is plausible that it is exported via AcrAB-TolC, thus yielding moderate resistance.

To test this hypothesis, we constructed isogenic *E. coli* strains with either overexpressed or inactivated AcrAB-TolC and measured susceptibility to a broad panel of antibiotics, including DT permeabilizers. As expected, modulating efflux pump activity affected susceptibility to various antibiotics, that are both DT non-permeabilizers and SCH79797, but had no impact on sensitivity to POL7306, tridecaptin M152-P3, or polymyxin B (Fig. 18).

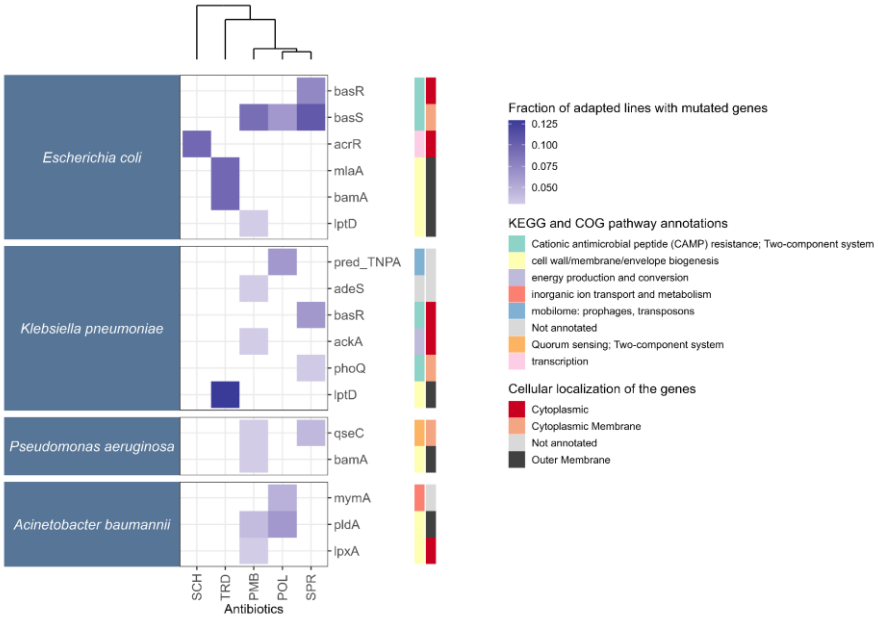

Figure 17. Functional and subcellular localization of commonly mutated genes in permeabilizer-adapted lines. This multi-panel heatmap focuses on genes mutated in at least three independent lines for each permeabilizer antibiotic. The main panel (left) shows the fraction of sequenced lines in which each gene was mutated (number of lines mutated / total lines sequenced for that antibiotic). Genes (rows) are grouped by cellular localization (per PSORT: *e.g.*, inner membrane, periplasm, cytoplasm) and by functional category according to KEGG pathways and COG classifications (displayed in the right panels). A hierarchical clustering dendrogram (average linkage) at top clusters antibiotics based on similarity of their mutational profiles. This composite visualization highlights patterns of gene involvement in cell envelope biogenesis, stress response, and other pathways relevant to resistance against ST and DT permeabilizers. Adapted from Maharramov et al., 2025.

Figure 18. Effect of AcrAB-TolC efflux pump modulation on antibiotic susceptibility. This bar graph compares MIC changes as level of resistance ($\log_2$ scale) for *E. coli* strains with either deletion of *acrB* (Δ*acrB* = red bars) or overexpression of acrAB (pUC*acrAB* = blue bars) relative to wild-type (BW25113). Each antibiotic's bar represents the average of three biological replicates, with error bars showing ±1 standard deviation. Negative $\log_2$ values (bars below zero) indicate increased susceptibility, whereas positive values indicate increased resistance. While overexpression or deletion of AcrAB-TolC significantly affects susceptibility to several antibiotics, it does not alter sensitivity to any of the ST or DT permeabilizer antibiotics, except for a modest impact on SCH79797. Reproduced from Maharramov et al., 2025.

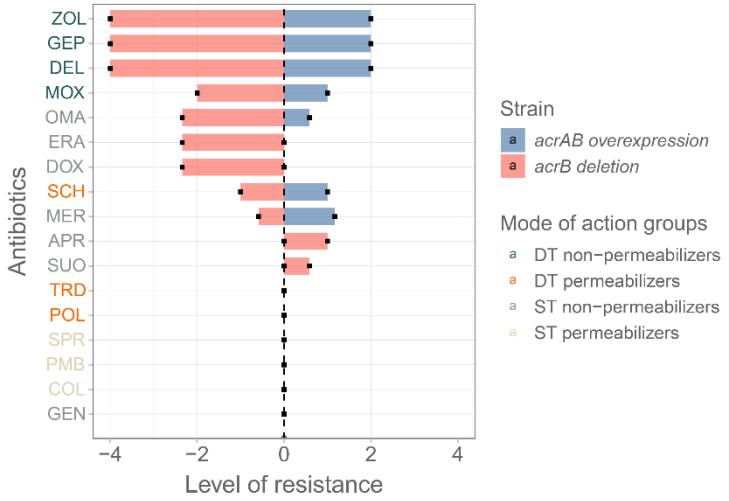

4.6. Cross-resistance of polymyxin adapted lines

To explore potential cross-resistance among membrane-targeting antibiotics, we selected 12 polymyxin B–resistant ALE lines and measured their susceptibilities to ST permeabilizers (SPR206, colistin) and to DT permeabilizers (SCH79797, tridecaptin M152-P3, POL7306). While polymyxin B resistance conferred cross-resistance to SPR206 and colistin, no change in susceptibility was observed for SCH79797 or tridecaptin M152-P3 (Fig. 19).

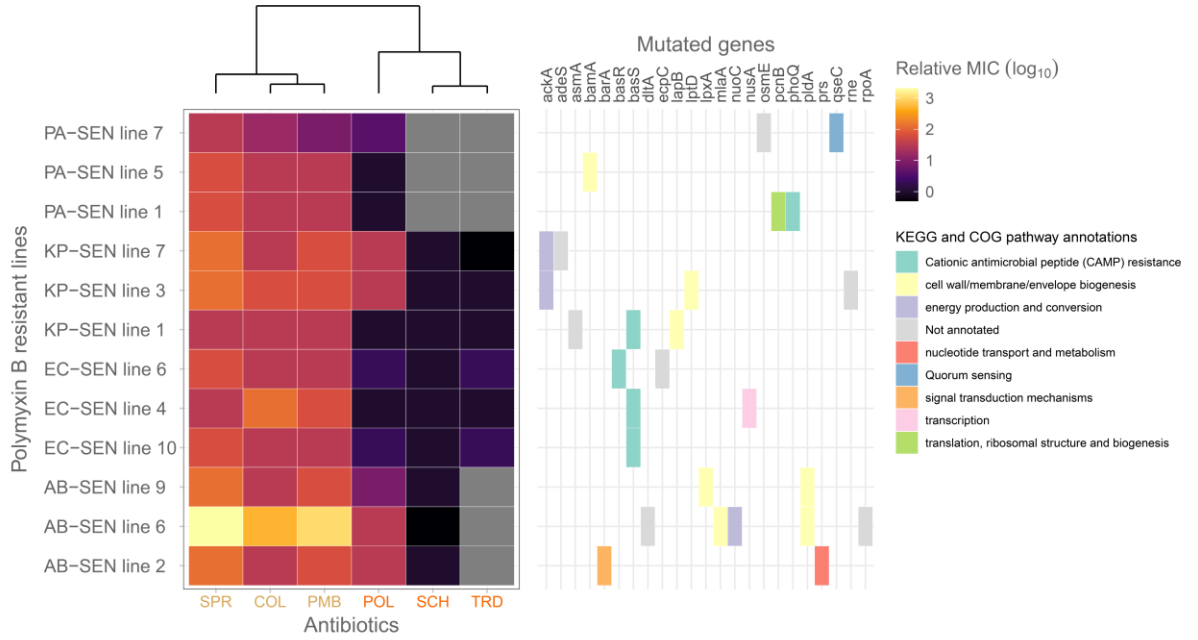

Figure 19. Cross-resistance profile of polymyxin B-resistant lines. This heatmap displays $\log_{10}$(relative MIC) = $MIC_{evolved}$ / $MIC_{ancestor}$ for twelve polymyxin B-resistant ALE lines (three independent lines per species: *E. coli* (EC), *K. pneumoniae* (KP), *A. baumannii* (AB), *P. aeruginosa* (PA)) against three ST permeabilizers (polymyxin B [PMB], colistin [COL], SPR206 [SPR]) and three DT permeabilizers (SCH79797 [SCH], tridecaptin M152-P3 [TRD], POL7306 [POL]). Gray cells indicate combinations not tested due to intrinsic resistance. To the right, a secondary heatmap annotates whether each PMB-resistant line harbors mutations in specific genes, with pathways grouped by KEGG and COG categories. Clustering (complete linkage, Euclidean distance) organizes antibiotics by similarity in cross-resistance profiles. PMB-resistant lines display cross-resistance to SPR206 and colistin but retain susceptibility to SCH79797 and tridecaptin M152-P3. Reproduced from Maharramov et al., 2025.

A subset of polymyxin B–resistant lines ($n = 7$) exhibited modestly reduced susceptibility to POL7306, but these changes were far less pronounced than those seen with SPR206 and colistin (Fig. 20) and were observed only in *K. pneumoniae* and *A. baumannii* (Fig. 19). These results indicate that resistance mechanisms against DT permeabilizers in development have limited overlap both among themselves and with those of other peptide-based antibiotics that primarily target the outer membrane, such as polymyxin B and SPR206.

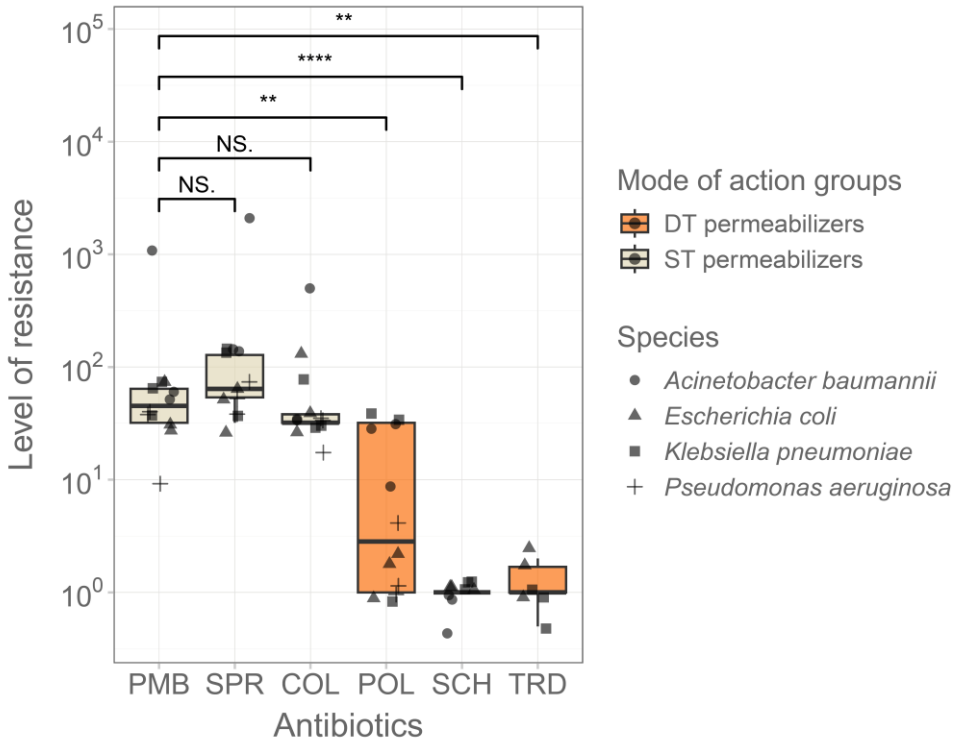

Figure 20. Cross-resistance of polymyxin B-resistant lines to other permeabilizers. Boxplots summarize relative MICs as level of resistance for twelve polymyxin B-resistant ALE lines tested against PMB, colistin (COL), SPR206 (SPR), and DT permeabilizers (SCH, TRD, POL). Each point is one evolved line. Dunn's post hoc test (Benjamini–Hochberg correction) reports significance: **, $p < 0.01$; ****, $p < 0.0001$; "NS" indicates not significant ($p > 0.05$). PMB-resistant lines show similar resistance levels to PMB, COL, and SPR, but no significant resistance to DT permeabilizers.

4.7. Resistance to dual-target permeabilizers by gene amplification is limited

Gene amplification can rapidly increase resistance by boosting the expression of resistance-conferring genes (Sandegren & Andersson, 2009). To investigate whether gene dosage effects could confer resistance to DT permeabilizers, we employed the ASKA library, which contains every *E. coli* open reading frame (ORF) cloned individually into an expression vector (Kitagawa et al., 2005). The pooled library was introduced into *E. coli*, and populations were challenged with rising antibiotic concentrations in standard drug-diffusion assays (Bryson & Szybalski, 1952; Spohn et al., 2019). Overall, the amplification of specific ORFs from the ASKA library yielded up to an eightfold increase in resistance for several antibiotics, indicating that gene amplification can contribute substantially to resistance. Sequence analysis of resistant clones identified 67 genes whose elevated expression reduced susceptibility to multiple drugs; many encode transcriptional regulators, including well-known MDR regulators such as *marA* and *soxS* (Barbosa & Levy, 2000; S. P. Cohen et al., 1993; R. G. Martin et al., 1996; Reyes-Fernández & Schuldiner, 2020), as well as stringent response factors *ytfK* and *dksA* (Germain et al., 2019; Wang et al., 2018). Crucially, however, the ASKA library screen did not reveal any ORFs whose overexpression conferred notable resistance to either DT or ST membrane permeabilizers (Fig. 21).

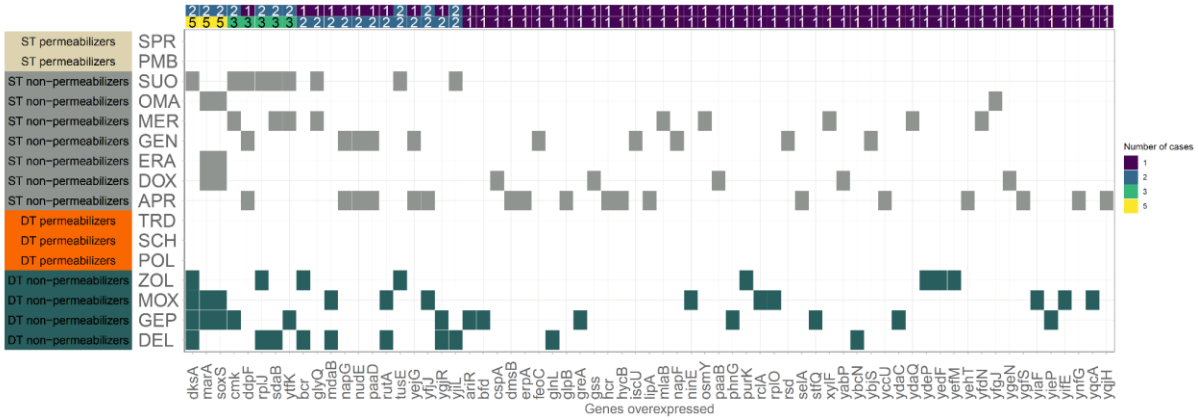

Figure 21. Genes whose overexpression reduces antibiotic susceptibility. This heatmap summarizes findings from ASKA library overexpression screen. The leftmost column indicates mode-of-action group for each antibiotic. Horizontal bars at the bottom show how many antibiotics a given gene affects when overexpressed (*i.e.*, reduces susceptibility). Vertical bars depict how many genes confer reduced susceptibility to each antibiotic group. Only genes meeting a ≥1% read-coverage threshold in each screen are included. Adapted from Maharramov et al., 2025.

This suggests that, although gene amplification can enhance resistance to some antibiotics, it does not substantially protect against membrane-targeting permeabilizers. It remains possible that overexpression of certain genes, alone or in combination, could modestly improve growth under sublethal antibiotic levels, but such effects were not detected in our screens.

4.8. Mobile resistance genes to dual-target permeabilizers are rare in the environment

Next, we explored the prevalence of mobile resistance genes that confer protection against the antibiotics studied here, using functional metagenomic libraries derived from soil, gut, and clinical microbiomes (Apjok et al., 2023). In total, 1,045 unique contigs were found across all antibiotics that caused decreased susceptibility. These unique contigs contained total of 539 non-redundant open reading frames (ORFs). For DT permeabilizers, only 4.2% of contigs were retrieved (17 for SCH79797 and 27 for POL7306). When comparing the number of resistance-conferring fragments across drug classes, we observed significantly fewer hits for DT permeabilizers than for ST permeabilizers or for DT non-permeabilizers (Fig. 22; Dunn's post hoc test with Benjamini–Hochberg correction, $p < 0.05$).

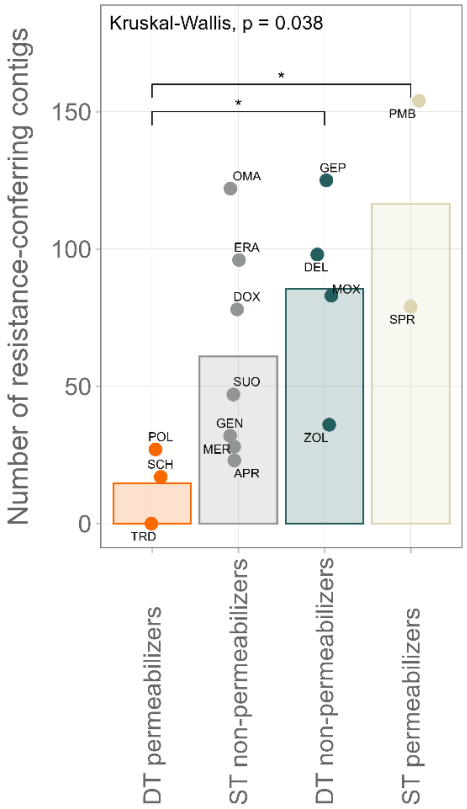

Figure 22. Influence of mobile DNA fragments on antibiotic resistance. This bar graph shows the average number of distinct resistance-conferring DNA contigs identified per mode-of-action group via functional metagenomic screens. Each dot represents one antibiotic within a group. Kruskal–Wallis test ($\chi^2 = 8.4475$, df = 3, $p = 0.038$) followed by Dunn's post hoc (Benjamini–Hochberg correction) indicates significantly fewer resistance contigs for DT permeabilizers compared to other groups ($p < 0.05$). Adapted from Maharramov et al., 2025.

Focusing solely on antibiotics currently in development further reinforced this trend: DT permeabilizers again yielded significantly fewer resistance fragments than other candidates (Fig. 23; Student's *t*-test, $p < 0.01$).

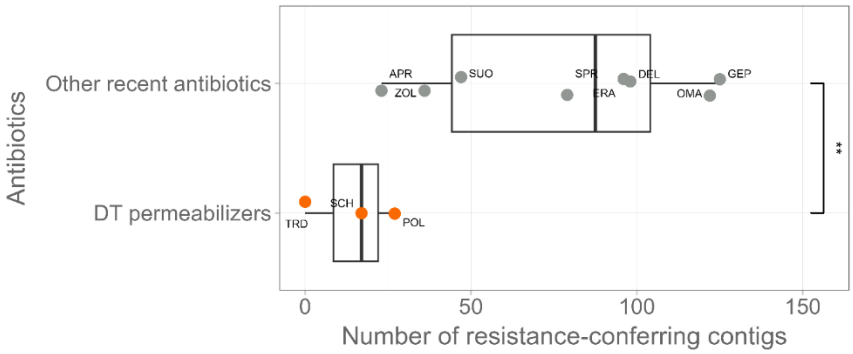

Figure 23. Resistance-conferring contigs for recently developed antibiotics. Focusing on antibiotics introduced since 2017 or currently in development, this boxplot shows the number of resistance-conferring contigs identified for DT permeabilizers versus other "recent" compounds via functional metagenomic screening. Each point represents one antibiotic. DT permeabilizers have significantly fewer resistance contigs than other recent antibiotics (Student's *t*-test, **, $p < 0.01$).

Notably, for tridecaptin M152-P3, no resistance-conferring DNA contig was detected following selection, underscoring its potential robustness against environmental resistance genes (Fig. 15). SCH79797 displayed the second-lowest number of resistance fragments ($n = 17$), further highlighting the distinct advantage of DT permeabilizers in circumventing LPS modification–based resistance mechanisms in nature.

Among the 14 non-redundant ORFs identified in screens against DT permeabilizers, only three exhibited close sequence similarity to known resistance genes catalogued in the Comprehensive Antibiotic Resistance Database (CARD) (Alcock et al., 2020; McArthur et al., 2013). These known genes primarily encode antibiotic efflux mechanisms, including *ramA*, an RND family regulator that upregulates AcrAB-TolC pump expression and downregulates porin production, thereby conferring an MDR phenotype (Masi & Pagès, 2013; Nishino et al., 2007; Ricci et al., 2014). This finding is consistent with our observation that overexpressing AcrAB-TolC in *E. coli* results in a modest but significant decrease in SCH79797 susceptibility (Fig. 18). In the soil metagenomic library screened against POL7306, we also detected an ORF with 77% identity to CRP, a global regulator that represses the MdtEF tripartite efflux pump (Nishino et al., 2008).

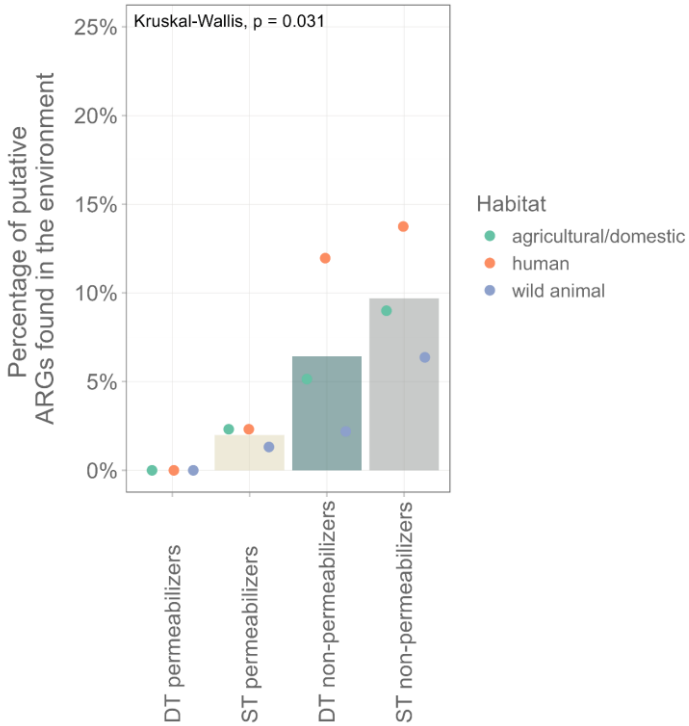

Figure 24. Habitat-specific prevalence of putative ARGs in natural *E. coli* genomes. For each antibiotic group, barplots depict the mean percentages of *E. coli* genomes from different habitats (agricultural, human, wild animal) that harbor at least one putative ARG identified in our screens. Individual points indicate mean percentages per antibiotic across habitats. A Kruskal–Wallis test ($\chi^2 = 8.8992$, df = 3, $p = 0.031$) shows significant variation in ARG prevalence among groups across habitats.

To determine whether these putative ARGs circulate among natural *E. coli* populations, we analyzed more than 16,000 genomes from diverse habitats, including agricultural, human, and wild animal hosts and spanning 11 phylogenetic groups (Luo et al., 2011; Pursey et al., 2023). Of the 539 non-redundant ORFs identified in our functional screens, only 48 had close homologs in the surveyed *E. coli* genomes, and these were generally rare (present in a small fraction of genomes). Strikingly, all 14 putative ARGs associated with DT permeabilizers (4 for SCH79797 and 10 for POL7306) were completely absent from the natural *E. coli* isolates across all habitats (Fig. 24). In contrast, when considering ST permeabilizers, DT non-permeabilizers, or other antibiotic classes, up to 8.4% of genomes carried at least one corresponding resistance gene (Fig. 25). These data underscore the rarity of mobile resistance determinants against DT permeabilizers in environmental reservoirs.

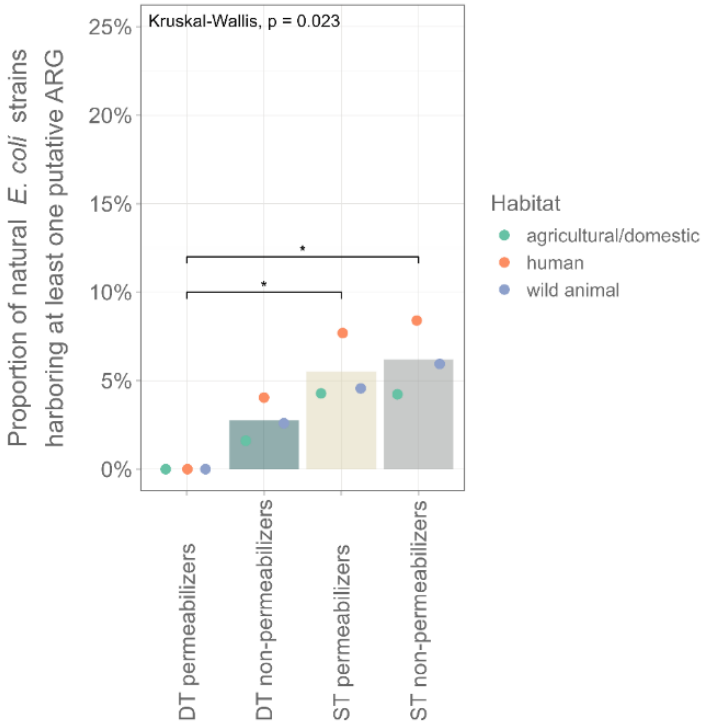

Figure 25. Prevalence of putative ARGs in natural *E. coli* genomes. This bar graph illustrates, for each mode-of-action group, the mean proportion of *E. coli* genomes (across three habitat categories) that carry at least one putative resistance gene identified in our functional metagenomic screens. Individual data points represent mean percentages for each antibiotic-habitat combination. A Kruskal–Wallis test ($\chi^2 = 9.4917$, df = 3, $p = 0.023$) and Dunn's post hoc comparisons (Benjamini–Hochberg correction) reveal that significantly fewer genomes harbor ARGs against DT permeabilizers compared to other groups ($p < 0.05$). Adapted from Maharramov et al., 2025.

4.9. Killing kinetics of dual-target permeabilizers

Finally, we quantified bacterial survival kinetics under fixed antibiotic exposure (10× MIC for 4 hours) in *E. coli*, *A. baumannii*, *K. pneumoniae*, and *P. aeruginosa* using automated image analysis. Strains were selected based on initial sensitivity (MIC ≤ 4 µg/mL), and survival was defined as the ratio of viable cells after treatment to the initial CFU count. Among all antibiotics tested, DT permeabilizers

ranked among the most efficacious killers. In particular, SCH79797 eradicated the entire population in all four species within 4 hours (Fig. 26). By comparison, colistin only achieved complete killing in *P. aeruginosa*.

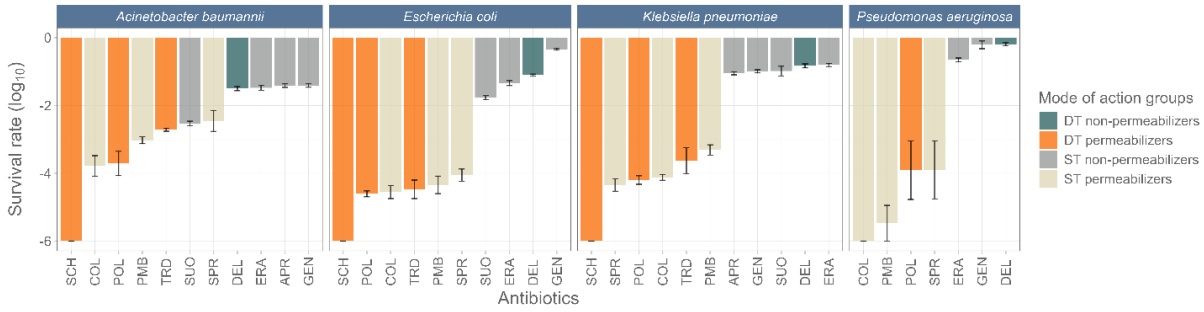

Figure 26. Bacterial survival following 4-hour exposure to 10× MIC. Bars represent mean survival rate (CFU_{after} / $CFU_{initial}$ in $\log_{10}$) for five biological replicates of each species (*E. coli*, *A. baumannii*, *K. pneumoniae*, *P. aeruginosa*) treated with antibiotics to which they were initially sensitive (MIC ≤ 4 μg/mL). Colors distinguish mode-of-action groups. DT permeabilizers, especially SCH79797 (SCH), yield the lowest survival rates across all species, indicating potent killing. Error bars indicate ± standard error. Adapted from Maharramov et al., 2025.

When we correlated the median relative MIC reached during ALE with the survival rate under each antibiotic, we observed a significant positive relationship (Fig. 27; Spearman's $\rho = 0.37$, $p = 0.0019$), indicating that drugs eliciting lower evolved resistance also tended to kill more effectively under these conditions.

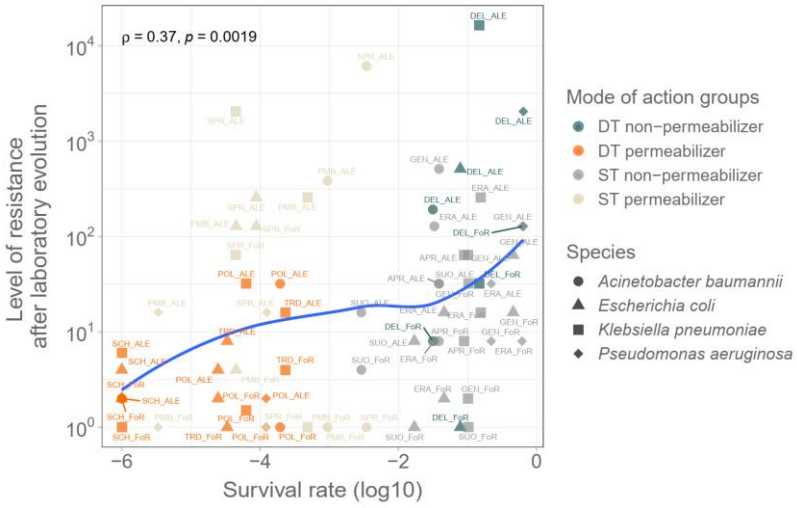

Figure 27. Correlation between survival rate and resistance level after ALE. Scatter plot of antibiotic–strain pairs showing the relationship between immediate survival and the extent of resistance after evolution. The x-axis is the survival rate ($\log_{10}$ scale) after acute drug exposure. The y-axis is the median relative MIC as level of resistance reached during adaptive laboratory evolution (ALE). Points are colored by mode-of-action group and shaped by species. The blue line shows a LOESS fit. We observed a significant positive correlation between survival and evolved resistance (Spearman's $\rho = 0.37$, $p = 0.0019$), indicating that antibiotics that achieve lower evolved resistance are also those that kill more effectively under these conditions.

To explore how dose influences the emergence of resistance, we performed detailed microplating assays coupled with automated image analysis to measure population survival across a range of antibiotic

concentrations (Lázár et al., 2022). For *E. coli*, we generated dose-response curves and calculated the Hill coefficient for each strain–antibiotic pair as a metric of dose-kill steepness (Fig. 28).

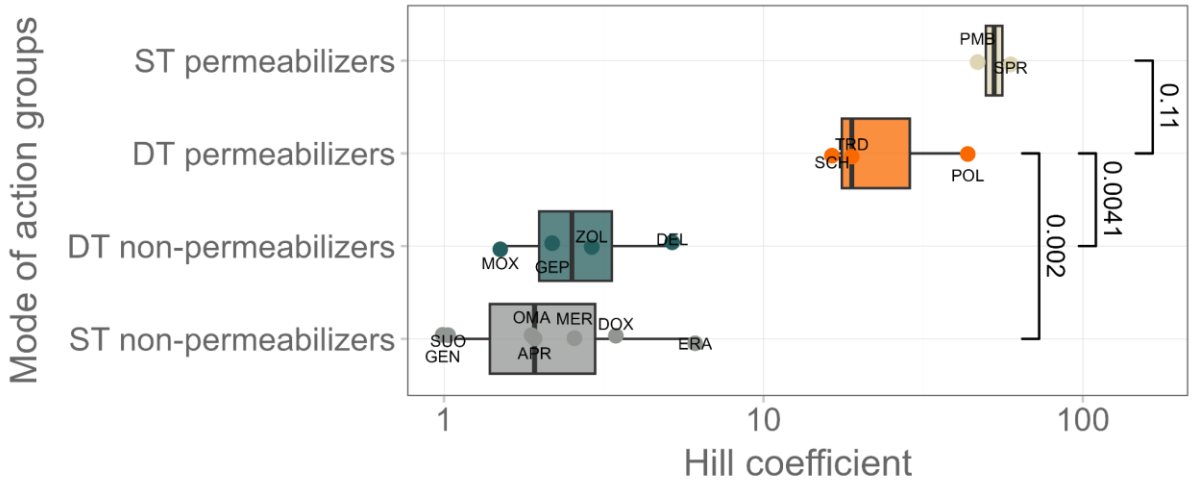

Figure 28. DT permeabilizers show favourable killing kinetics in dose-response experiments. The effect of different levels of antibiotic exposure (dose-response curves) was measured on a sensitive *E. coli* clinical isolate (ATCC25922). The y-axis indicates the magnitude of the Hill coefficient that was calculated to sigmoidal dose-response curves to quantify the killing kinetics of each antibiotic. Mode of action group differentiation is denoted by colour. P-values were calculated using an independent two-sample *t*-test. We found that DT permeabilizers show superior killing kinetics compared to non-permeabilizers and similarly to ST permeabilizer antibiotics.

The resulting curves revealed that both DT and ST permeabilizers exhibit remarkably steep dose–response profiles, with substantial bacterial elimination occurring over a narrow concentration window (Fig. 29). Together, these findings demonstrate that dual-target permeabilizers combine potent killing kinetics with limited potential for resistance development, highlighting their promise as next-generation antibiotics.

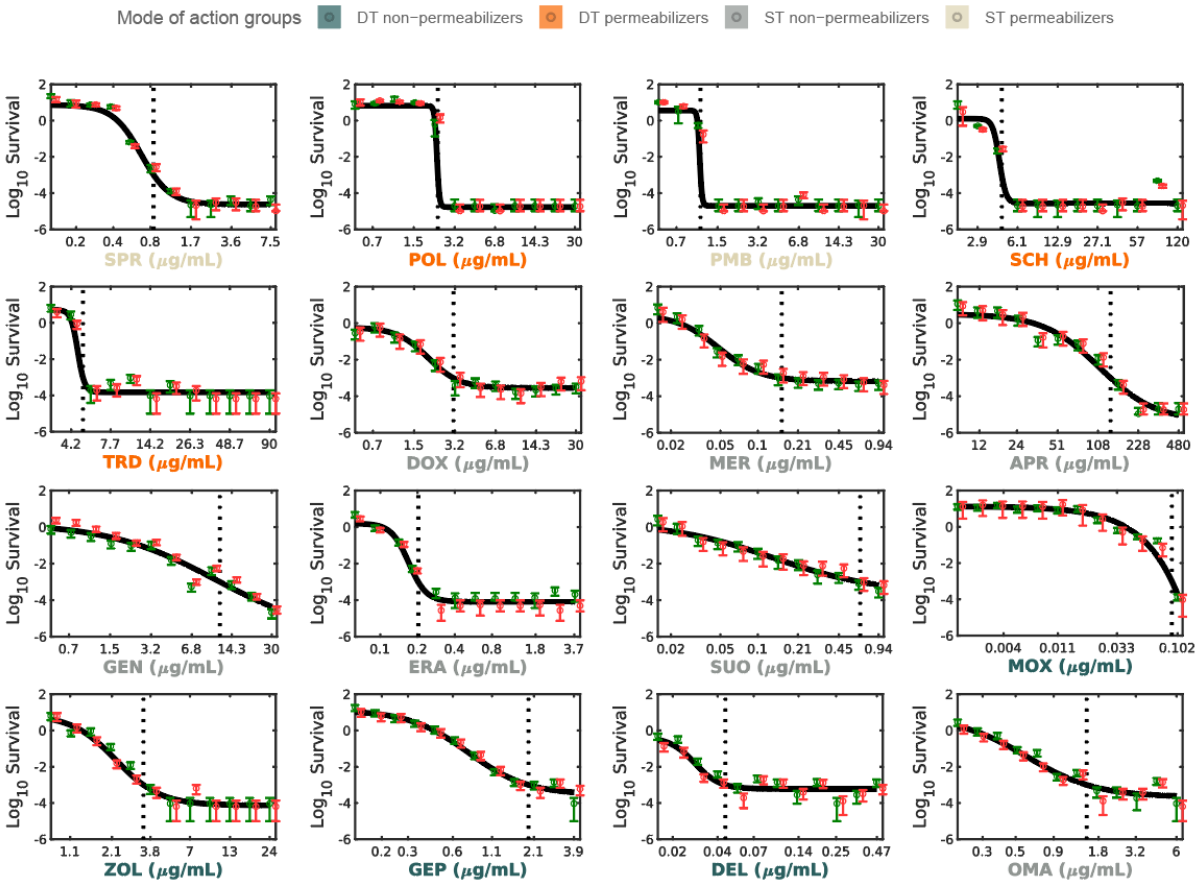

Figure 29. Dose–response curves for *E. coli* ATCC 25922. Dose–response relationships were measured by counting CFU/mL after 4 hours of exposure to various concentrations of each of the 16 antibiotics. Points represent means of two biological replicates; error bars show Poisson-based standard errors. Each curve is a Hill fit to the data. A vertical dashed line marks the concentration that kills 99.9% of the population. Hill coefficients quantify how steeply survival falls with concentration: lower Hill values indicate steeper killing. Statistical comparisons show that DT permeabilizers have significantly lower Hill coefficients than DT non-permeabilizers and ST non-permeabilizers (two-sample Student's t-test, $p < 0.01$), but do not differ significantly from ST permeabilizers ($p = 0.218$). X-axis labels are color-coded by mode-of-action group. Reproduced from (Maharramov et al., 2025)

5. Discussion

Given the urgent need for new antimicrobial strategies to combat rising resistance (Bertagnolio et al., 2024), this study explores guiding principles for developing antibiotics that remain effective in the long term. We propose that, to restrict resistance evolution, candidate drugs should combine two features: disruption of membrane integrity and a second physiological target. In contrast, compounds that inhibit two intracellular pathways without affecting the membrane remain prone to rapid resistance.

Among the agents we examined, three preclinical candidates, such as SCH79797, tridecaptin M152-P3, and POL7306, best illustrate this concept. Each of these dual-target permeabilizers not only permeabilizes the bacterial envelope but also binds a distinct intracellular target, although their precise mechanisms differ (Table 2; Figs. 7-8). Several factors appear to impede resistance development against these compounds. First, spontaneous and long-term laboratory evolution yielded only modest increases in MIC for SCH79797, tridecaptin M152-P3, or POL7306 (Figs. 9-11). Because bacteria would need to alter both their membrane composition and a second pathway, the mutational landscape for achieving high-level resistance is greatly constrained. Cross-resistance between these dual-target permeabilizers and other antibiotic classes was extremely rare (Figs. 15-17). Notably, lineages evolved to resist polymyxin B, a typical membrane disruptor, remained completely susceptible to SCH79797, POL7306, and tridecaptin M152-P3 (Fig. 19), underscoring that modifications of LPS alone cannot confer protection against agents that also binds another cellular target. Moreover, the few mutations that did arise in dual-target permeabilizer–adapted lines often carried significant fitness costs, as evidenced by negative correlations between resistance level and growth in antibiotic-free medium (Fig. 14). Thus, even when rare resistance mutations emerge, they tend to impair bacterial fitness, further restricting their spread. This result reflects the organism's relative growth rate under defined laboratory conditions and serves as a proxy for the cost of resistance in the absence of selective pressure. However, fitness effects are context dependent and may differ across environments, microbial communities, or *in vivo* settings, where resistance-associated costs can be mitigated or amplified. Thus, further research is needed to validate these results across different conditions, especially *in vivo*.

Second, gene amplification, which may serve as a stepping-stone resistance mechanism by which bacteria overexpress latent resistance determinant (Sandegren & Andersson, 2009), proved ineffective against membrane-permeabilizing agents. In our ASKA library screens, overexpressing any single gene failed to elevate resistance to SCH79797, tridecaptin M152-P3, or POL7306 (Fig. 21). This suggests that, when the membrane is compromised, boosting individual gene products cannot overcome the simultaneous disruption of both envelope integrity and a secondary target.

Third, mobile resistance determinants against dual-target permeabilizers are scarce both in human-associated microbiomes and in clinical pathogens. Functional metagenomic screens yielded no resistance fragments for tridecaptin M152-P3 and only a handful for SCH79797 and POL7306 (Fig. 22).

Furthermore, among over 16,000 natural *E. coli* genomes surveyed, none carried homologs of resistance genes against POL7306, SCH79797 or tridecaptin M152-P3; in contrast, up to 8.4% of genomes contained ARGs against other antibiotic classes (Fig. 25). This scarcity of mobile resistance elements significantly reduces the likelihood of horizontal gene transfer conferring dual-target permeabilizer resistance.

Fourth, dual-target permeabilizers exhibit potent bactericidal activity with steep dose–response curves. In four-hour kill assays at 10× MIC, SCH79797 eradicated nearly all cells across *E. coli*, *A. baumannii*, *K. pneumoniae*, and *P. aeruginosa* (Fig. 26). Although polymyxin B and colistin also demonstrate strong killing, they remain vulnerable to resistance via LPS modification (Fig. 27). By fitting Hill functions to dose–response data in *E. coli*, we found that dual-target permeabilizers cause bacterial death over a narrow concentration window (high Hill coefficients; Figs. 28, 29), further limiting the opportunity for resistant mutants to persist at sublethal drug levels.

Taken together, these findings indicate that conventional resistance pathways, such as target-site mutation, efflux pump upregulation, or enzymatic inactivation, offer little protection against dual-target permeabilizers. For example, SCH79797 binds the mechanosensitive channel MscL (Wray et al., 2022) and inhibits folate biosynthesis (J. K. Martin et al., 2020), yet no mutations appeared in *mscL* or folate pathway genes in SCH79797-adapted lines. Similarly, POL7306's target, the outer membrane protein BamA (Luther et al., 2019), remained unaltered, and tridecaptin M152-P3's primary target, lipid II (Jangra et al., 2019), likewise showed no mutational changes in biosynthesis genes (Kumar et al., 2022). Although SCH79797-adapted bacteria did exhibit a modest reduction in susceptibility due to increased AcrAB-TolC efflux (Fig. 18), these shifts were minor compared to the dramatic resistance seen with other compounds. Importantly, we found no evidence of enzymatic inactivation for any dual-target permeabilizer, neither in evolved genomes nor in metagenomic libraries.

A major advantage of embedding membrane permeabilization and intracellular inhibition within a single scaffold is the avoidance of pharmacokinetic (PK) and pharmacodynamic (PD) mismatches that frequently undermine combination therapies. Indeed, SCH79797 outperformed a matched combination of its functional counterparts, trimethoprim and a membrane-disrupting agent, where antagonism was observed for the drug mixture but not for the single compound (J. K. Martin et al., 2020). This aligns with broader evidence that interactions between membrane-targeting moieties and intracellular antibiotics can be either synergistic or antagonistic (Brochado et al., 2018). By physically linking both activities, multitarget compounds reduce the risk of antagonism and eliminate spatial or temporal monotherapy caused by differential tissue penetration. While combination therapies are often proposed to enhance efficacy (Tyers & Wright, 2019), these findings argue that single-molecule multitarget designs may represent a more robust and evolutionary stable strategy.

This principle is reinforced by recent independent studies. Y. Li et al., (2025) developed bifunctional antibacterial peptides by covalently linking modified PbgA-derived peptides to a colistin analogue via a small-molecule linker. These compounds exhibited potent activity against polymyxin-resistant Gram-negative pathogens and acted through dual mechanisms: outer membrane disruption via LPS binding and inhibition of BamA. Notably, serial passaging of polymyxin-resistant *A. baumannii* and polymyxin- and carbapenem-resistant *P. aeruginosa* resulted in no more than an eight-fold increase in MIC over 25 passages, whereas the individual peptide components evolved resistance exceeding 256-fold within 15 passages. These results support our findings and reinforce the advantage of combining membrane disruption with a second target in a single molecule.

Dual mechanisms of action are well documented in the Gram-positive literature, where targeting multiple components of the cell envelope often results in high antibacterial efficacy and reduced resistance potential. Teixobactin, for example, binds two essential precursors in cell-wall biosynthesis, lipid II (peptidoglycan) and lipid III (teichoic acids), and early screens failed to identify resistant mutants (Ling et al., 2015). Although Martins et al., (2025) recently reported modest MIC increases in *Staphylococcus aureus*, resistance levels remained low, and, notably, SCH79797 tested in the same study yielded no detectable resistance. Additional support comes from the discovery of paenimicin, an 11-mer depsi-lipopeptide that binds lipid A in Gram-negative bacteria while simultaneously sequestering teichoic acids in Gram-positive species, with no resistance detected (W. He et al., 2025). Together, these findings suggest that the dual-target permeabilizer strategy may extend beyond Gram-negative pathogens and could enable the development of genuinely broad-spectrum antibiotics, although further research is needed to evaluate these claims.

In contrast, dual-target antibiotics that lack membrane-permeabilizing activity remain highly vulnerable to resistance evolution. Dual target topoisomerase inhibitors, which are drugs that inhibit both DNA gyrase and topoisomerase IV, readily select for high level resistance in our screens. Adaptive laboratory evolution in this class of antibiotics yielded a median 128-fold MIC increase (Fig. 11), with frequent mutations in *gyrA*, *parC*, and efflux regulators. Moreover, functional metagenomics screens uncovered target protection proteins (*e.g.*, Qnr family) that confer dual target topoisomerase resistance (Jacoby et al., 2015; Jacoby & Hooper, 2013). These findings are further supported by literature in recently developed dual topoisomerase inhibitors. In *K. pneumoniae*, a single initial mutation to gepotidacin acts as a steppingstone, enabling acquisition of a second mutation that produces an approximately 2,000-fold MIC increase (Szili et al., 2019). Similarly, delafloxacin resistance can arise through efflux pump gene amplification, effectively bypassing the need for multiple target-site mutations (Silva et al., 2023). These examples demonstrate that dual intracellular targeting alone is insufficient to prevent resistance evolution and underscore the critical role of membrane permeabilization in constraining bacterial adaptations.

Our findings further distinguish dual-target permeabilizers from outer-membrane permeabilizers used as adjuvants. While polymyxin-derived compounds such as SPR741 can transiently sensitize Gram-negative bacteria to otherwise inactive antibiotics, such approaches often fail to consider long-term evolutionary outcomes and face translational challenges, including narrow therapeutic windows and tolerance mechanisms (French et al., 2020). Thus, this compound was discontinued and replaced by the next-generation analogue SPR206 in 2020 (Prasad et al., 2022). By delivering both activities within a single scaffold, DT permeabilizers avoid spatial monotherapy and ensure matched PK/PD profiles, a principle shown to be critical for suppressing resistance evolution (Moreno-Gamez et al., 2015).

Finally, it is informative to compare dual-target permeabilizers with monotherapeutic membrane disruptors such as polymyxin B and SPR206, which bind lipid A in LPS (Ezadi et al., 2019; Zhang et al., 2020). Bacteria can readily resist these by modifying LPS, but they cannot evade dual-target permeabilizers because those drugs also demand a second, essential interaction beyond the membrane. In particular, SCH79797's inhibition of MscL presents a promising alternative membrane-targeting strategy: MscL is broadly conserved among bacteria, essential for survival, and absent in mammals (Wang & Blount, 2023). It remains active in stationary phase and does not depend on metabolic activity, suggesting that MscL inhibitors could kill dormant or persister cells. Indeed, SCH79797 cleared bacterial populations within four hours (Fig. 26), yet no *mscL* mutations arose under this selective pressure.

In summary, our comprehensive experimental approach, that span from spontaneous resistance assays, adaptive laboratory evolution, metagenomic screens, and kill-kinetic analyses, reveals that antibiotics combining membrane permeabilization with a second intracellular mechanism impose a formidable barrier to resistance. Although *in vivo* validation is still needed, these dual-target permeabilizers represent a promising direction for next-generation therapies against multidrug-resistant Gram-negative pathogens. Ultimately, my results highlight the strategic advantage of simultaneously targeting the bacterial envelope and a critical intracellular pathway to outpace the evolution of resistance.

6. Summary

Antibiotic resistance poses a critical threat to global health, undermining decades of medical progress and leading to higher morbidity, mortality, and healthcare costs. As resistance emerges even against novel agents in development and pharmaceutical pipelines diminish, there is an urgent need to identify the core principles that govern long-term antibiotic efficacy. My PhD research addresses this challenge by introducing and experimentally validating a rational design framework for "dual-target permeabilizers," a new mechanism of antibiotics that combine membrane disruption with a second, distinct intracellular mechanism to limit resistance evolution.

To test this framework, we employed two complementary laboratory evolution strategies across four clinically relevant Gram-negative species (*Escherichia coli*, *Klebsiella pneumoniae*, *Acinetobacter baumannii*, and *Pseudomonas aeruginosa*). First, short-term experiments selected for single-step resistance mutations by exposing populations to high antibiotic concentrations. Second, long-term evolution gradually increased antibiotic doses to drive high-level resistance. In parallel, we conducted functional metagenomic screens of environmental and clinical microbiomes to identify mobile resistance genes capable of horizontal transfer. These combined approaches allowed us to compare resistance trajectories under diverse selective pressures and assess both genetic adaptation and the risk of resistance gene dissemination.

Through these studies, three preclinical compounds (SCH79797, tridecaptin M152-P3, and POL7306) emerged as prime examples of our dual-target permeabilizer concept. Each agent disrupts membrane integrity while engaging a distinct secondary target: SCH79797 activates and binds the mechanosensitive channel (MscL) and inhibits folate synthesis; tridecaptin M152-P3 binds lipid II; and POL7306 targets the BamA protein in the outer membrane. Remarkably, bacteria evolved under these drugs showed only small increases in minimum inhibitory concentrations (MICs) and few or no mutations in the genes encoding these targets. Cross-resistance to conventional antibiotics was also rare. For instance, polymyxin B–adapted lines remained fully susceptible to dual-target permeabilizers, demonstrating the limited pathways available for resistance.

When resistance mutations did arise, they frequently carried significant fitness costs, manifesting as slower growth rates that likely limit their spread. Unlike many intracellular antibiotics, dual-target permeabilizers also prevent resistance by gene amplification, since perturbations to membrane composition are inherently detrimental. Our functional metagenomic analysis reinforced these findings by revealing a scarcity of mobile resistance genes against SCH79797, tridecaptin M152-P3, and POL7306 in both clinical and environmental microbiomes. This low prevalence suggests a minimal risk of horizontal gene transfer propagating resistance.

Dose–response assays further demonstrated that dual-target permeabilizers achieve steep, bactericidal killing over a narrow concentration range. While polymyxin B and colistin also show abrupt bactericidal kinetics, they remain vulnerable to resistance via lipopolysaccharide (LPS) modifications. In contrast, the additional intracellular activities of dual-target permeabilizers preserve potency even when LPS is altered. Mechanistically, no target-site mutations were observed in genes encoding SCH79797's MscL channel or folate enzymes, tridecaptin's lipid II pathway, or POL7306's BamA target. Efflux-pump mutations were similarly rare, with only SCH79797–adapted lines showing a modest AcrAB-TolC upregulation. By comparison, dual-target topoisomerase inhibitors, acting on DNA gyrase and topoisomerase IV, enabled high-level resistance (median 128-fold MIC increase) through target-site changes, efflux upregulation, and protective proteins.

Taken together, these results define clear principles for designing "resistance-evading" antibiotics: combining membrane permeabilization with a secondary target constrains genetic adaptation, imposes fitness costs on resistant mutants, and minimizes horizontal gene transfer. The mechanosensitive MscL channel exemplifies an especially promising target due to its conservation across bacteria, absence in mammals, and activity in both growing and dormant cells. These findings not only deliver critical insights into bacterial resistance but also provide a practical roadmap for next-generation antibiotic development, offering hope for sustainable therapies against multidrug-resistant pathogens.

7. Personal contributions

The results presented in this PhD dissertation are based on work I carried out in the Csaba Pál Laboratory of Microbial Experimental Evolution, Institute of Biochemistry, HUN-REN Biological Research Centre, Szeged.

I performed the majority of the data analysis and conducted a substantial portion of the experiments necessary for this study. The initial adaptive laboratory evolution and frequency-of-resistance (FoR) datasets were obtained from a previously published paper, in which I am also a co-author (Daruka et al., 2025). Building on these datasets, I carried out the additional analyses that form the core of this thesis.

My contributions to the experimental work include designing and implementing the genome-wide overexpression screens, as well as preparing plasmid DNA samples for sequencing. Sequencing and initial ORF identification from the overexpression library were performed by Márton Enyedi and colleagues at Delta Bio 2000 Ltd., Szeged. I was responsible for the downstream analysis of these data, including quality control, ORF quantification, clustering, statistical evaluation, and visualization.

Microplating assays combined with automated image analysis for quantifying population survival across antibiotic gradients were performed by Bence Bognár and Terézia Kovács from Viktória Lázár's laboratory (Systems Biology of Antibiotic Action, HUN-REN BRC). *In vitro* growth measurements were carried out by my colleague Petra Szili.

Additionally, I investigated the AcrAB efflux system activity and its impact on antibiotic resistance. Measurements of cross-resistance profiles, survival-rate dynamics and membrane permeabilization assay were performed jointly with my colleague Márton Czikkely, with whom I share first authorship on the publication forming the foundation of this dissertation (Maharramov et al., 2025).

I independently carried out all data analyses presented in this thesis, including clustering analyses of cross-resistance patterns, comparison of mutational profiles between ST- and DT-permeabilizer–adapted populations, and KEGG pathway annotation and functional categorization of mutated genes, all of which were performed using R. With the exception of *Figure 28*, all figures included in this thesis were generated by me.

8. Acknowledgement

To begin, I would like to express my heartfelt appreciation to my supervisor, Csaba Pál, for his unwavering support and guidance throughout my PhD journey. His dedicated attention, constructive feedback, and insightful discussions have been invaluable and played a central role in shaping my scientific development. It has truly been a privilege to work with him, and I am deeply grateful for the opportunity.

I would also like to thank my colleagues for making all these years in the lab both enjoyable and enriching. My sincere thanks go to Márton Czikkely, Zoltán Farkas, Lejla Daruka, and Petra Szili for their help, kindness, and friendship. I am equally grateful to Andreea Daraba and Andrea Tóth for their exceptional technical assistance and for keeping the lab running smoothly.

I am especially thankful to our collaborators, Balázs Papp, Gábor Grézal, and Viktória Lázár for their thoughtful input, encouragement, and support during the publication process. Their constructive suggestions significantly strengthened my research.

Furthermore, I would like to thank my thesis reviewers, Péter Galajda and Tamás Beke-Somfai, for their valuable comments and recommendations, which helped refine this thesis.

I am deeply grateful to all my friends in Hungary, who made my time here enjoyable and fulfilling, as well as to those close friends abroad whose support I felt despite the distance.

A very special thanks goes to my girlfriend, Jéssica, for standing by me through the most challenging moments and encouraging me to keep going. Her support has meant more than words can express.

Last but certainly not least, I owe my sincerest gratitude to my family for their unconditional love and support throughout this journey.

9. References

Abouzeed, Y. M., Baucheron, S., & Cloeckaert, A. (2008). ramR Mutations Involved in Efflux-Mediated Multidrug Resistance in Salmonella enterica Serovar Typhimurium. *Antimicrobial Agents and Chemotherapy*, *52*(7), 2428. https://doi.org/10.1128/AAC.00084-08

Alav, I., Kobylka, J., Kuth, M. S., Pos, K. M., Picard, M., Blair, J. M. A., & Bavro, V. N. (2021). Structure, Assembly, and Function of Tripartite Efflux and Type 1 Secretion Systems in Gram-Negative Bacteria. *Chemical Reviews*, *121*(9), 5479–5596. https://doi.org/10.1021/ACS.CHEMREV.1C00055/ASSET/IMAGES/MEDIUM/CR1C00055_0021.GIF

Alcock, B. P., Raphenya, A. R., Lau, T. T. Y., Tsang, K. K., Bouchard, M., Edalatmand, A., Huynh, W., Nguyen, A. L. V., Cheng, A. A., Liu, S., Min, S. Y., Miroshnichenko, A., Tran, H. K., Werfalli, R. E., Nasir, J. A., Oloni, M., Speicher, D. J., Florescu, A., Singh, B., … McArthur, A. G. (2020). CARD 2020: antibiotic resistome surveillance with the comprehensive antibiotic resistance database. *Nucleic Acids Research*, *48*(D1), D517–D525. https://doi.org/10.1093/NAR/GKZ935

Altschul, S. F., Gish, W., Miller, W., Myers, E. W., & Lipman, D. J. (1990). Basic local alignment search tool. *Journal of Molecular Biology*, *215*(3), 403–410. https://doi.org/10.1016/S0022-2836(05)80360-2

Apjok, G., Számel, M., Christodoulou, C., Seregi, V., Vásárhelyi, B. M., Stirling, T., Eszenyi, B., Sári, T., Vidovics, F., Nagrand, E., Kovács, D., Szili, P., Lantos, I. I., Méhi, O., Jangir, P. K., Herczeg, R., Gálik, B., Urbán, P., Gyenesei, A., … Kintses, B. (2023). Characterization of antibiotic resistomes by reprogrammed bacteriophage-enabled functional metagenomics in clinical strains. *Nature Microbiology 2023 8:3*, *8*(3), 410–423. https://doi.org/10.1038/s41564-023-01320-2

Baba, T., Ara, T., Hasegawa, M., Takai, Y., Okumura, Y., Baba, M., Datsenko, K. A., Tomita, M., Wanner, B. L., & Mori, H. (2006). Construction of Escherichia coli K-12 in-frame, single-gene knockout mutants: the Keio collection. *Molecular Systems Biology*, *2*. https://doi.org/10.1038/MSB4100050

Balibar, C. J., & Grabowicz, M. (2015). Mutant Alleles of lptD Increase the Permeability of Pseudomonas aeruginosa and Define Determinants of Intrinsic Resistance to Antibiotics. *Antimicrobial Agents and Chemotherapy*, *60*(2), 845–854. https://doi.org/10.1128/AAC.01747-15

Bann, S. J., Ballantine, R. D., & Cochrane, S. A. (2021). The tridecaptins: non-ribosomal peptides that selectively target Gram-negative bacteria. *RSC Medicinal Chemistry*, *12*(4), 538–551. https://doi.org/10.1039/D0MD00413H

Baquero, F., & Alenazy, R. (2022). Drug Efflux Pump Inhibitors: A Promising Approach to Counter Multidrug Resistance in Gram-Negative Pathogens by Targeting AcrB Protein from AcrAB-TolC Multidrug Efflux Pump from Escherichia coli. *Biology 2022, Vol. 11, Page 1328*, *11*(9), 1328. https://doi.org/10.3390/BIOLOGY11091328

Barbosa, T. M., & Levy, S. B. (2000). Differential expression of over 60 chromosomal genes in Escherichia coli by constitutive expression of MarA. *Journal of Bacteriology*, *182*(12), 3467–3474. https://doi.org/10.1128/JB.182.12.3467-3474.2000

Bell, G., & MacLean, C. (2018). The Search for "Evolution-Proof" Antibiotics. *Trends in Microbiology*, *26*(6), 471–483. https://doi.org/10.1016/J.TIM.2017.11.005

Bertagnolio, S., Dobreva, Z., Centner, C. M., Olaru, I. D., Donà, D., Burzo, S., Huttner, B. D., Chaillon, A., Gebreselassie, N., Wi, T., Hasso-Agopsowicz, M., Allegranzi, B., Sati, H., Ivanovska, V., Kothari, K. U., Balkhy, H. H., Cassini, A., Hamers, R. L., Weezenbeek, K. Van, … Zignol, M. (2024). WHO global research priorities for antimicrobial resistance in human health. *The Lancet Microbe*, *0*(0). https://doi.org/10.1016/S2666-5247(24)00134-4

Bianco, G., Boattini, M., Cricca, M., Diella, L., Gatti, M., Rossi, L., Bartoletti, M., Sambri, V., Signoretto, C., Fonnesu, R., Comini, S., & Gaibani, P. (2024). Updates on the Activity, Efficacy and Emerging Mechanisms of Resistance to Cefiderocol. *Current Issues in Molecular Biology*, *46*(12), 14132. https://doi.org/10.3390/CIMB46120846

Blair, J. M. A., Richmond, G. E., & Piddock, L. J. V. (2014). Multidrug Efflux Pumps in Gram-Negative Bacteria and Their Role in Antibiotic Resistance. *Future Microbiology*, *9*(10), 1165–1177. https://doi.org/10.2217/FMB.14.66

Blanco, P., Hernando-Amado, S., Reales-Calderon, J. A., Corona, F., Lira, F., Alcalde-Rico, M., Bernardini, A., Sanchez, M. B., & Martinez, J. L. (2016). Bacterial Multidrug Efflux Pumps: Much More Than Antibiotic Resistance Determinants. *Microorganisms 2016, Vol. 4, Page 14*, *4*(1), 14. https://doi.org/10.3390/MICROORGANISMS4010014

Bódi, Z., Farkas, Z., Nevozhay, D., Kalapis, D., Lázár, V., Csörgő, B., Nyerges, Á., Szamecz, B., Fekete, G., Papp, B., Araújo, H., Oliveira, J. L., Moura, G., Santos, M. A. S., Székely, T., Balázsi, G., & Pál, C. (2017). Phenotypic heterogeneity promotes adaptive evolution. *PLOS Biology*, *15*(5), e2000644. https://doi.org/10.1371/JOURNAL.PBIO.2000644

Bordeleau, E., Stogios, P. J., Evdokimova, E., Koteva, K., Savchenko, A., & Wright, G. D. (2021). ApmA Is a Unique Aminoglycoside Antibiotic Acetyltransferase That Inactivates Apramycin. *MBio*, *12*(1), 1–11. https://doi.org/10.1128/MBIO.02705-20

Bortolaia, V., Kaas, R. S., Ruppe, E., Roberts, M. C., Schwarz, S., Cattoir, V., Philippon, A., Allesoe, R. L., Rebelo, A. R., Florensa, A. F., Fagelhauer, L., Chakraborty, T., Neumann, B., Werner, G., Bender, J. K., Stingl, K., Nguyen, M., Coppens, J., Xavier, B. B., … Aarestrup, F. M. (2020). ResFinder 4.0 for predictions of phenotypes from genotypes. *The Journal of Antimicrobial Chemotherapy*, *75*(12), 3491–3500. https://doi.org/10.1093/JAC/DKAA345

Botte, M., Ni, D., Schenck, S., Zimmermann, I., Chami, M., Bocquet, N., Egloff, P., Bucher, D., Trabuco, M., Cheng, R. K. Y., Brunner, J. D., Seeger, M. A., Stahlberg, H., & Hennig, M. (2022). Cryo-EM structures of a LptDE transporter in complex with Pro-macrobodies offer insight into lipopolysaccharide translocation. *Nature Communications 2022 13:1*, *13*(1), 1–10. https://doi.org/10.1038/s41467-022-29459-2

Breukink, E., & de Kruijff, B. (2006). Lipid II as a target for antibiotics. *Nature Reviews. Drug Discovery*, *5*(4), 321–323. https://doi.org/10.1038/NRD2004

Brochado, A. R., Telzerow, A., Bobonis, J., Banzhaf, M., Mateus, A., Selkrig, J., Huth, E., Bassler, S., Zamarreño Beas, J., Zietek, M., Ng, N., Foerster, S., Ezraty, B., Py, B., Barras, F., Savitski, M. M., Bork, P., Göttig, S., & Typas, A. (2018). Species-specific activity of antibacterial drug combinations. *Nature 2018 559:7713*, *559*(7713), 259–263. https://doi.org/10.1038/s41586-018-0278-9

Bryson, V., & Szybalski, W. (1952). Microbial selection. *Science*, *116*(3003), 45–51. https://doi.org/10.1126/SCIENCE.116.3003.45/ASSET/E75827E3-B3F8-4BAD-9E32-2695EF5F5221/ASSETS/SCIENCE.116.3003.45.FP.PNG

Bush, K., & Jacoby, G. A. (2010). Updated functional classification of β-lactamases. *Antimicrobial Agents and Chemotherapy*, *54*(3), 969–976. https://doi.org/10.1128/AAC.01009-09/ASSET/F4B63627-1C12-41AA-9BF0-DE454FCC87AE/ASSETS/GRAPHIC/ZAC9991087260003.JPEG

Butler, M. S., Henderson, I. R., Capon, R. J., & Blaskovich, M. A. T. (2023). Antibiotics in the clinical pipeline as of December 2022. *The Journal of Antibiotics 2023 76:8*, *76*(8), 431–473. https://doi.org/10.1038/s41429-023-00629-8

Calcott, M. J., Owen, J. G., & Ackerley, D. F. (2020). Efficient rational modification of non-ribosomal peptides by adenylation domain substitution. *Nature Communications*, *11*(1), 4554. https://doi.org/10.1038/S41467-020-18365-0

Cannatelli, A., Giani, T., D'Andrea, M. M., Pilato, V. Di, Arena, F., Conte, V., Tryfinopoulou, K., Vatopoulos, A., & Rossolini, G. M. (2014). MgrB inactivation is a common mechanism of colistin resistance in KPC-producing Klebsiella pneumoniae of clinical origin. *Antimicrobial Agents and Chemotherapy*, *58*(10), 5696–5703. https://doi.org/10.1128/AAC.03110-14

Chamberlain S, A. Z. S. T. (2024). taxizedb: Tools for Working with "Taxonomic" Databases. *R Package Version 0.3.1*.

Chubiz, L. M. (2023). The Mar, Sox, and Rob Systems. *EcoSal Plus*, *11*(1), eesp-0010-2022. https://doi.org/10.1128/ECOSALPLUS.ESP-0010-2022

Clermont, O., Christenson, J. K., Denamur, E., & Gordon, D. M. (2013). The Clermont Escherichia coli phylo-typing method revisited: improvement of specificity and detection of new phylo-groups. *Environmental Microbiology Reports*, *5*(1), 58–65. https://doi.org/10.1111/1758-2229.12019

Cochrane, S. A., Findlay, B., Bakhtiary, A., Acedo, J. Z., Rodriguez-Lopez, E. M., Mercier, P., & Vederas, J. C. (2016). Antimicrobial lipopeptide tridecaptin A1selectively binds to Gram-negative lipid II. *Proceedings of the National Academy of Sciences of the United States of America*, *113*(41), 11561–11566. https://doi.org/10.1073/PNAS.1608623113/SUPPL_FILE/PNAS.1608623113.SAPP.PDF

Codjoe, F. S., & Donkor, E. S. (2017). Carbapenem Resistance: A Review. *Medical Sciences*, *6*(1), 1. https://doi.org/10.3390/MEDSCI6010001

Cohen, F., Aggen, J. B., Andrews, L. D., Assar, Z., Boggs, J., Choi, T., Dozzo, P., Easterday, A. N., Haglund, C. M., Hildebrandt, D. J., Holt, M. C., Joly, K., Jubb, A., Kamal, Z., Kane, T. R., Konradi, A. W., Krause, K. M., Linsell, M. S., Machajewski, T. D., … Cirz, R. T. (2019). Optimization of LpxC Inhibitors for Antibacterial Activity and Cardiovascular Safety. *ChemMedChem*, *14*(16), 1560–1572. https://doi.org/10.1002/CMDC.201900287

Cohen, S. P., Hachler, H., & Levy, S. B. (1993). Genetic and functional analysis of the multiple antibiotic resistance (mar) locus in Escherichia coli. *Journal of Bacteriology*, *175*(5), 1484–1492. https://doi.org/10.1128/jb.175.5.1484-1492.1993

Darby, E. M., Trampari, E., Siasat, P., Gaya, M. S., Alav, I., Webber, M. A., & Blair, J. M. A. (2023). Molecular mechanisms of antibiotic resistance revisited. In *Nature Reviews Microbiology* (Vol. 21, Issue 5, pp. 280–295). Nature Research. https://doi.org/10.1038/s41579-022-00820-y

Daruka, L., Czikkely, M. S., Szili, P., Farkas, Z., Balogh, D., Grézal, G., Maharramov, E., Vu, T. H., Sipos, L., Juhász, S., Dunai, A., Daraba, A., Számel, M., Sári, T., Stirling, T., Vásárhelyi, B. M., Ari, E., Christodoulou, C., Manczinger, M., … Pál, C. (2025). ESKAPE pathogens rapidly develop resistance against antibiotics in development in vitro. *Nature Microbiology 2025 10:2*, *10*(2), 313–331. https://doi.org/10.1038/s41564-024-01891-8

Davin-Regli, A., Pagès, J. M., & Vergalli, J. (2024). The contribution of porins to enterobacterial drug resistance. *Journal of Antimicrobial Chemotherapy*, *79*(10), 2460–2470. https://doi.org/10.1093/JAC/DKAE265

Dcosta, V. M., King, C. E., Kalan, L., Morar, M., Sung, W. W. L., Schwarz, C., Froese, D., Zazula, G., Calmels, F., Debruyne, R., Golding, G. B., Poinar, H. N., & Wright, G. D. (2011). Antibiotic resistance is ancient. *Nature 2011 477:7365*, *477*(7365), 457–461. https://doi.org/10.1038/nature10388

Delcour, A. H. (2008). Outer Membrane Permeability and Antibiotic Resistance. *Biochimica et Biophysica Acta*, *1794*(5), 808. https://doi.org/10.1016/J.BBAPAP.2008.11.005

Dhanda, G., Singh, H., Gupta, A., Abdul Mohid, S., Biswas, K., Mukherjee, R., Mukherjee, S., Bhunia, A., Nair, N. N., & Haldar, J. (2025). Dual-Functional Antibiotic Adjuvant Displays Potency against Complicated Gram-Negative Bacterial Infections and Exhibits Immunomodulatory Properties. *ACS Central Science*, *11*(2), 279–293. https://doi.org/10.1021/ACSCENTSCI.4C02060/ASSET/IMAGES/LARGE/OC4C02060_0006.JPEG

Dunai, A., Spohn, R., Farkas, Z., Lázár, V., Györkei, Apjok, G., Boross, G., Szappanos, B., Grézal, G., Faragó, A., Bodai, L., Papp, B., & Pál, C. (2019). Rapid decline of bacterial drug-resistance in an antibiotic-free environment through phenotypic reversion. *ELife*, *8*. https://doi.org/10.7554/ELIFE.47088

Emms, D. M., & Kelly, S. (2015). OrthoFinder: solving fundamental biases in whole genome comparisons dramatically improves orthogroup inference accuracy. *Genome Biology*, *16*(1), 1–14. https://doi.org/10.1186/S13059-015-0721-2/FIGURES/7

Emms, D. M., & Kelly, S. (2019). OrthoFinder: Phylogenetic orthology inference for comparative genomics. *Genome Biology*, *20*(1), 1–14. https://doi.org/10.1186/S13059-019-1832-Y/FIGURES/5

Ezadi, F., Ardebili, A., & Mirnejad, R. (2019). Antimicrobial Susceptibility Testing for Polymyxins: Challenges, Issues, and Recommendations. *Journal of Clinical Microbiology*, *57*(4). https://doi.org/10.1128/JCM.01390-18

Falagas, M. E., & Kasiakou, S. K. (2006). Toxicity of polymyxins: a systematic review of the evidence from old and recent studies. *Critical Care (London, England)*, *10*(1). https://doi.org/10.1186/CC3995

Felnagle, E. A., Jackson, E. E., Chan, Y. A., Podevels, A. M., Berti, A. D., McMahon, M. D., & Thomas, M. G. (2008). Nonribosomal peptide synthetases involved in the production of medically relevant

natural products. *Molecular Pharmaceutics*, *5*(2), 191–211. https://doi.org/10.1021/MP700137G/ASSET/IMAGES/MEDIUM/MP-2007-00137G_0012.GIF

French, S., Farha, M., Ellis, M. J., Sameer, Z., Côté, J. P., Cotroneo, N., Lister, T., Rubio, A., & Brown, E. D. (2020). Potentiation of Antibiotics against Gram-Negative Bacteria by Polymyxin B Analogue SPR741 from Unique Perturbation of the Outer Membrane. *ACS Infectious Diseases*, *6*(6), 1405–1412. https://doi.org/10.1021/ACSINFECDIS.9B00159/ASSET/IMAGES/LARGE/ID9B00159_0006.JPEG

Fu, L., Niu, B., Zhu, Z., Wu, S., & Li, W. (2012). CD-HIT: accelerated for clustering the next-generation sequencing data. *Bioinformatics (Oxford, England)*, *28*(23), 3150–3152. https://doi.org/10.1093/BIOINFORMATICS/BTS565

Garrison, E., Kronenberg, Z. N., Dawson, E. T., Pedersen, B. S., & Prins, P. (2022). A spectrum of free software tools for processing the VCF variant call format: vcflib, bio-vcf, cyvcf2, hts-nim and slivar. *PLOS Computational Biology*, *18*(5), e1009123. https://doi.org/10.1371/JOURNAL.PCBI.1009123

Garrison, E., & Marth, G. (2012). *Haplotype-based variant detection from short-read sequencing*. https://arxiv.org/abs/1207.3907v2

Gasparrini, A. J., Markley, J. L., Kumar, H., Wang, B., Fang, L., Irum, S., Symister, C. T., Wallace, M., Burnham, C. A. D., Andleeb, S., Tolia, N. H., Wencewicz, T. A., & Dantas, G. (2020). Tetracycline-inactivating enzymes from environmental, human commensal, and pathogenic bacteria cause broad-spectrum tetracycline resistance. *Communications Biology*, *3*(1). https://doi.org/10.1038/S42003-020-0966-5

Germain, E., Guiraud, P., Byrne, D., Douzi, B., Djendli, M., & Maisonneuve, E. (2019). YtfK activates the stringent response by triggering the alarmone synthetase SpoT in Escherichia coli. *Nature Communications 2019 10:1*, *10*(1), 1–12. https://doi.org/10.1038/s41467-019-13764-4

Grabowicz, M., Yeh, J., & Silhavy, T. J. (2013). Dominant negative LptE mutation that supports a role for LptE as a plug in the LptD barrel. *Journal of Bacteriology*, *195*(6), 1327–1334. https://doi.org/10.1128/JB.02142-12/SUPPL_FILE/ZJB999092486SO1.PDF

Grenié, M., Berti, E., Carvajal-Quintero, J., Dädlow, G. M. L., Sagouis, A., & Winter, M. (2023). Harmonizing taxon names in biodiversity data: A review of tools, databases and best practices. *Methods in Ecology and Evolution*, *14*(1), 12–25. https://doi.org/10.1111/2041-210X.13802

Gu, Y., Stansfeld, P. J., Zeng, Y., Dong, H., Wang, W., & Dong, C. (2015). Lipopolysaccharide is inserted into the outer membrane through an intramembrane hole, a lumen gate, and the lateral opening of LptD. *Structure (London, England : 1993)*, *23*(3), 496–504. https://doi.org/10.1016/J.STR.2015.01.001

Halat, D. H., & Moubareck, C. A. (2020). The Current Burden of Carbapenemases: Review of Significant Properties and Dissemination among Gram-Negative Bacteria. *Antibiotics*, *9*(4), 186. https://doi.org/10.3390/ANTIBIOTICS9040186

Han, W., Ma, X., Balibar, C. J., Baxter Rath, C. M., Benton, B., Bermingham, A., Casey, F., Chie-Leon, B., Cho, M. K., Frank, A. O., Frommlet, A., Ho, C. M., Lee, P. S., Li, M., Lingel, A., Ma, S., Merritt, H., Ornelas, E., De Pascale, G., … Uehara, T. (2020). Two Distinct Mechanisms of Inhibition of LpxA Acyltransferase Essential for Lipopolysaccharide Biosynthesis. *Journal of the*

American Chemical Society, *142*(9), 4445–4455. https://doi.org/10.1021/JACS.9B13530/SUPPL_FILE/JA9B13530_SI_002.ZIP

He, T., Wang, R., Liu, D., Walsh, T. R., Zhang, R., Lv, Y., Ke, Y., Ji, Q., Wei, R., Liu, Z., Shen, Y., Wang, G., Sun, L., Lei, L., Lv, Z., Li, Y., Pang, M., Wang, L., Sun, Q., … Wang, Y. (2019). Emergence of plasmid-mediated high-level tigecycline resistance genes in animals and humans. *Nature Microbiology 2019 4:9*, *4*(9), 1450–1456. https://doi.org/10.1038/s41564-019-0445-2

He, W., Huan, X., Li, Y., Deng, Q., Chen, T., Xiao, W., Chen, Y., Ma, L., Liu, N., Shang, Z., & Wang, Z. (2025). A broad-spectrum antibiotic targets multiple-drug-resistant bacteria with dual binding targets and no detectable resistance. *Nature Communications 2025 16:1*, *16*(1), 7048-. https://doi.org/10.1038/s41467-025-62407-4

Helander, I. M., & Mattila-Sandholm, T. (2000). Fluorometric assessment of Gram-negative bacterial permeabilization. *Journal of Applied Microbiology*, *88*(2), 213–219. https://doi.org/10.1046/J.1365-2672.2000.00971.X

Hooper, D. C., & Jacoby, G. A. (2016). Topoisomerase Inhibitors: Fluoroquinolone Mechanisms of Action and Resistance. *Cold Spring Harbor Perspectives in Medicine*, *6*(9), a025320. https://doi.org/10.1101/CSHPERSPECT.A025320

Huang, L., Wu, C., Gao, H., Xu, C., Dai, M., Huang, L., Hao, H., Wang, X., & Cheng, G. (2022). Bacterial Multidrug Efflux Pumps at the Frontline of Antimicrobial Resistance: An Overview. *Antibiotics*, *11*(4), 520. https://doi.org/10.3390/ANTIBIOTICS11040520

Hyatt, D., Chen, G. L., LoCascio, P. F., Land, M. L., Larimer, F. W., & Hauser, L. J. (2010). Prodigal: Prokaryotic gene recognition and translation initiation site identification. *BMC Bioinformatics*, *11*(1), 1–11. https://doi.org/10.1186/1471-2105-11-119/TABLES/5

Ikuta, K. S., Swetschinski, L. R., Aguilar, G. R., Sharara, F., Mestrovic, T., Gray, A. P., Weaver, N. D., Wool, E. E., Han, C., Hayoon, A. G., Aali, A., Abate, S. M., Abbasi-Kangevari, M., Abbasi-Kangevari, Z., Abd-Elsalam, S., Abebe, G., Abedi, A., Abhari, A. P., Abidi, H., … Naghavi, M. (2022). Global mortality associated with 33 bacterial pathogens in 2019: a systematic analysis for the Global Burden of Disease Study 2019. *The Lancet*, *400*(10369), 2221–2248. https://doi.org/10.1016/S0140-6736(22)02185-7

Jacoby, G. A., Corcoran, M. A., & Hooper, D. C. (2015). Protective Effect of Qnr on Agents Other than Quinolones That Target DNA Gyrase. *Antimicrobial Agents and Chemotherapy*, *59*(11), 6689. https://doi.org/10.1128/AAC.01292-15

Jacoby, G. A., & Hooper, D. C. (2013). Phylogenetic Analysis of Chromosomally Determined Qnr and Related Proteins. *Antimicrobial Agents and Chemotherapy*, *57*(4), 1930. https://doi.org/10.1128/AAC.02080-12

Jangra, M., Kaur, M., Tambat, R., Rana, R., Maurya, S. K., Khatri, N., Ghafur, A., & Nandanwar, H. (2019). Tridecaptin M, a new variant discovered in mud bacterium, shows activity against colistin-And extremely drug-resistant Enterobacteriaceae. *Antimicrobial Agents and Chemotherapy*, *63*(6). https://doi.org/10.1128/AAC.00338-19/SUPPL_FILE/AAC.00338-19-S0001.PDF

Karaiskos, I., Galani, I., Daikos, G. L., & Giamarellou, H. (2025). Breaking Through Resistance: A Comparative Review of New Beta-Lactamase Inhibitors (Avibactam, Vaborbactam, Relebactam) Against Multidrug-Resistant Superbugs. *Antibiotics*, *14*(5), 528. https://doi.org/10.3390/ANTIBIOTICS14050528

Karakonstantis, S., Rousaki, M., Vassilopoulou, L., & Kritsotakis, E. I. (2024). Global prevalence of cefiderocol non-susceptibility in Enterobacterales, Pseudomonas aeruginosa, Acinetobacter baumannii, and Stenotrophomonas maltophilia: a systematic review and meta-analysis. *Clinical Microbiology and Infection*, *30*(2), 178–188. https://doi.org/10.1016/J.CMI.2023.08.029

Kaur, M., & Mingeot -Leclercq, M. P. (2024). Maintenance of bacterial outer membrane lipid asymmetry: insight into MlaA. *BMC Microbiology 2023 24:1*, *24*(1), 1–14. https://doi.org/10.1186/S12866-023-03138-8

Khunsri, I., Prombutara, P., Htoo, H. H., Wanvimonsuk, S., Samernate, T., Pornsing, C., Tharntada, S., Jaree, P., Chaikeeratisak, V., Somboonwiwat, K., & Nonejuie, P. (2023). Roles of qseC mutation in bacterial resistance against anti-lipopolysaccharide factor isoform 3 (ALFPm3). *PLOS ONE*, *18*(6). https://doi.org/10.1371/JOURNAL.PONE.0286764

Kintses, B., Méhi, O., Ari, E., Számel, M., Györkei, Á., Jangir, P. K., Nagy, I., Pál, F., Fekete, G., Tengölics, R., Nyerges, Á., Likó, I., Bálint, A., Molnár, T., Bálint, B., Vásárhelyi, B. M., Bustamante, M., Papp, B., & Pál, C. (2019). Phylogenetic barriers to horizontal transfer of antimicrobial peptide resistance genes in the human gut microbiota. *Nature Microbiology*, *4*(3), 447–458. https://doi.org/10.1038/s41564-018-0313-5

Kitagawa, M., Ara, T., Arifuzzaman, M., Ioka-Nakamichi, T., Inamoto, E., Toyonaga, H., & Mori, H. (2005). Complete set of ORF clones of Escherichia coli ASKA library (A complete set of E. coli K-12 ORF archive): unique resources for biological research. *DNA Research*, *12*(5), 291–299. https://doi.org/10.1093/dnares/dsi012

Krishnamoorthy, G., Leus, I. V., Weeks, J. W., Wolloscheck, D., Rybenkov, V. V., & Zgurskaya, H. I. (2017). Synergy between active efflux and outer membrane diffusion defines rules of antibiotic permeation into gram-negative bacteria. *MBio*, *8*(5). https://doi.org/10.1128/MBIO.01172-17/SUPPL_FILE/MBO005173551SF4.TIF

Kroeck, K. G., Sacco, M. D., Smith, E. W., Zhang, X., Shoun, D., Akhtar, A., Darch, S. E., Cohen, F., Andrews, L. D., Knox, J. E., & Chen, Y. (2019). Discovery of dual-activity small-molecule ligands of Pseudomonas aeruginosa LpxA and LpxD using SPR and X-ray crystallography. *Scientific Reports 2019 9:1*, *9*(1), 1–12. https://doi.org/10.1038/s41598-019-51844-z

Kumar, S., Mollo, A., Kahne, D., & Ruiz, N. (2022). The Bacterial Cell Wall: From Lipid II Flipping to Polymerization. *Chemical Reviews*, *122*(9), 8884–8910. https://doi.org/10.1021/ACS.CHEMREV.1C00773/ASSET/IMAGES/MEDIUM/CR1C00773_0012.GIF

Lázár, V., Snitser, O., Barkan, D., & Kishony, R. (2022). Antibiotic combinations reduce Staphylococcus aureus clearance. *Nature*, *610*(7932), 540–546. https://doi.org/10.1038/S41586-022-05260-5

Lee, J., Tomasek, D., Santos, T. M., May, M. D., Meuskens, I., & Kahne, D. (2019). Formation of a β-barrel membrane protein is catalyzed by the interior surface of the assembly machine protein BamA. *ELife*, *8*. https://doi.org/10.7554/ELIFE.49787

Lewis, K. (2020). The Science of Antibiotic Discovery. *Cell*, *181*(1), 29–45. https://doi.org/10.1016/J.CELL.2020.02.056

Lewis, K., Lee, R. E., Brötz-Oesterhelt, H., Hiller, S., Rodnina, M. V., Schneider, T., Weingarth, M., & Wohlgemuth, I. (2024). Sophisticated natural products as antibiotics. In *Nature* (Vol. 632, Issue 8023, pp. 39–49). Nature Research. https://doi.org/10.1038/s41586-024-07530-w

Li, H., & Durbin, R. (2009). Fast and accurate short read alignment with Burrows-Wheeler transform. *Bioinformatics (Oxford, England)*, *25*(14), 1754–1760. https://doi.org/10.1093/BIOINFORMATICS/BTP324

Li, H., Luo, Y. F., Williams, B. J., Blackwell, T. S., & Xie, C. M. (2012). Structure and function of OprD protein in Pseudomonas aeruginosa: From antibiotic resistance to novel therapies. *International Journal of Medical Microbiology*, *302*(2), 63–68. https://doi.org/10.1016/J.IJMM.2011.10.001

Li, Q., Cebrián, R., Montalbán-López, M., Ren, H., Wu, W., & Kuipers, O. P. (2021). Outer-membrane-acting peptides and lipid II-targeting antibiotics cooperatively kill Gram-negative pathogens. *Communications Biology 2021 4:1*, *4*(1), 1–11. https://doi.org/10.1038/s42003-020-01511-1

Li, Y., Mei, H., Dong, Y., Lu, J., Yang, X., Zhang, Y., Feng, M., & Feng, J. (2025). Novel bifunctional antibacterial peptides mediated by a covalent conjugation strategy combat priority multidrug-resistant gram-negative pathogens through dual targets. *The Journal of Antibiotics 2025 78:6*, *78*(6), 359–369. https://doi.org/10.1038/s41429-025-00822-x

Ling, L. L., Schneider, T., Peoples, A. J., Spoering, A. L., Engels, I., Conlon, B. P., Mueller, A., Schäberle, T. F., Hughes, D. E., Epstein, S., Jones, M., Lazarides, L., Steadman, V. A., Cohen, D. R., Felix, C. R., Fetterman, K. A., Millett, W. P., Nitti, A. G., Zullo, A. M., … Lewis, K. (2015a). A new antibiotic kills pathogens without detectable resistance. *Nature 2015 517:7535*, *517*(7535), 455–459. https://doi.org/10.1038/nature14098

Ling, L. L., Schneider, T., Peoples, A. J., Spoering, A. L., Engels, I., Conlon, B. P., Mueller, A., Schäberle, T. F., Hughes, D. E., Epstein, S., Jones, M., Lazarides, L., Steadman, V. A., Cohen, D. R., Felix, C. R., Fetterman, K. A., Millett, W. P., Nitti, A. G., Zullo, A. M., … Lewis, K. (2015b). A new antibiotic kills pathogens without detectable resistance. *Nature 2015 517:7535*, *517*(7535), 455–459. https://doi.org/10.1038/nature14098

Lo Sciuto, A., Martorana, A. M., Fernández-Piñar, R., Mancone, C., Polissi, A., & Imperi, F. (2018). Pseudomonas aeruginosa LptE is crucial for LptD assembly, cell envelope integrity, antibiotic resistance and virulence. *Virulence*, *9*(1), 1718–1733. https://doi.org/10.1080/21505594.2018.1537730

Luo, C., Walk, S. T., Gordon, D. M., Feldgarden, M., Tiedje, J. M., & Konstantinidis, K. T. (2011). Genome sequencing of environmental Escherichia coli expands understanding of the ecology and speciation of the model bacterial species. *Proceedings of the National Academy of Sciences of the United States of America*, *108*(17), 7200–7205. https://doi.org/10.1073/PNAS.1015622108/SUPPL_FILE/ST03.DOCX

Luria, S. E., & Delbrück, M. (1943). Mutations of Bacteria from Virus Sensitivity to Virus Resistance. *Genetics*, *28*(6), 491–511. https://doi.org/10.1093/GENETICS/28.6.491

Luther, A., Urfer, M., Zahn, M., Müller, M., Wang, S. Y., Mondal, M., Vitale, A., Hartmann, J. B., Sharpe, T., Monte, F. Lo, Kocherla, H., Cline, E., Pessi, G., Rath, P., Modaresi, S. M., Chiquet, P., Stiegeler, S., Verbree, C., Remus, T., … Obrecht, D. (2019). Chimeric peptidomimetic antibiotics against Gram-negative bacteria. *Nature 2019 576:7787*, *576*(7787), 452–458. https://doi.org/10.1038/s41586-019-1665-6

MacNair, C. R., Rutherford, S. T., & Tan, M. W. (2024). Alternative therapeutic strategies to treat antibiotic-resistant pathogens. In *Nature Reviews Microbiology* (Vol. 22, Issue 5, pp. 262–275). Nature Research. https://doi.org/10.1038/s41579-023-00993-0

Maharramov, E., Czikkely, M. S., Szili, P., Farkas, Z., Grézal, G., Daruka, L., Kurkó, E., Mészáros, L., Daraba, A., Kovács, T., Bognár, B., Juhász, S., Papp, B., Lázár, V., & Pál, C. (2025). Exploring the principles behind antibiotics with limited resistance. *Nature Communications 2025 16:1*, *16*(1), 1842-. https://doi.org/10.1038/s41467-025-56934-3

Markley, J. L., & Wencewicz, T. A. (2018). Tetracycline-Inactivating Enzymes. *Frontiers in Microbiology*, *9*(MAY), 1058. https://doi.org/10.3389/FMICB.2018.01058

Martin, J. K., Sheehan, J. P., Bratton, B. P., Moore, G. M., Mateus, A., Li, S. H. J., Kim, H., Rabinowitz, J. D., Typas, A., Savitski, M. M., Wilson, M. Z., & Gitai, Z. (2020). A Dual-Mechanism Antibiotic Kills Gram-Negative Bacteria and Avoids Drug Resistance. *Cell*, *181*(7), 1518-1532.e14. https://doi.org/10.1016/J.CELL.2020.05.005

Martin, R. G., Jair, K. W., Wolf, R. E., & Rosner, J. L. (1996). Autoactivation of the marRAB multiple antibiotic resistance operon by the marA transcriptional activator in Escherichia coli. *Journal of Bacteriology*, *178*(8), 2216–2223. https://doi.org/10.1128/jb.178.8.2216-2223.1996

Martins, A., Judák, F., Farkas, Z., Szili, P., Grézal, G., Csörgő, B., Czikkely, M. S., Maharramov, E., Daruka, L., Spohn, R., Balogh, D., Daraba, A., Juhász, S., Vágvölgyi, M., Hunyadi, A., Cao, Y., Sun, Z., Li, X., Papp, B., & Pál, C. (2025). Antibiotic candidates for Gram-positive bacterial infections induce multidrug resistance. *Science Translational Medicine*, *17*(780). https://doi.org/10.1126/SCITRANSLMED.ADL2103/SUPPL_FILE/SCITRANSLMED.ADL2103_MDAR_REPRODUCIBILITY_CHECKLIST.PDF

Masi, M., & Pagès, J.-M. (2013). Structure, Function and Regulation of Outer Membrane Proteins Involved in Drug Transport in Enterobactericeae: the OmpF/C - TolC Case. *The Open Microbiology Journal*, *7*(1), 22–33. https://doi.org/10.2174/1874285801307010022

Masi, M., Vergalli, J., Ghai, I., Barba-Bon, A., Schembri, T., Nau, W. M., Lafitte, D., Winterhalter, M., & Pagès, J. M. (2022). Cephalosporin translocation across enterobacterial OmpF and OmpC channels, a filter across the outer membrane. *Communications Biology 2022 5:1*, *5*(1), 1–10. https://doi.org/10.1038/s42003-022-04035-y

May, K. L., & Grabowicz, M. (2018). The bacterial outer membrane is an evolving antibiotic barrier. *Proceedings of the National Academy of Sciences of the United States of America*, *115*(36), 8852–8854. https://doi.org/10.1073/PNAS.1812779115/ASSET/4CA14952-2515-429D-AEEA-DD8428CE9524/ASSETS/GRAPHIC/PNAS.1812779115FIG01.JPEG

McArthur, A. G., Waglechner, N., Nizam, F., Yan, A., Azad, M. A., Baylay, A. J., Bhullar, K., Canova, M. J., De Pascale, G., Ejim, L., Kalan, L., King, A. M., Koteva, K., Morar, M., Mulvey, M. R., O'Brien, J. S., Pawlowski, A. C., Piddock, L. J. V., Spanogiannopoulos, P., … Wright, G. D. (2013). The comprehensive antibiotic resistance database. *Antimicrobial Agents and Chemotherapy*, *57*(7), 3348–3357. https://doi.org/10.1128/AAC.00419-13/ASSET/81B6EA0E-6DD1-48A2-801B-ECB1FDE2D281/ASSETS/GRAPHIC/ZAC9991019770005.JPEG

Melnyk, A. H., Wong, A., & Kassen, R. (2015). The fitness costs of antibiotic resistance mutations. *Evolutionary Applications*, *8*(3), 273–283. https://doi.org/10.1111/EVA.12196

Miller, W. R., & Arias, C. A. (2024). ESKAPE pathogens: antimicrobial resistance, epidemiology, clinical impact and therapeutics. In *Nature Reviews Microbiology* (Vol. 22, Issue 10, pp. 598–616). Nature Research. https://doi.org/10.1038/s41579-024-01054-w

Moreno-Gamez, S., Hilla, A. L., Rosenbloom, D. I. S., Petrov, D. A., Nowak, M. A., & Pennings, P. S. (2015). Imperfect drug penetration leads to spatial monotherapy and rapid evolution of multidrug resistance. *Proceedings of the National Academy of Sciences of the United States of America*, *112*(22), E2874–E2883. https://doi.org/10.1073/PNAS.1424184112/SUPPL_FILE/PNAS.1424184112.SAPP.PDF

Murray, C. J., Ikuta, K. S., Sharara, F., Swetschinski, L., Robles Aguilar, G., Gray, A., Han, C., Bisignano, C., Rao, P., Wool, E., Johnson, S. C., Browne, A. J., Chipeta, M. G., Fell, F., Hackett, S., Haines-Woodhouse, G., Kashef Hamadani, B. H., Kumaran, E. A. P., McManigal, B., … Naghavi, M. (2022). Global burden of bacterial antimicrobial resistance in 2019: a systematic analysis. *The Lancet*, *399*(10325), 629–655. https://doi.org/10.1016/S0140-6736(21)02724-0

Myers, A. G., & Clark, R. B. (2021). Discovery of Macrolide Antibiotics Effective against Multi-Drug Resistant Gram-Negative Pathogens. *Accounts of Chemical Research*, *54*(7), 1635–1645. https://doi.org/10.1021/ACS.ACCOUNTS.1C00020/ASSET/IMAGES/LARGE/AR1C00020_0005.JPEG

Naas, T., Oueslati, S., Bonnin, R. A., Dabos, M. L., Zavala, A., Dortet, L., Retailleau, P., & Iorga, B. I. (2017). Beta-lactamase database (BLDB) - structure and function. *Journal of Enzyme Inhibition and Medicinal Chemistry*, *32*(1), 917–919. https://doi.org/10.1080/14756366.2017.1344235

Naghavi, M., Vollset, S. E., Ikuta, K. S., Swetschinski, L. R., Gray, A. P., Wool, E. E., Robles Aguilar, G., Mestrovic, T., Smith, G., Han, C., Hsu, R. L., Chalek, J., Araki, D. T., Chung, E., Raggi, C., Gershberg Hayoon, A., Davis Weaver, N., Lindstedt, P. A., Smith, A. E., … Murray, C. J. L. (2024). Global burden of bacterial antimicrobial resistance 1990–2021: a systematic analysis with forecasts to 2050. *The Lancet*, *404*(10459), 1199–1226. https://doi.org/10.1016/S0140-6736(24)01867-1

Nishino, K., Nikaido, E., & Yamaguchi, A. (2007). Regulation of multidrug efflux systems involved in multidrug and metal resistance of Salmonella enterica serovar Typhimurium. *Journal of Bacteriology*, *189*(24), 9066–9075. https://doi.org/10.1128/JB.01045-07

Nishino, K., Senda, Y., & Yamaguchi, A. (2008). CRP regulator modulates multidrug resistance of Escherichia coli by repressing the mdtEF multidrug efflux genes. *The Journal of Antibiotics*, *61*(3), 120–127. https://doi.org/10.1038/JA.2008.120

Nishino, K., & Yamaguchi, A. (2001). Analysis of a complete library of putative drug transporter genes in Escherichia coli. *Journal of Bacteriology*, *183*(20), 5803–5812. https://doi.org/10.1128/JB.183.20.5803-5812.2001

Ntallis, C., Martin, N. I., Edwards, A. M., & Weingarth, M. (2025). Bacterial cell envelope-targeting antibiotics. *Nature Reviews Microbiology 2025*, 1–14. https://doi.org/10.1038/s41579-025-01247-x

Nyerges, A., Tomašič, T., Durcik, M., Revesz, T., Szili, P., Draskovits, G., Bogar, F., Skok, Ž., Zidar, N., Ilaš, J., Zega, A., Kikelj, D., Daruka, L., Kintses, B., Vasarhelyi, B., Foldesi, I., Kata, D., Welin, M., Kimbung, R., … Pal, C. (2020). Rational design of balanced dual-targeting antibiotics with

limited resistance. *PLOS Biology*, *18*(10), e3000819. https://doi.org/10.1371/JOURNAL.PBIO.3000819

Okuda, S., Sherman, D. J., Silhavy, T. J., Ruiz, N., & Kahne, D. (2016). Lipopolysaccharide transport and assembly at the outer membrane: the PEZ model. *Nature Reviews Microbiology 2016 14:6*, *14*(6), 337–345. https://doi.org/10.1038/nrmicro.2016.25

Olaitan, A. O., Morand, S., & Rolain, J. M. (2014). Mechanisms of polymyxin resistance: acquired and intrinsic resistance in bacteria. *Frontiers in Microbiology*, *5*(NOV). https://doi.org/10.3389/FMICB.2014.00643

O'Leary, N. A., Wright, M. W., Brister, J. R., Ciufo, S., Haddad, D., McVeigh, R., Rajput, B., Robbertse, B., Smith-White, B., Ako-Adjei, D., Astashyn, A., Badretdin, A., Bao, Y., Blinkova, O., Brover, V., Chetvernin, V., Choi, J., Cox, E., Ermolaeva, O., … Pruitt, K. D. (2016). Reference sequence (RefSeq) database at NCBI: current status, taxonomic expansion, and functional annotation. *Nucleic Acids Research*, *44*(D1), D733–D745. https://doi.org/10.1093/NAR/GKV1189

Partridge, S. R., Kwong, S. M., Firth, N., & Jensen, S. O. (2018). Mobile Genetic Elements Associated with Antimicrobial Resistance. *Clinical Microbiology Reviews*, *31*(4), e00088-17. https://doi.org/10.1128/CMR.00088-17

Poirel, L., Jayol, A., & Nordmanna, P. (2017). Polymyxins: Antibacterial activity, susceptibility testing, and resistance mechanisms encoded by plasmids or chromosomes. *Clinical Microbiology Reviews*, *30*(2), 557–596. https://doi.org/10.1128/CMR.00064-16/ASSET/F24ADD26-A033-40E2-9AA1-A534A4E95FBA/ASSETS/GRAPHIC/ZCM0021725860005.JPEG

Prasad, N. K., Seiple, I. B., Cirz, R. T., & Rosenberg, O. S. (2022). Leaks in the Pipeline: a Failure Analysis of Gram-Negative Antibiotic Development from 2010 to 2020. *Antimicrobial Agents and Chemotherapy*, *66*(5). https://doi.org/10.1128/AAC.00054-22/ASSET/5CADBC2C-2BBB-4A7D-8E33-8D6E543CD129/ASSETS/IMAGES/LARGE/AAC.00054-22-F002.JPG

Pursey, E., Dimitriu, T., Gaze, W. H., Westra, E. R., & Houte, S. van. (2023). The distribution of antimicrobial resistance genes across phylogroup, host species and geography in 16,000 publicly-available E. coli genomes. *MedRxiv*, 2022.08.05.22278465. https://doi.org/10.1101/2022.08.05.22278465

R Core Team. (2022). *R: A Language and Environment for Statistical Computing*. R Foundation for Statistical Computing.

Ramirez, D. M., Ramirez, D., Arthur, G., Zhanel, G., & Schweizer, F. (2022). Guanidinylated Polymyxins as Outer Membrane Permeabilizers Capable of Potentiating Rifampicin, Erythromycin, Ceftazidime and Aztreonam against Gram-Negative Bacteria. *Antibiotics*, *11*(10), 1277. https://doi.org/10.3390/ANTIBIOTICS11101277/S1

Ramirez, M. S., & Tolmasky, M. E. (2010). Aminoglycoside modifying enzymes. *Drug Resistance Updates*, *13*(6), 151–171. https://doi.org/10.1016/J.DRUP.2010.08.003

Reyes-Fernández, E. Z., & Schuldiner, S. (2020). Acidification of Cytoplasm in Escherichia coli Provides a Strategy to Cope with Stress and Facilitates Development of Antibiotic Resistance. *Scientific Reports 2020 10:1*, *10*(1), 1–13. https://doi.org/10.1038/s41598-020-66890-1

Reygaert, W. C. (2018). An overview of the antimicrobial resistance mechanisms of bacteria. *AIMS Microbiology*, *4*(3), 482. https://doi.org/10.3934/MICROBIOL.2018.3.482

Ricci, V., Blair, J. M. A., & Piddock, L. J. V. (2014). RamA, which controls expression of the MDR efflux pump AcrAB-TolC, is regulated by the Lon protease. *Journal of Antimicrobial Chemotherapy*, *69*(3), 643–650. https://doi.org/10.1093/JAC/DKT432

Ricci, V., Tzakas, P., Buckley, A., Coldham, N. C., & Piddock, L. J. V. (2006). Ciprofloxacin-Resistant Salmonella enterica Serovar Typhimurium Strains Are Difficult To Select in the Absence of AcrB and TolC. *Antimicrobial Agents and Chemotherapy*, *50*(1), 38. https://doi.org/10.1128/AAC.50.1.38-42.2006

Robinson, J. T., Thorvaldsdóttir, H., Winckler, W., Guttman, M., Lander, E. S., Getz, G., & Mesirov, J. P. (2011). Integrative genomics viewer. *Nature Biotechnology 2011 29:1*, *29*(1), 24–26. https://doi.org/10.1038/nbt.1754

Romano, K. P., & Hung, D. T. (2023). Targeting LPS biosynthesis and transport in gram-negative bacteria in the era of multi-drug resistance. *Biochimica et Biophysica Acta (BBA) - Molecular Cell Research*, *1870*(3), 119407. https://doi.org/10.1016/J.BBAMCR.2022.119407

Sandegren, L., & Andersson, D. I. (2009). Bacterial gene amplification: implications for the evolution of antibiotic resistance. *Nature Reviews Microbiology 2009 7:8*, *7*(8), 578–588. https://doi.org/10.1038/nrmicro2174

Saxena, D., Maitra, R., Bormon, R., Czekanska, M., Meiers, J., Titz, A., Verma, S., & Chopra, S. (2023). Tackling the outer membrane: facilitating compound entry into Gram-negative bacterial pathogens. *Npj Antimicrobials and Resistance 2023 1:1*, *1*(1), 1–22. https://doi.org/10.1038/s44259-023-00016-1

Sethuvel, D. P. M., Bakthavatchalam, Y. D., Karthik, M., Irulappan, M., Shrivastava, R., Periasamy, H., & Veeraraghavan, B. (2023). β-Lactam Resistance in ESKAPE Pathogens Mediated Through Modifications in Penicillin-Binding Proteins: An Overview. *Infectious Diseases and Therapy*, *12*(3), 829. https://doi.org/10.1007/S40121-023-00771-8

Sheu, C. C., Chang, Y. T., Lin, S. Y., Chen, Y. H., & Hsueh, P. R. (2019). Infections Caused by Carbapenem-Resistant Enterobacteriaceae: An Update on Therapeutic Options. *Frontiers in Microbiology*, *10*(JAN), 80. https://doi.org/10.3389/FMICB.2019.00080

Shukla, R., Peoples, A. J., Ludwig, K. C., Maity, S., Derks, M. G. N., De Benedetti, S., Krueger, A. M., Vermeulen, B. J. A., Harbig, T., Lavore, F., Kumar, R., Honorato, R. V., Grein, F., Nieselt, K., Liu, Y., Bonvin, A. M. J. J., Baldus, M., Kubitscheck, U., Breukink, E., … Weingarth, M. (2023). An antibiotic from an uncultured bacterium binds to an immutable target. *Cell*, *186*(19), 4059-4073.e27. https://doi.org/10.1016/J.CELL.2023.07.038

Si, Z., Pethe, K., & Chan-Park, M. B. (2023). Chemical Basis of Combination Therapy to Combat Antibiotic Resistance. *JACS Au*, *3*(2), 276–292. https://doi.org/10.1021/JACSAU.2C00532/ASSET/IMAGES/LARGE/AU2C00532_0007.JPEG

Silver, L. L. (2007). Multi-targeting by monotherapeutic antibacterials. *Nature Reviews Drug Discovery 2006 6:1*, *6*(1), 41–55. https://doi.org/10.1038/nrd2202

Smith, T. F., & Waterman, M. S. (1981). Identification of common molecular subsequences. *Journal of Molecular Biology*, *147*(1), 195–197. https://doi.org/10.1016/0022-2836(81)90087-5

Spohn, R., Daruka, L., Lázár, V., Martins, A., Vidovics, F., Grézal, G., Méhi, O., Kintses, B., Számel, M., Jangir, P. K., Csörgő, B., Györkei, Á., Bódi, Z., Faragó, A., Bodai, L., Földesi, I., Kata, D.,

Maróti, G., Pap, B., … Pál, C. (2019). Integrated evolutionary analysis reveals antimicrobial peptides with limited resistance. *Nature Communications 2019 10:1*, *10*(1), 1–13. https://doi.org/10.1038/s41467-019-12364-6

Srinivas, N., Jetter, P., Ueberbacher, B. J., Werneburg, M., Zerbe, K., Steinmann, J., Van Der Meijden, B., Bernardini, F., Lederer, A., Dias, R. L. A., Misson, P. E., Henze, H., Zumbrunn, J., Gombert, F. O., Obrecht, D., Hunziker, P., Schauer, S., Ziegler, U., Käch, A., … Robinson, J. A. (2010). Peptidomimetic antibiotics target outer-membrane biogenesis in pseudomonas aeruginosa. *Science*, *327*(5968), 1010–1013. https://doi.org/10.1126/SCIENCE.1182749/SUPPL_FILE/SRINIVAS.SOM.PDF

Surivet, J. P., Panchaud, P., Specklin, J. L., Diethelm, S., Blumstein, A. C., Gauvin, J. C., Jacob, L., Masse, F., Mathieu, G., Mirre, A., Schmitt, C., Lange, R., Tidten-Luksch, N., Gnerre, C., Seeland, S., Herrmann, C., Seiler, P., Enderlin-Paput, M., Mac Sweeney, A., … Rueedi, G. (2020). Discovery of Novel Inhibitors of LpxC Displaying Potent in Vitro Activity against Gram-Negative Bacteria. *Journal of Medicinal Chemistry*, *63*(1), 66–87. https://doi.org/10.1021/ACS.JMEDCHEM.9B01604/SUPPL_FILE/JM9B01604_SI_001.CSV

Szili, P., Draskovits, G., Révész, T., Bogár, F., Balogh, D., Martinek, T., Daruka, L., Spohn, R., Vásárhelyi, B. M., Czikkely, M., Kintses, B., Grézal, G., Ferenc, G., Pál, C., & Nyerges, Á. (2019). Rapid evolution of reduced susceptibility against a balanced dual-targeting antibiotic through stepping-stone mutations. *Antimicrobial Agents and Chemotherapy*, *63*(9). https://doi.org/10.1128/AAC.00207-19/SUPPL_FILE/AAC.00207-19-SD002.XLSX

Szybalski, W. (1954). Genetic studies on microbial cross resistance to toxic agents. IV. Cross resistance of Bacillus megaterium to forty-four antimicrobial drugs. *Applied Microbiology*, *2*(2), 57–63. https://doi.org/10.1128/AM.2.2.57-63.1954

Tatusov, R. L., Koonin, E. V., & Lipman, D. J. (1997). A genomic perspective on protein families. *Science (New York, N.Y.)*, *278*(5338), 631–637. https://doi.org/10.1126/SCIENCE.278.5338.631

Theuretzbacher, U. (2025a). Evaluating the innovative potential of the global antibacterial pipeline. *Clinical Microbiology and Infection*, *31*(6), 903–909. https://doi.org/10.1016/j.cmi.2023.09.024

Theuretzbacher, U. (2025b). The global resistance problem and the clinical antibacterial pipeline. In *Nature Reviews Microbiology* (Vol. 23, Issue 8, pp. 491–508). Nature Research. https://doi.org/10.1038/s41579-025-01169-8

Theuretzbacher, U., Blasco, B., Duffey, M., & Piddock, L. J. V. (2023). Unrealized targets in the discovery of antibiotics for Gram-negative bacterial infections. In *Nature Reviews Drug Discovery* (Vol. 22, Issue 12, pp. 957–975). Nature Research. https://doi.org/10.1038/s41573-023-00791-6

Theuretzbacher, U., Jumde, R. P., Hennessy, A., Cohn, J., & Piddock, L. J. V. (2025). Global health perspectives on antibacterial drug discovery and the preclinical pipeline. *Nature Reviews Microbiology 2025 23:8*, *23*(8), 474–490. https://doi.org/10.1038/s41579-025-01167-w

Tooke, C. L., Hinchliffe, P., Bragginton, E. C., Colenso, C. K., Hirvonen, V. H. A., Takebayashi, Y., & Spencer, J. (2019). β-Lactamases and β-Lactamase Inhibitors in the 21st Century. *Journal of Molecular Biology*, *431*(18), 3472–3500. https://doi.org/10.1016/J.JMB.2019.04.002

Törönen, P., & Holm, L. (2022). PANNZER-A practical tool for protein function prediction. *Protein Science : A Publication of the Protein Society*, *31*(1), 118–128. https://doi.org/10.1002/PRO.4193

Törönen, P., Medlar, A., & Holm, L. (2018). PANNZER2: a rapid functional annotation web server. *Nucleic Acids Research*, *46*(W1), W84–W88. https://doi.org/10.1093/NAR/GKY350

Tyers, M., & Wright, G. D. (2019). Drug combinations: a strategy to extend the life of antibiotics in the 21st century. *Nature Reviews Microbiology 2018 17:3*, *17*(3), 141–155. https://doi.org/10.1038/s41579-018-0141-x

Vaara, M. (1993). Outer membrane permeability barrier to azithromycin, clarithromycin, and roxithromycin in gram-negative enteric bacteria. *Antimicrobial Agents and Chemotherapy*, *37*(2), 354. https://doi.org/10.1128/AAC.37.2.354

Varughese, L. R., Rajpoot, M., Goyal, S., Mehra, R., Chhokar, V., & Beniwal, V. (2018). Analytical profiling of mutations in quinolone resistance determining region of gyrA gene among UPEC. *PLOS ONE*, *13*(1), e0190729. https://doi.org/10.1371/JOURNAL.PONE.0190729

Wang, J., & Blount, P. (2023). Feeling the tension: the bacterial mechanosensitive channel of large conductance as a model system and drug target. *Current Opinion in Physiology*, *31*, 100627. https://doi.org/10.1016/J.COPHYS.2022.100627

Wang, J., Cao, L., Yang, X., Wu, Q., Lu, L., & Wang, Z. (2018). Transcriptional analysis reveals the critical role of RNA polymerase-binding transcription factor, DksA, in regulating multi-drug resistance of Escherichia coli. *International Journal of Antimicrobial Agents*, *52*(1), 63–69. https://doi.org/10.1016/j.ijantimicag.2018.05.002

Waters, N. R., Abram, F., Brennan, F., Holmes, A., & Pritchard, L. (2020). Easy phylotyping of Escherichia coli via the EzClermont web app and command-line tool. *Access Microbiology*, *2*(9), e000143. https://doi.org/10.1099/ACMI.0.000143

Wiegand, I., Hilpert, K., & Hancock, R. E. W. (2008). Agar and broth dilution methods to determine the minimal inhibitory concentration (MIC) of antimicrobial substances. *Nature Protocols*, *3*(2), 163–175. https://doi.org/10.1038/nprot.2007.521

World Health Organization. (2017). *Prioritization of pathogens to guide discovery, research and development of new antibiotics for drug-resistant bacterial infections, including tuberculosis.* https://www.who.int/publications/i/item/WHO-EMP-IAU-2017.12

World Health Organization. (2024). WHO Bacterial Priority Pathogens List, 2024- Bacterial pathogens of public health importance to guide research, development and strategies to prevent and control antimicrobial resistance. *World Health Organization*, 1–72. https://iris.who.int/bitstream/handle/10665/376776/9789240093461-eng.pdf

Wray, R., Wang, J., Blount, P., & Iscla, I. (2022). Activation of a Bacterial Mechanosensitive Channel, MscL, Underlies the Membrane Permeabilization of Dual-Targeting Antibacterial Compounds. *Antibiotics (Basel, Switzerland)*, *11*(7). https://doi.org/10.3390/ANTIBIOTICS11070970

Wu, T., Hu, E., Xu, S., Chen, M., Guo, P., Dai, Z., Feng, T., Zhou, L., Tang, W., Zhan, L., Fu, X., Liu, S., Bo, X., & Yu, G. (2021). clusterProfiler 4.0: A universal enrichment tool for interpreting omics data. *The Innovation*, *2*(3), 100141. https://doi.org/10.1016/J.XINN.2021.100141

Yan, A., Shi, Y., Matson, J. S., & Vaara, M. (2019). Polymyxins and Their Potential Next Generation as Therapeutic Antibiotics. *Frontiers in Microbiology*, *10*(JULY), 1689–1689. https://doi.org/10.3389/FMICB.2019.01689

Yosef, I., Goren, M. G., Globus, R., Molshanski-Mor, S., & Qimron, U. (2017). Extending the Host Range of Bacteriophage Particles for DNA Transduction. *Molecular Cell*, *66*(5), 721-728.e3. https://doi.org/10.1016/j.molcel.2017.04.025

Zhang, Y., Zhao, C., Wang, Q., Wang, X., Chen, H., Li, H., Zhang, F., & Wang, H. (2020). Evaluation of the in vitro activity of new polymyxin B analogue SPR206 against clinical MDR, colistin-resistant and tigecycline-resistant Gram-negative bacilli. *Journal of Antimicrobial Chemotherapy*, *75*(9), 2609–2615. https://doi.org/10.1093/JAC/DKAA217

Zhu, L., Lin, J., Ma, J., Cronan, J. E., & Wang, H. (2010). Triclosan resistance of Pseudomonas aeruginosa PAO1 is due to FabV, a triclosan-resistant enoyl-acyl carrier protein reductase. *Antimicrobial Agents and Chemotherapy*, *54*(2), 689–698. https://doi.org/10.1128/AAC.01152-09/ASSET/EF857DB6-79E4-4B4D-BF8D-0247602539F8/ASSETS/GRAPHIC/ZAC0021087930006.JPEG

10. List of publications

Number of scientific publications: 4 (+ 2 pre-print)

Number of citations: 132

H-index: 4

Total impact factor: 61.1

MTMT identification number: 10082508

Peer-reviewed publications

* **Maharramov, E**., Czikkely, M. S., Szili, P., Farkas, Z., Grézal, G., Daruka, L., Kurkó, E., Mészáros, L., Daraba, A., Kovács, T., Bognár, B., Juhász, S., Papp, B., Lázár, V., & Pál, C. *Exploring the principles behind antibiotics with limited resistance.* Nat. Commun. 16, 1842 (2025). IF: 17.2

Daruka, L., Czikkely, M. S., Szili, P., Farkas, Z., Balogh, D., Grézal, G., **Maharramov, E.**, Vu, T.-H., Sipos, L., Juhász, S., Dunai, A., Daraba, A., Számel, M., Sári, T., Stirling, T., Vásárhelyi, B. M., Ari, E., Christodoulou, C., Manczinger, M., Enyedi, M. Z., Jaksa, G., Kovács, K., van Houte, S., Pursey, E., Pintér, L., Haracska, L., Kintses, B., Papp, B., & Pál, C. *ESKAPE pathogens rapidly develop resistance against antibiotics in development in vitro.* Nat. Microbiol. 10, 313–331 (2025). IF: 20.7

Martins, A., Judák, F., Farkas, Z., Szili, P., Grézal, G., Csörgő, B., Czikkely, M. S., **Maharramov, E.**, Daruka, L., Spohn, R., Balogh, D., Daraba, A., Juhász, S., Vágvölgyi, M., Hunyadi, A., Cao, Y., Sun, Z., Li, X., Papp, B., & Pál, C. *Antibiotic candidates for Gram-positive bacterial infections induce multidrug resistance.* Sci. Transl. Med. 17, eadl2103 (2025). IF: 16.0

Durcik, M., Cotman, A. E., Toplak, Z., Mozina, S., Skok, Z., Szili, P. E., Czikkely, M., **Maharramov, E.**, Vu, T. H., Piras, M. V., Zidar, N., Ilas, J., Zega, A., Trontelj, J., Pardo, L. A., Hughes, D., Huseby, D., Berruga-Fernández, T., Cao, S., Simoff, I., Svensson, R., Korol, S. V., Jin, Z., Vicente, F., Ramos, M. C., Mundy, J. E. A., Maxwell, A., Stevenson, C. E. M., Lawson, D. M., Glinghammar, B., Sjostrom, E., Bohlin, M., Oreskar, J., Alvér, S., Janssen, G. V., Sterk, G. J., Kikelj, D., Pál, C., Tomašić, T., & Peterlin Mašič, L. *New dual inhibitors of bacterial topoisomerases with broad-spectrum antibacterial activity and in vivo efficacy against vancomycin-intermediate Staphylococcus aureus.* J. Med. Chem. 66(6), 3968–3994 (2023). IF: 7.2

** This publication serves as the basis of this PhD dissertation.*

Preprints

Szili, P., Daruka, L., Spohn, R., Vu, T.-H., **Maharramov, E.**, Grézal, G., Czikkely, M., Csernyák, M., Vonyó, A., Benedek, B., Daraba, A., Judák, F., Martins, A., Balogh, D., Csörgő, B., Dunai, A., Kovács, T., Ábrahám, A., Lázár, V., Stirling, T., Vásárhelyi, B., Kintses, B., Réthi-Nagy, Z., Juhász, S., Papp, B., & Pál, C. *A comprehensive analysis reveals biocides with limited resistance in ESKAPE pathogens.* (2025). Under review in Nature Microbiology.

Kalapis, D., Kovács, K., Balogh, D., **Maharramov, E.**, Ajibola, W., Silander, O., Fehér, T., Pál, C., & Papp, B. *Gene loss promotes the evolution of metabolic innovations through transcriptional rewiring.* (2025). Under review in PLOS Biology.